Self-Assembled Antibody Nanorings as Prosthetic Antigen Receptors for Redirecting T Cells against Tumor Cells and as Platform for Delivery of Vaccine Adjuvants for Cancer Immunotherapy

A DISSERTATION
SUBMITTED TO THE FACULTY OF
UNIVERSITY OF MINNESOTA
BY

Jingjing Shen

IN PARTIAL FULFILLMENT OF THE REQUIREMENTS
FOR THE DEGREE OF DOCTOR OF PHILOSOPHY

Dr. Carston Rick Wagner, Advisor

May, 2016

Acknowledgements

Firstly, I would like to express my sincere gratitude to my advisor Dr. Carston Rick Wagner, for the continuous support of my Ph.D study and related research, for his patience, motivation, and immense knowledge. His technical and editorial advice was essential to the completion of this dissertation and has taught me innumerable lessons and insights on the workings of academic research in general.

I am very grateful to my committee members, Dr. Elizabeth Ambrose, Dr. Mark Distefano and Dr. Daniel Harki, for their encouragement, insightful comments, and valuable feedback throughout my graduate studies. I also want to thank my collaborators Dr. Daniel Vallera and Dr, Jeffrey Miller. I specially want to thank Dr. Thomas S Griffith, Dr. Katherine Murphy and Tamara Kucaba for their help with the animal study.

The friendship of all members of Dr. Wagner's research group is much appreciated and has led to many interesting and good-spirited discussions relating to this research.

Last, but not least, I would like to thank my family especially my husband for his understanding and love during the past few years. Their constant support, encouragement and sacrifices have made this accomplishment possible. I specially want to thank my little boy, for so much love, joy and happiness he has brought to me. He is such a blessing for me and for my family.

Abstract

We have previously demonstrated that in the presence of the chemical dimerizer bisMTX, DHFR-DHFR ($DHFR^2$) and DHFR-DHFR-antiCD3 ($DHFR^2$-antiCD3) fusion proteins can spontaneously assemble into a range of chemically self-assembled nanorings (CSANs) whose size varies depending on the length and composition of the linker peptide between the DHFRs. If the linker is a single glycine, we observed that rings containing 7 to 10 $DHFR^2$ fusion proteins with an average ring size were composed of 8 monomers.

The research presented in the thesis focused on exploring our methodology for engineering multivalent CSANs for delivery of vaccine adjuvants and for redirecting immune cells specificity for cancer immunotherapy. In the first part, we have synthesized a MTX analog for the purpose of driving the equilibrium towards formation of heterodimers of CSANs. The binding affinities of this MTX analog with either wild type DHFR or several DHFR mutants were determined.

In the second part of the thesis, we assembled bispecific antiCD3/CD22 CSANs by mixing of an equal proportion of two $DHFR^2$ linked by a single glycine and fused to two different antibodies: antiCD3 scFv that binds to the CD3 receptor on immune T-cells and antiCD22 scFv targeting CD22, an antigen widely expressed on B-leukemias or lymphomas. We firstly determined the binding affinity of engineered antiCD22 CSANs to CD22+ B lymphoma cells by comparison with those for the parental monoclonal antibody followed by investigations of their internalization by these cells using confocal

microscopy. In addition, we studied the activation of T cells by cytokine profiling, immunophenotyping and T cell functional assays *in vitro* after treatment with bispecific antiCD3/CD22 CSANs. In the presence of target B lymphoma cells, cytolytic efficacy of redirected T cells was also determined. Finally, we assessed the ability of trimethoprim, a non-toxic FDA approved competitive inhibitor of DHFR to carry out disassembly of the bispecific antibody nanorings.

Finally, to explore the potential of $DHFR^2$ based CSANs to be used as vaccines by the multivalent display of an antigen and adjuvant, we prepared CSANs assembled with the bisMTX dimerizer and CSANs assembled with the bisMTX-CpG, bisMTX dimerizer linked to CpG oligonucleotides, and compared their immune responses in mice. We studied the immunogenicity of CpG CSANs as well as CSANs by cytokine profiling, immunophenotyping using mouse immune cells *in vitro*. And we determined titers of neutralization antibodies in the sera of immunized mice.

Table of Contents

List of Tables

Chapter One

Chapter Two

List of Figures

Chapter One

Chapter Two

Chapter Three

Chapter Four

List of Abbreviations

1DHFR^{2}antiCD3	DHFR-1amino acid linker-DHFR
13DHFR^{2}antiCD3	DHFR-13amino acid linker-DHFR
Ab	Antibody
AFM	Atom force microscopy
bisMTX	bis-methotrexate
CpG ODN	Cytosine triphosphate guanine triphosphate oligodeoxynucleotides
DEAE	Diethyl aminoethyl
DHF	Dihydrofolate
ESI-MS	Electrospray ionization mass spectrometry
FDA	U S Food and Drug Administration
FITC	Fluorescein isothiocyanate
FKBP	FK 506 binding protein
IL-2	Interleukin-2
IFN-γ	Interferon gamma
IPTG	Isopropylthiogalactoside
Kd	Dissociation constant
KDa	Kilodaltons
LB	Luria bertani
mAb	Monoclonal antibody
Mw	Molecular weight
NADPH	Nicotinamide adenine dinucleotide phosphate
PBMC	Peripheral blood mononuclear cell
PCR	Polymerase chain reaction
scFv	Single chain variable fragment
SDS-PAGE	sodium dodecyl sulfate polyacrylamide gel electrophoresis
SEC	Size exclusion chromatography

TCR	T cell receptor
TNF	Tumor necrosis factor
UV	Ultraviolet
WT	Wild type

Chapter One: Introduction-Cancer immunotherapy

More than a century ago, the concept of cancer immunotherapy arose. The bone surgeon William Coley, who worked at what later became the Memorial Sloan Kettering Cancer Center in New York, injected his patients with a killed bacteria vaccine during the late 1800s in the hope of stimulating the body's defenses.[1] During the 1990s, physicians began treating people with cancer with high doses of interleukin-2 (IL-2) and interferon-γ (IFNγ) - inflammatory cytokines released by infection-fighting white blood cells called T cells.[2] A sub-set of cancer patients have lived for decades with the help of cytokine treatment.[3] However, there can be life-threatening side effects, including vascular leakage and kidney damage, because systemic inflammation is generated by high-dose cytokines release.[3] Great progresses have been made in the field of cancer immunology in the past decade. Immunotherapy is a central component of many cancer treatment regimens, which is the use of drugs and/or biological agents to initiate, modulate and control an immune response.[4] A wide range of immunotherapeutic strategies is currently being investigated for both prophylactic and therapeutic purposes.

I. **Antitumor vaccine**

Starting from the discovery of the cowpox/smallpox vaccine by Jenner, the field of vaccines against infectious diseases has focused on preventive applications with numerous successes, mainly because the causative agents of most infectious diseases are recognized by the immune system as “non-self”.[5] Although many tumors are well known to over-express distinct antigens, these antigens can be expressed on other tissues as well, making the development of tumor vaccines problematic. The immune system can be forced to respond against tumor-associated antigens by means of vaccination.[6] Cancer vaccines aimed at the generation of strong neutralization antibody responses against

vaccine antigens and the induction of robust tumor-specific T cell responses have been a focus of translational cancer immunotherapies. Multiple immunization strategies have been studied including the use of recombinant viruses encoding cancer antigens,[7] immunization with whole tumor cells,[8] antigen-loaded dendritic cells,[9] or immunogenic peptides derived from cancer antigens (**Figure 1**).[10]

A. Vaccines derived from viral subunit-like particles (VLPs)

A substantial proportion of the world's cancer burden can be attributed to the consequences of chronic infection with viruses, bacteria, and parasites.[11] The infections with hepatitis B (HBV) viruses and C viruses (HCV) are associated with occurrence of hepatocellular carcinoma (HCC). HBV and HCV infections were estimated to account for 4.9% of all cancer cases and specifically to be associated with 85.5% of all HCC cases in the world, making it the ninth leading cause of death.[11] HPV infections were estimated to account for 5.2% of all cancers in the world, being responsible for 3% of mouth cancers, 12% of oropharynx cancers, 40% of penis cancers, 40% of vulva/vagina cancers and virtually 100% of uterine cervical cancers.[7] The U.S. Food and Drug Administration (FDA) has approved two prophylactic vaccines against human papillomavirus (HPV), Gardasil® and Cervarix®, protecting against infection by the two types of HPV (type 16 and 18) that cause approximately 70 percent of all cases of cervical cancer worldwide.[12] Both vaccines are derived from viral subunit-like particles (VLPs) composed of a single viral protein, L1, which is the major structural (capsid) protein of the virus and hence contains its immunodominant neutralization epitope.[13] Cervarix®, manufactured by GlaxoSmithKline, is a bivalent vaccine, composed of VLPs made with proteins from HPV-16 and HPV-18. Conversely, Gardasil®, produced by Merck, is a quadrivalent

vaccine that contains VLPs from HPV-6, HPV-11, HPV-16 and HPV-18. The FDA has also approved a cancer preventive vaccine that protects against hepatitis B virus (HBV) infection. The anti-HBV vaccine is based on 22-nm particles containing the recombinant HBV surface antigen (HBsAg). It is highly immunogenic and has been shown to convey lifelong immunity.[14]

Figure 1. Cancer vaccine approaches. [15]

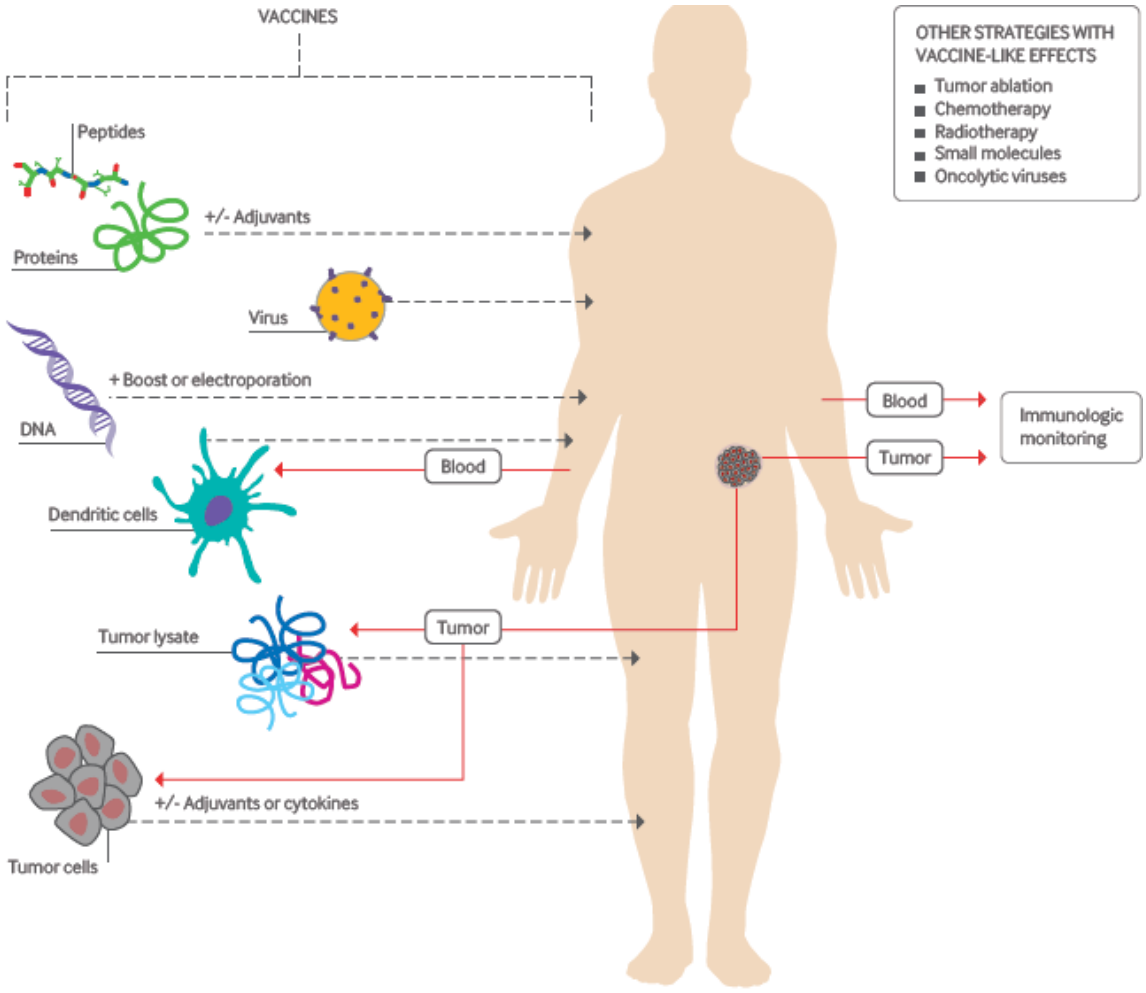

Vaccines include short peptides, full length proteins,viruses, DNA, dendritic cells, tumor cells (killed), and tumor lysates. These elements can be modified, added to adjuvants, or combined together. Standard of care approaches such as tumor ablation, certain chemotherapies, and radiation can also have vaccine-like effects, promoting tumor specific immunity.[15] They do this by increasing the expression of tumor antigens within the tumor or causing the release of antigens from dying tumor cells and by promoting antitumor immunity for therapeutic benefit.[16] Figure 1 is reprinted from ref 15 with permission. Copyright 2015 BMJ.

B. Peptide-based vaccines

The vast majority of pre-clinical and clinical vaccination studies involving peptide-based vaccines have employed formulations comprising short peptides that match the exact, minimal sequences of major histocompatibility complex (MHC) class I-binding CD8+ T cell (CTL) epitopes.[17,18,19] The immunogenic peptides have been delivered in a variety of adjuvant formulations (including cytokines and toll-like receptor (TLR) ligands) to promote *in vivo* presentation by endogenous APCs. Candidate peptide epitopes are tested experimentally for those that bind commonly expressed HLA molecules and are naturally processed and presented by tumor cells. These peptides have been shown to be the most immunogenic, since they are capable of activating CD8+ cells.

A benefit of peptide based vaccine approaches is that nine to ten amino acid peptides are simple and cheap to manufacture. However, people who do not express common HLA types cannot be treated with this type of vaccine, because of HLA restriction. In addition, they can bind exogenously to all cells that express MHC-I, including T cells and B cells.[20] Without proper co-stimulatory molecule expression, the peptides are capable of causing exhausting of CTL and tolerance of the immunizing antigens rather than immuity.[17, 21,22] Therefore, longer peptides of 25–35 amino acids in length, called synthetic long peptides (SLP) have been developed. Such SLP covering the entire sequence of the native protein Ag to which an immune response is targeted, require internalization and processing by dendritic cell (DC), therefore induce a robust therapeutic T-cell response.[23,24] An additional advantage of SLP based vaccines is the increased duration of *in vivo* epitope presentation from $CD11c^{+}$ DC in the lymph node draining the vaccination site.[20]

However, there are still limitations to peptide based vaccine approaches which stems from the concept of "tumor escape". Tumor cells can undergo antigenic variations or lose the expression of immunogenic antigens and/or HLA molecules, thereby avoiding recognition by the immune system (cancer immunoediting).[25] Thus, antigen-negative tumor variants will be positively selected under the pressure of T cells targeting antigen positive cells. To overcome cancer immunoediting, current immunotherapeutic strategies involve simultaneous immunization with multiple peptide antigens. A Phase 2 multi-peptide vaccine IMA901 trial with metastatic renal cell carcinoma (RCC) patients has been recently reported by Walter *et al*.[10] The IMA901 trial is the first therapeutic vaccine for renal cell cancer (RCC) consisting of multiple tumor-associated peptides (TUMAPs) confirmed to be naturally present in human cancer tissue.[10] The randomized phase 2 trial confirmed that immune responses to multiple TUMAPs were associated with longer overall survival.[10]

C. Therapeutic vaccination via DCs.

a. Antigen-loaded dendritic cells

Upon differentiation from common myeloid bone marrow progenitors, DCs migrate to tissues in an immature state. In response to microbial and endogenous stimuli, immature DCs (iDCs) undergo a significant functional shift as they mature. The mature DCs bear MHC class II molecules (mDCs) and upregulate co-stimulatory molecules such as CD40, CD70, CD86 and the tumor necrosis factor (ligand) superfamily member 4 (TNFSF4, best known as OX40L) on the cell surface.[26, 27] The mDCs also express chemokine receptors, such as chemokine (C-C motif) receptor 7 (CCR7), that allow them to

efficiently migrate to lymph nodes[28] and secrete increased quantities of cytokines and chemokines.[29] Therefore, mDCs acquire a robust capacity to elicit adaptive immunity.

Vaccination strategies involving DCs which are often called 'nature's adjuvants' have been developed owing to their properties in coordinating innate (antigen-nonspecific) and adaptive immune responses (antigen-specific).[30] The aim of DC vaccination is to induce tumor-specific effector T cells that can reduce tumor mass and can induce immunological memory to control tumor relapse. DCs derived from patients that have been dosed with an adjuvant (that induces DC maturation) can be cultured *ex vivo* and then re-injected back into the patients.[26] The main DC-based anticancer interventions involve: (1) intratumoral administration of *ex vivo*-generated, gene-modified murine bone marrow-derived dendritic cells (DC);[31,32] (2) DCs co-cultured with one or more TAAs *ex vivo*;[33,34] (3) strategies that allow for the loading of DCs with TAAs *in vivo*;[35,36] and (4) DC-derived exosomes.[37,38,39]

In 2010, the first DC based "cancer vaccine" (sipuleucel-T, also known as Provenge) was approved by the US Food and Drug Administration (FDA) for use in humans for the treatment of certain types of prostate cancer.[9] The vaccine consists of dendritic cells loaded with prostate acid phosphatase as a tumor associated antigen that is fused to granulocyte-macrophage colony-stimulating factor, an immune-cell activator. In a Phase III trial, the protein fusion based vaccine has been shown to prolong by a median of 4-months the life of patients with hormone-resistant prostate cancer.[9] The studies involving *ex vivo* generated DC‑based vaccines are summarized in **Table 1**.

Antigens can be directly delivered to DCs *in vivo* using chimeric proteins that are comprised of an antibody that is specific for a DC receptor fused to a selected antigen.

Specific targeting of antigens to DCs *in vivo* has been shown to elicit potent antigen-specific CD4+ and CD8+ T cell-mediated immunity.[35,40,41] To target antigens to dendritic cells, the Steinman group incorporated ovalbumin protein into an anti-DEC-205 mAb.[40] DEC-205 is an endocytic receptor that is abundant on DC cells in lymphoid tissues. Receptor-mediated presentation of peptides was shown to be more efficient at inducing T-cell division than unconjugated OVA.[40] However, the activated T cells were then deleted and the mice became specifically unresponsive to rechallenge with OVA in complete Freund's adjuvant.[40] Simultaneously, they injected agonistic anti-CD40 antibody, which has been shown to induce the maturation of DCs.[40] They demonstrated that the DEC-205 antigen conjugates initiated immunity from the naive CD4+ and CD8+ T cell repertoire.[40] The mice immunized with the DEC-205 antigen conjugates were shown to have enhanced resistance to an established rapidly growing tumor and to viral infection at a mucosal site.

D. Immunotherapeutic whole-cell

The use of vaccines consisting of irradiated, whole tumor-cell preparations might induce the most effective tumor-specific CD4+ and CD8+ T-cell responses by providing the immune system with the opportunity to react to multiple TAAs.[42] Earlier strategies included the use of irradiated, autologous tumor cells.[42] The potential limitations of this approach encompass the difficulties associated with obtaining patient-specific cells in large amounts and concerns about reproducibly generating vaccine preparations free of contaminants.

Table 1. Examples of clinical trials testing vaccination with *ex vivo* DCs. [30]

Vaccine and antigen	**Indication**
GM-CSF–IL-4 DCs with or without HLA-A*0201- restricted peptides or peptides alone	Metastatic prostate cancer
GM-CSF–IL-4 DCs with peptides, tumor lysates or autologous tumor-eluted peptides	Stage IV melanoma, renal cell carcinoma and malignant glioma
FLT3 ligand-expanded blood DCs and altered peptides	Advanced CEA^+ cancer
GM-CSF–IL-4 DCs and tumor lysates	Refractory paediatric solid tumors
DCs loaded with autologous tumor RNA	Colon cancer
DCs loaded with killed allogeneic tumor cells	Stage IV melanoma
Monocyte-derived DCs loaded with the NKT cell ligand α-galactosylceramide	Advanced cancer
Comparative study of $CD34^+$ HPC-derived Langerhans cells versus monocyte-derived DCs	Melanoma

CEA, carcinoembryonic antigen; DC, dendritic cell; IL-4, interleukin-4; GM-CSF, granulocyte–macrophage colony-stimulating factor; HLA, human leukocyte antigen; HPC, haematopoietic progenitor cell; NK cell, natural killer cell.

Table adapted from Palucka *et al.*[30]

An irradiated, syngeneic, granulocyte-macrophage colony-stimulating factor (GM-CSF)-expressing tumor-cell vaccine (Gvax) has been shown to induce dense intratumoral infiltrates of APCs displaying superior antigen-presenting activity.[8] These APCs (mainly activated dendritic cells) efficiently process dying tumor cells and traffic to lymph nodes, where they prime tumor-specific T cells, generating a potent and sustained antitumor immune response.[8] An allogeneic variant of Gvax derived from tumor cell lines, which were originally derived from lymph node (LNCaP) and bone (PC-3) metastases, has been tested in both pancreatic cancer and hormone-resistant prostate cancer patients and is still under clinical investigation.[43,44,45] The allogeneic variant of Gvax vaccine approach seems to be nontoxic and can induce dose-dependent systemic antitumor immunity.[43,44,45]

E. Endogenous vaccination

Classical cancer chemotherapies seem to not only kill tumor cells but also induce immune response. For example, cytotoxic treatment such as anthracyclines, oxaliplatin, and γ-radiation induce tumor cells to undergo apoptosis, which is associated with cell surface exposure of a protein that is normally found in the lumen of the endoplasmic reticulum (ER), namely the Ca^{2+}-binding chaperone calreticulin (CRT).[46,47] When elicited by cytotoxic treatments, the CRT exposure pathway is turned on, resulting in CRT translocation from the ER onto the plasma membrane surface and apoptotic cancer cell death. Dendritic cells (DCs) might capture those apoptotic bodies of tumor cells that have expression of CRT on their surface and thus might elicit tumor-specific CD8+ T cell-mediated immune responses, which then would seek out residual tumor cells.[46,47]

II. T-cell-based Immunotherapy

T-lymphocytes are multi-functional effector cells that circulate through the bloodstream to detect and destroy diseased cells. Tumor cells process and present antigenic peptides as major histocompatibility complexes (MHC) on their surface. Upon T cell receptor (TCR) recognition of a peptide-MHC complex (pMHC) displayed on tumor cell surface, the response of the T cells is initiated. T-cell-based immunotherapies include adoptive cell transfer of tumor-infiltrating lymphocytes,[48] genetically engineered T cells,[49] bispecific antibodies[50] and immune checkpoint inhibitor antibodies (**Figure 2**).[51]

A. Adoptive transfer of tumor infiltration lymphocytes (TILs)

The World Health Organization (WHO) estimates that worldwide there are 66,000 deaths annually from skin cancer, with approximately 80% due to melanoma. The median survival of patients with melanoma who have distant metastases (American Joint Committee on Cancer stage IV) is less than 1 year.[52] Tumor-infiltration lymphocytes are a heterogeneous cell population found within tumor lesions and mainly consist of T cells. Adoptive T-Cell Therapy was firstly described in 1988 for treatment of patients of metastatic melanomas.[53] However, these cells were unable to persist and proliferate *in vivo*, despite simultaneous administration of the T-cell growth factor, IL-2. Following lymphodepleting by chemotherapy with drugs such as cyclophosphamide and fludarabine and with or without total-body irradiation (TBI), this approach was significantly improved.[54] Fifty percent of patients with metastatic melanoma refractory to all other treatments experienced durable responses regardless of the organ site, including the brain.[48] Among patients who achieved a complete tumor regression (22 out of 93

Figure 2. Strategies for use of T-cell therapies for cancer. [55]

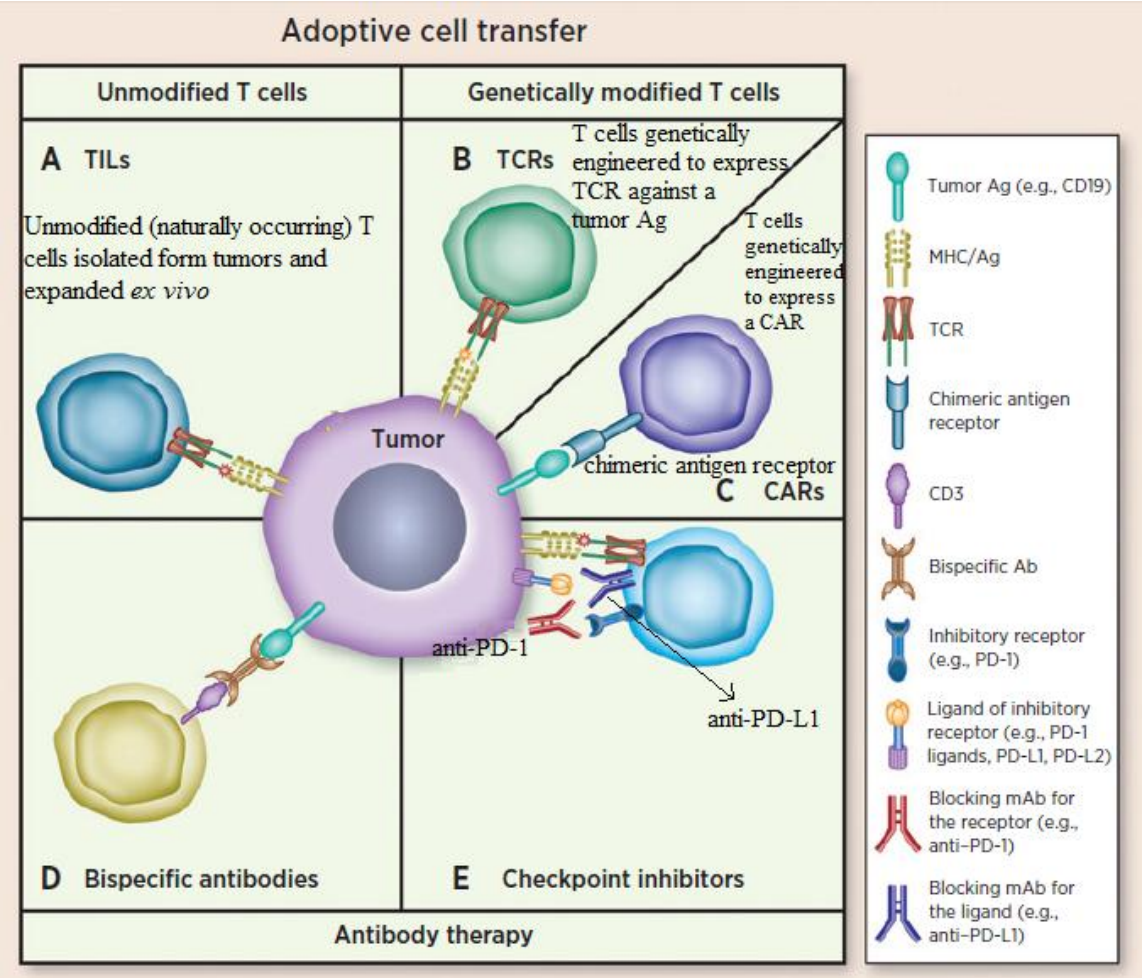

Anticancer T-cell-based therapy can be performed (A, B, C) by *ex vivo* manipulation of T cells through Adoptive Cell Transfer (ACT) of unmodified (TILs) or genetically modified T cells (TCRs, CARs) and (D, E) by *in vivo* manipulation of T cells using antibodies (bispecific and checkpoint inhibitors). These approaches may induce monoclonal (TCRs, CARs, bispecific antibodies) or polyclonal (TILs, checkpoint inhibitors) antitumor T cells. Ag, antigen. Figure adapted from Houot *et al.* [55]

patients), 19 patients have ongoing complete regressions beyond 5 years and may be cured, indicating expansion and persistence of polyclonal antitumor T cells.[48]

However, the major limitation of this approach is that the process to prepare TILs is laborious and expensive. The tumor needs to be resected for TILs isolation. The patient needs to tolerate lymphodepletion and high dose IL-2 infusion. Another critical factor has been the ability to generate TILs in a short period of time so that the TILs can be expanded to sufficient numbers to be administered to patients before their disease progresses. Most importantly, this approach seems to be primarily effective for the treatment of melanoma, possibly due to high expression of immunogenic mutational epitopes due to the high frequency of somatic mutations found for melanoma.[56] Therefore, the large numbers of melanoma infiltrating T cells possess specific cytolysis against the tumors.[57]

Adoptive T therapy has also been an attractive strategy for the treatment and prevention of Epstein-Barr virus (EBV)-associated lymphoproliferative disease occurring after haemopoietic stem-cell transplant or solid organ transplantation, which is a potentially life threatening condition.[58] EPV mainly infects B-cells resulting in the expression of viral latency-associated proteins, which could be targeted by T cells. EBV-specific cytotoxic T lymphocytes (EBV-CTL) have been isolated and successfully used to treat post-transplant lymphoproliferative diseases (PTLD).[58] In addition, autologous EBV–specific T cells have been shown to induce durable complete responses without significant toxicity in EBV-associated tumors such as nasopharyngeal carcinoma[59] and Hodgkin disease. Approximately 40% of patients with Hodgkin or non-Hodgkin

lymphoma express the type II latency Epstein-Barr virus (EBV) antigens latent membrane protein.[60]

B. Genetically modified T cells (TCRs, CARs)

The major limitations of TILs therapy include the requirement that patients have preexisting tumor-reactive cells that can be expanded *ex vivo*. The difficulty in identifying antigen-specific T cells in the cancer types other than melanoma and the complex T cells preparation process starting from surgical resection for TILs isolation and consistent active T cells generation and expansion to preserve anti-tumor function are significant hurdles to their broad application. Recent studies have demonstrated that patients' peripheral blood lymphocytes can be genetically engineered to recognize tumor-associated antigens.[61] The modified lymphocytes have been shown to mediate cancer regression *in vivo*, thus potentially enhancing and extending ACT to patients with a wide variety of cancer types. Genetically modified T cells (TCRs or CARs) are transfected using virus vectors (retroviruses or lentiviruses) or a transposon system (Sleeping Beauty). Following transfection, genetically modified T cells are expanded and transferred into patients who have undergone lymphodepletion similar to the protocols used for TILs.

a. TCRs

The T cell receptor (TCR) is composed of the TCR alpha and beta chains and recognizes Tumor-associated antigens (TAAs) when they were presented as peptides by the major histocompatibility complex proteins, MHC I and MHC II. While MHC II is largely associated with the recognition of bacterial antigens, MHC I is associated with the recognition of viral and tumor associated antigens. The first report of investigating

genetically engineered peripheral blood lymphocytes (PBLs) was described by the Rosenberg group in 2006.[61] Objective regression of metastatic melanoma lesions was observed after the administration of autologous TCRs specific for MART1.[61] Since these early results, TCRs specific to other antigens, including NY-ESO-1[62] and MAGE-A3[63] in melanoma and synovial sarcoma, gp100 in melanoma[64] and carcinoembryonic antigen (CEA) in colorectal cancer[65], have been investigated.

The major obstacle to the widespread application of TCRs therapy has been the observation of on or off target toxicity.[64] Antigens such as MART1 and gp100 are expressed by normal melanocytes present in the skin, retina, and inner ear. TCR gene therapy against MART1 and gp100 resulted in skin rash characterized by a dense infiltrate of CD3+ T lymphocytes, predominantly CD8+, uveitis (cellular infiltrate of the eye), and hearing loss.[64] Dose-limiting inflammatory colitis was observed in patients treated with CEA TCRs with colorectal adenocarcinoma due to the expression of CEA on normal epithelial cells throughout the gastrointestinal tract.[65] In addition, patients with myeloma and melanoma, experienced off-target and organ-specific toxicities when treated with MAGE-A3-specific TCRs. They developed cardiogenic shock and died within a few days of T-cell infusion due to recognition of the unrelated cardiac peptide antigen titin.[66]

b. Chimeric antigen receptors (CARs) for T cell immunotherapy

Chimeric antigen receptors (CAR) are recombinant receptors that provide both antigen-binding and T-cell-activating functions. CARs are modular polypeptides typically consisting of three distinct modules: an extracellular target-binding module, a transmembrane module anchoring the CAR into the cell membrane, and an intracellular

signaling module (**Figure 3**).[67] The extracellular target binding module is usually derived from a recombinantly derived single chain antibody (scFv) and linked through a polypeptide sequence to a transmembrane module. The transmembrane modules are usually costimulatory domains derived from CD8 and CD4 coreceptor molecules.[68] The major advantage of CAR-based strategies is that the target-binding scFv is derived from antibodies with affinities several orders of magnitude higher than TCRs. In principle, any tumor cell surface antigen could be targeted by a CAR, therefore overriding MHC restriction, and tolerance to self-antigens.[69] Therefore, CARs are more broadly applicable to patient populations with a diverse expression of MHCs, otherwise known as HLAs.[68] In addition, CARs not only have the ability to recognize proteins but also carbohydrate and glycolipid structures, again expanding the range of potential targets.[70,71] The antigens targeted to date by CARs are summarized in **Table 2** and **Table 3**.

Results from early studies in adoptive T cell therapy required transferring large numbers of effector T cells, which were found to be unable to expand in the patient to a sufficient degree in order to achieve an effector-to-target ratio *in vivo* necessary to eradicate advanced cancers. In contrast, recent results from trials with engineered T cells have shown that the infusion of small numbers of cells may suffice since T cell expansion can occur in the host once they are engaged with the target tumor. The protocol of chimeric antigen receptor (CAR) therapy is shown in **Figure 4**.

Figure 3. Antibodies can bind to surface antigens expressed on tumor cells. [67]

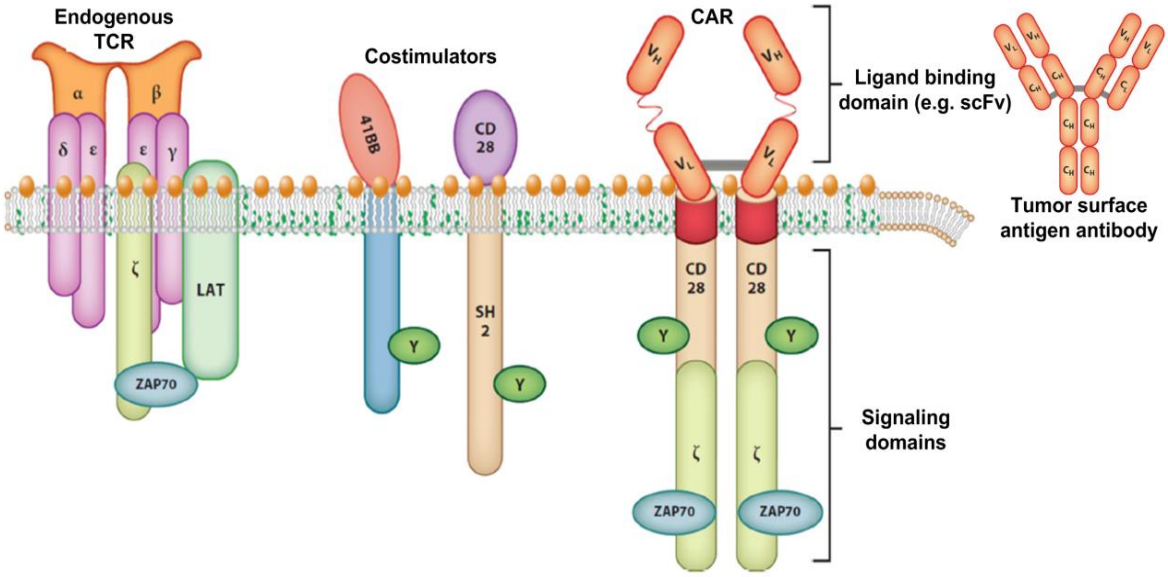

Chimeric antigen receptors (CARs) have a single-chain antibody fragment (scFv), expressed in tandem with signaling elements derived from the T cell receptor (TCR) and costimulatory domains such as 4-1BB or CD28. Figure adapted from Barrett *et al*.[67]

Figure 4. Chimeric antigen receptor (CAR) therapy procedure. [67]

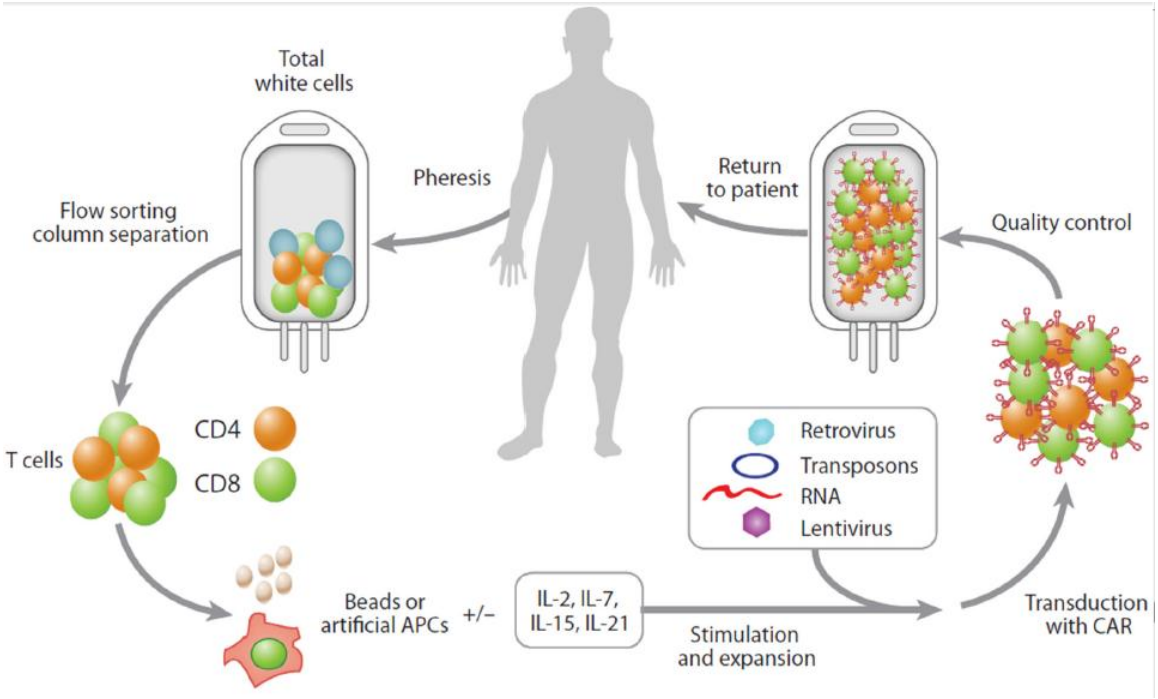

Chimeric antigen receptor (CAR) therapy is similar to an autologous bone marrow transplantation procedure. T cells are collected from the patient by apheresis, and the T cells are expanded and genetically modified using several approaches before they are returned to the patient. Abbreviation: APCs, antigen-presenting cells.[67] Figure 4 is reprinted from ref 67 with permission. Copyright 2014 Annual Reviews.

Table 2. Classification of antigenic targets for engineered T cells. [67]

Overexpressed self-antigens	mesothelin	pancreatic cancer
	PSA	prostate cancer
	c-erbB2	breast cancer
Cancer-testes (germ cell) antigens	NY-ESO-1, MAGE	myeloma, melanoma
mutational antigens	$BRAF_{V600E}$ mutations	melanoma
	BCR-ABL translocations	leukemia
Viral antigens	EBV	Hodgkin lymphoma
	HPV	cervical cancer
	polyomavirus	Merkel cancer

Table adapted from Barrett *et al*. [67]

Table 3. Antigens targeted by CARs. [68]

Target antigen	Associated malignancy	Receptor type (other specificity)	*In vivo* studies
α-Folate receptor	Ovarian cancer	scFv-FcεRIγ	Phase I
	Epithelial cancers	scFv-41BB-CD3-ζ	+
CAIX	Renal cell carcinoma	scFv-CD4- FcεRIγ	Phase I
	Renal cell carcinoma	G250-FcεRIγ	–
CD19	B-cell malignancies	scFv-CD3-ζ (EBV)	–
	B-cell malignancies	scFv-CD3-ζ	+
	B cell malignancies	scFv-CD28-CD3-ζ	+
	Refractory follicular lymphoma	scFv-CD3-ζ	Phase I
	B-cell malignancies	scFv-CD28-CD3-ζ	+
	ALL	scFv-41BB-CD3-ζ	–
	ALL	scFv-41BB-CD3-ζ	+
	B-cell malignancies	scFv-CD3-ζ (Influenza MP-1)	+
	B-cell malignancies	scFv-CD3-ζ (VZV)	–
	ALL	FMC63-CD28-41BB-CD3-ζ	+,–
	B-cell malignancies	FMC63-41BB-CD3-ζ	+
	Follicular lymphoma	FMC63-CD28-CD3-ζ	NCT00924326
	B-cell malignancies	FMC63-CD28-CD3-ζ	NCT00924326
	CLL and ALL	SJ25C1-CD28-CD3-ζ	(NCT00466531 NCT01044069)
	CLL	FMC63-41BB-CD3-ζ	NCT01029366
	Lymphoma	scFv-CD3-ζ + scFv-CD28-CD3-ζ	Phase I
CD20	Lymphomas	scFv-CD28-CD3-ζ	–
	B-cell malignancies	scFv-CD4-CD3-ζ	–
	B-cell lymphomas	scFv-CD3-ζ	–
	Mantle cell lymphoma and indolent B-cell lymphomas	scFv-CD28-41BB-CD3-ζ	NCT00621452
CD22	B-cell malignancies	scFV-CD4-CD3-ζ	–
CD23	CLL	scFv-CD28-CD3-ζ	+
CD24	Pancreatic adenocarcinoma	scFv- CD28-FcεRIγ	+
CD30	Lymphomas	scFv-FcεRIγ	–
	Hodgkin lymphoma	scFv-CD3-ζ (EBV)	+
		scFv-CD28-CD3-ζ (EBV)	+
CD33	AML	scFv-CD28-CD3-ζ	–
		cFv-41BB-CD3-ζ	
		scFv-CD28-CD3-ζ (EBV)	+
CD38	Non-Hodgkin lymphoma	scFv-41BB-CD3-ζ	+
CD44v7/8	Cervical carcinoma	scFv-CD8-CD3-ζ	+
CEA	Colorectal cancer	scFv-CD3-ζ	+
		scFv-FcεRIγ	+
		scFv-CD3ε	–
		scFv-CD28-CD3-ζ	–
		scFv-CD28-CD3-ζ	+
EGFRvIII	Glioblastoma	scFv-CD28-41BB-CD3-ζ	NCT01454596
EGP-2	Multiple malignancies	scFv-CD3-ζ	–
		scFv-FcεRIγ	–
EGP-40	Colorectal cancer	scFv-FcεRIγ	–
EphA2	Glioblastoma	scFv-CD28-CD3-ζ	+
Erb-B2	Breast cancer and others	scFv-CD28-CD3-ζ	+
		scFv-CD28-CD3-ζ (Influenza)	+
		scFv-CD28mut.-CD3-ζ	+
	Prostate cancer, colon cancer	scFv-FcεRIγ	+
	Various tumors	scFv-CD28-41BB- CD3-ζ	+

Target antigen	Associated malignancy	Receptor type (other specificity)	*In vivo* studies
Erb-B 2,3,4	Breast cancer and others	Heregulin-CD3-ζ	–
		scFv-CD3-ζ	+
FBP	Ovarian cancer	scFv-FcεRIγ	+
	Ovarian cancer	scFv-FcεRIγ (alloantigen)	+
Fetal acethylcholine receptor	Rhabdomyosarcoma	scFv-CD3-ζ	–
G_{D2}	Neuroblastoma, melanoma	scFv-CD3-ζ	–
		scFv-CD3-ζ	NCT00085930
		scFv-CD28-OX40-CD3-ζ	–, +
		scFv-CD3-ζ (VZV)	–
	Ewing sarcoma	scFv-CD28-CD3-ζ	+
G_{D3}	Melanoma	scFv-CD3-ζ, ScFv-CD3ε	–
		scFv-CD28-CD3-ζ	+
HER2	Medulloblastoma	scFv-CD3-ζ	+
		scFv-CD28-CD3-ζ	+
	Pancreatic adenocarcinoma	scFv-CD28-41BB-CD3-ζ	+
	Glioblastoma		Phase I
	Osteosarcoma	scFv-CD28-CD3-ζ	+
	Ovarian cancer	scFv-CD28-CD3-ζ	+
HMW-MAA	Melanoma	scFv-CD3-ζ, ScFv-CD28-CD3-ζ	–
IL-11Rα	Osteosarcoma	scFv-CD28-CD3-ζ	+
IL-13Rα2	Glioma	IL-13-CD28-4-1BB-CD3-ζ	+
	Glioblastoma	IL-13-CD3-ζ	+
	Medulloblastoma	IL-13-CD3-ζ	+
KDR	Tumor neovasculature	scFv-FcεRIγ	–
κ-light chain	B-cell malignancies (B-NHL, CLL)	scFv-CD3-ζ	+
		scFv-CD28-CD3-ζ	+
Lewis Y	Various carcinomas	scFv-FcεRIγ	–
	Epithelial-derived tumors	scFv-CD28-CD3-ζ	+
L1-cell adhesion molecule	Neuroblastoma	scFv-CD3-ζ	Phase I
MAGE-A1	Melanoma	scFV-CD4-FcεRIγ	–
		scFV-CD28-FcεRIγ	
Mesothelin	Mesothelioma	scFv-41BB-CD3-ζ	+
Murine CMV infected cells	Murine CMV	Ly49H-CD3-ζ	+
MUC1	Breast and ovarian cancer	scFV-CD28-OX40-CD3-ζ	+
MUC16	Ovarian cancer	scFV-CD28-CD3-ζ	
NKG2D Ligands	Myeloma, ovarian, and other tumors	NKG2D-CD3-ζ	+
NY-ESO-1 (157–165)	Multiple myeloma	scFv-CD28-CD3-ζ	+
Oncofetal antigen (h5T4)	Various tumors	scFV-CD3-ζ (vaccination)	+
PSCA	Prostate carcinoma	7F5-β2-CD3-ζ	–
		scFv-CD3-ζ	
PSMA	Prostate cancer/tumor vasculature	scFv-CD3-ζ	+
	Prostate/tumor vasculature	scFv-CD28-CD3-ζ	–
		scFv-CD3-ζ	+
ROR1	B-CLL and mantle cell lymphoma	scFv-CD28-CD3-ζ	+
Targeting via mAb IgE	Various tumors	FcεRI-CD28-CD3-ζ	+
TAG-72	Adenocarcinomas	scFv-CD3-ζ	+
VEGF-R2	Tumor neovasculature	scFv-CD3-ζ	–
Biotinylated molecules	Various tumors, ovarian cancer	BBIR-z/CD28z	+

Table adapted from Sadelain *et al*. Table 3 is reprinted from ref 68 with permission. Copyright 2013 AACR.[68]

Approaches for T cell engineering

For lymphocyte-based therapies, chromosome-integrating vectors derived from gamma retroviruses or lentiviruses have been most useful for long-term gene expression, Foamy virus vectors derived from the Spumavirus genus of retroviruses, have advantages over gammaretroviruses and lentiviruses, because of being non-pathogenic in non-human primates and humans. These vectors may be the safest of the integrating viral approaches. Ongoing clinical trials will determine their potential toxicity and efficacy.[72,73]

For non-virus-based approaches without the use of an integrating vector system, RNA-based electroporation of lymphocytes with *in vitro* transcribed mRNA results in the transient expression of proteins. CAR expression and function of RNA-electroporated T cells could be detected up to a week after electroporation.[74] Multiple, more frequent injections of RNA CAR–electroporated T cells mediated regression of large vascularized flank mesothelioma tumors in mice.[74] This approach may genetic modify T cells without the safety concerns posed by viral vector genomic integration. Another non-virus-based approach is the use of transposon-based systems, which can integrate transgenes more efficiently than plasmids that do not contain an integrating element. Transposons are most commonly introduced into cells by electroporation or lipofection and in the presence of transposase enzymes. For example, the Sleeping Beauty (SB) transposon system is a non-viral DNA delivery system in which a transposase directs integration of an SB transposon into the genome at 5'-TA-3' sequences.[49,75]

Ligand binding domains

The extracellular domains that bind to antigen are classified into three general categories: (i) single-chain variable fragments (scFvs) derived from antibodies; (ii)

fragment antigen-binding domains (Fabs) selected from libraries; or (iii) nature ligands that engage their cognate receptor (**Table 3**). Most commonly used ligands are scFvs derived from murine immunoglobulins, since they encoded by a single contiguous recombinant gene typically derived from either a well-characterized monoclonal antibody or selected by phage display libraries.[76] Immunogenicity issues are a concern for mouse monoclonal based antibodies and libraries, however, the extensive development of humanization methodologies and human antibody based libraries has provided workable solutions to this important problem.[77]

The position of the epitope and its distance to the target cell surface are expected to affect the binding to the antigen and the optimal formation of T-cell target conjugates and synapses.[78,79] It has recently been shown that that CARs exhibit diminished signaling efficiency as the distance of the epitope from the target cell membrane increases. James *et al* constructed two CD22-specific CARs by the genetic modification of CTL.[78] One CAR contains an engineered scFv that binds to the first Ig-like domain of the CD22 molecule (far from the cell membrane), whereas the second CAR was constructed with a scFv, which is situated closer to the cell surface. Diminished Ag sensitivity was observed when targeting membrane-distal epitopes. However, lower Ag sensitivity can be an advantage and allow discrimination between targets with differing levels of Ag expression. Consequently, the anti-CD22 CARs are highly cytotoxic to B cell lymphoma lines expressing high levels of CD22, but have minimal lytic activity against autologous normal B cells, which express lower levels of CD22.[78]

CAR signaling

Chimeric fusion receptors were shown to have T cell-activating potential with different fusion combinations between CD3-ζ or Fc receptor γ and CD8, CD4, CD25 or CD16. [80] The T cell antigen receptor (TCR) is a complex, multi-chains structure composed of an antigen binding heterodimer (α/β) and three conserved signal transducing modules: CD3-ε/γ and CD3-ε/δ heterodimers and a TCR-ζ homodimer.[81] Irving *et al* constructed a chimeric protein linking the extracellular and transmembrane domains of CD8 to the cytoplasmic domain of the ζ chain and found that the CD8/ ζ chimera can be expressed in the absence of CD3 γ, δ,and ε, and is capable of generating inositol trisphosphate, tyrosine phosphorylation, release of interleukin-2, and expression of CD69 in response of antibody crosslinking stimuli.[80]

The ζ chain of TCR is a dimeric transmembrane protein that triggers T cell effector function when aggregated by extracellular stimuli, with a very short extracellular domain and an extended cytoplasmic tail.[82] Protein chimeras were prepared by Romeo *et al*, in which the extracellular domain of CD4 is fused to the transmembrane and the intracellular domains of the TCR and IgG Fc receptor signal transducing elements. CTLs expressing the CD4/ζ or CD4/Fcγ show potent MHC-independent destruction of cellular targets expressing HIV envelope proteins gp120.[83] Like ζ, the Fc receptor-associated γ chain is associated with other polypeptides for mediating ligand recognition or other undefined functions. γ bears a homodimeric structure and has an overall organization very similar to that of ζ and is a component of monocytes/macrophages, dendritic cells (DCs) and NK cells. Activating hFcγRI and hFcγRIIIA requires the association of the FcRγ subunit (F*cer1g*) to be expressed and functional at the cell surface. hFcγRI (CD64)

is restricted by monocytes/macrophages and dendritic cells (DCs) and, inducibly expressed on neutrophils and mast cells. hFcγRIIIA (CD16A) is a low affinity IgG Fc receptors, expressed on NK cells and monocytes/macrophages.[84] Romeo *et al* further supported the role of CD3 ζ or FcRγ in facilitating the coupling of the TCR to intracellular signal transduction.[83] As an extension of this work, Letourneur *et al* constructed chimeric proteins consisting of the extracellular domain of the α chain of the interleukin 2 receptor (CD25) and the cytoplasmic domain of either ζ or FcRγ to activate cells when expressed in either T cells or rat basophilic leukemia cells.[85]

Although the signaling delivered by the CD3-ζ CARs cytoplasmic domain is well suited for activating cytolytic stimulus, the optimal activation of T cells requires the engagement of one or more co-stimulatory receptors (signal 2).[86] The best characterized co-stimulatory molecule is CD28.[87,88] In the absence of CD28 signaling, CD3-ζ CARs can result in a very poor T-cell proliferative response or in the induction of anergy or apoptosis.[87] For example, CD3-ζ CARs against prostate-specific membrane antigen (PSMA, a cell-surface glycoprotein expressed on prostate cancer cells and the neovascular endothelium of multiple carcinomas) failed to elicit a robust and sustained cytokine response, including interleukin-2, and support T cell expansion upon repeated exposure to antigen in the absence of costimulatory signal CD28.[89,88] Other cytoplasmic domains of a costimulatory receptors such as 4-1BB, DAP10, OX40 or ICOS have been also reported to construct the second generation of CARs (**Figure 5**).The dual-signaling CARs conferred enhanced signaling and persistence to T cells, which has been confirmed in patients treated with a mixture of T cells transduced with either a CD28/CD3ζ or CD3ζ-only CAR.[90]

Figure 5. Structure of first-generation to fourth-generation CARs.

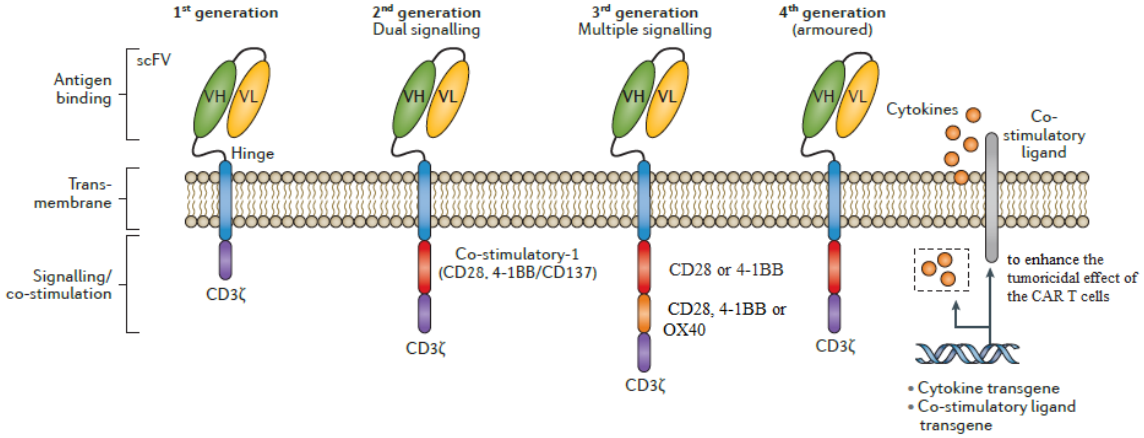

The first-generation CAR contains one intracellular CD3ζ signaling domain to allow for TCR signaling. The second-generation CARs have two intracellular signaling domains: a co-stimulatory domain comprising either a CD28 or a 4-1BB signaling domain, coupled with a CD3ζ signaling domain to enable T-cell activation and proliferation upon antigen recognition. The third-generation CARs have two co-stimulatory domains and a CD3ζ signaling domain. The first co-stimulatory domain is either a CD28 or a 4-1BB domain, with the second co-stimulatory domain consisting of either a CD28, a 4-1BB or a OX40 domain. Fourth-generation 'armoured CAR T cells' combine a second-generation CAR with the addition of various genes, including cytokine and co-stimulatory ligands. Figure adapted from Batlevi et al. [91]

Costimulatory ligands, chimeric costimulatory receptors and cytokines

Costimulatory support, such as costimulatory receptor ligands and cytokines, can be engineered into cells to modulate the function and/or survival of CAR-transduced T cells. The combination of CD80 and 4-1BBL has been shown to result in sustained *in vivo* T cell expansion and persistence, associated with the rejection of massive, established tumor burdens.[92] Several ligands for Ig super-family and TNF receptor family costimulatory receptor, including CD80, CD86, 4-1BBL, OX40L and CD70, have been shown to enhance T cell proliferation and cytokine secretion upon antigen engagement.[68] Both auto- and trans-costimulation have been shown to contribute to enhanced T cell activity in this context, which may enhance adoptive cell therapies utilizing CAR- or TCR-transduced T cells.

Another approach to enhance the potency of CAR-targeted T cells is to further genetically modify the T cells to secrete pro-inflammatory or pro-proliferative cytokines. Numerous cytokines profoundly affect T-cell development, differentiation, and homeostasis. IL-2, IL-7, IL-15, and IL-21 are members of a cytokine family whose heteromeric receptors share the common γ chain (γ_c). They are T-cell growth factors and can augment the T-cell antitumor immune response. Human primary T cells were genetically modified to recognize the CD19 antigen and overexpress a γ_c-cytokine. IL-7 and IL-21 were found to be superior to IL-2 and IL-15 in enhancing γ_c cytokine secretion and tumor rejection in a xenotransplant model of human CD19+ tumor.[93] In an immune competent syngeneic tumor model, CD19-specific CAR-T cells expressing IL-12 showed greater efficacy than CAR-modified T cells alone.[94] They are able to safely eradicate

established disease in the absence of prior cyclophosphamide conditioning and acquire intrinsic resistance to T regulatory cell-mediated inhibition.[94]

Clinical applications

Over the last decade, many groups have shown that CAR-T cells have potent anti-tumor effects against a variety of advanced hematologic malignancies of the B-cell lineage. The central issue facing the field is whether the technology can be extended to non-B cell derived malignancies, and in particular carcinomas. Solid tumors overall have less sensitivity to T cell mediated cytotoxicity and the microenvironment is usually immunosuppressive.[95] In addition, solid tumors tend to lack specific target antigens, thus identifying valid targets is an essential goal that requires further investigation.[95]

In terms of practical limitations, CAR-T based therapies are restricted to target cell surface antigens. Furthermore, since CARs are chimeric modular polypeptides contain unique junctional fragments, CAR-T cells have the potential to be targeted by a patient's humoral and cellular immune responses. For example, humoral immune responses have been shown to neutralize CAR–mediated T-cell function toward the renal cancer antigen, carbonic anhydrase IX (CAIX).[96] In rare instances, CAR-T cells can provoke anaphylaxis most likely by inducing an IgE antibody specific for the murine-based antibody sequences present in the CAR-modified T cell product.[97] Cellular immune responses have been shown to be directed to the complementarity-determining and framework regions of the CAR scFv.

The viral based methods for introducing the genes required to produce CAR-T cells have raised additional immunogenicity concerns. The retroviral transduction of T cells has been shown to introduce vector-derived immunogenic epitopes in to a patient's T

cells.[96] The herpes simplex virus thymidine kinase (HSV-TK) gene has been used most extensively in the clinic for regulating cell survival. The first study to administer HSV-TK-modified T cells to patients used a retrovirus (HyTK) that encodes hygromycin phosphotransferase (Hy) and HSV-TK to transduce autologous HIV gag-specific CD8+ T-cell clones that were infused into HIV-infected individuals to augment virus-specific immunity. The viral TK, in contrast to the mammalian TK, efficiently phosphorylates the nucleoside analogue ganciclovir, resulting in the formation of a toxic metabolite to mammalian cells. Therefore, ganciclovir can be administered to ablate the CAR-Ts if toxicity occurs after their infusion. However, rapid clearance of HyTK positive T cells after repeated infusions, and the elimination of T cells coincided with the induction of CD8+ cytotoxic T lymphocyte (CTL) responses directed against Hy and HSV-TK derived protein.[98]

CAR Safety

The immune-mediated rejection of normal tissues that express the targeted antigen is referred to as an "on-target, off-tumor" response. Other than "on-target, off-tumor" responses similarly observed for TCR therapy, anti-tumor responses mediated by a large number of activated T cells has the potential to initiate cytokine storms syndrome (CSS), which is characterized by high fever, hypotension and organ failure. The use of steroids, vasopressors and/or supportive therapy delivered in the intensive care unit has been used to clinically manage this highly deleterious and potentially life threatening response. Grupp and colleagues have observed that IL-6 blockade utilizing Tocilizumab may be effective in steroid-refractory circumstances, without compromising T cell efficacy.[99] Unlike many conventional drug-induced side effects, CSS cannot be controlled by simply

reducing drug dosage, as proliferating T cells will increase in numbers and eventually reach critical levels where a synchronous cytokine response may exceed patient tolerability. Split T cell dosing or short-lived T cells may partially reduce this effect, but more fundamental solutions are needed to reduce and ideally prevent the side effects associated with the large scale activation of T-cells.

C. Checkpoint blockade

A crucial breakthrough in cancer immunotherapy came in 1996, when James Allison, an immunologist at MD Anderson Cancer Center, and his colleagues showed that it was possible to amplify anti-cancer immunity by taking the brakes off a molecular checkpoint that would otherwise dampen the immune response.[51] Apart from the well-documented inhibitory cells including regulatory T cells (Tregs) and myeloid-derived suppressor cells (MDSC) that are upregulated in the tumor microenvironment, T cells have intrinsic regulatory mechanisms that negatively regulate their effector function. Activated T cells upregulate surface inhibitory receptors including cytotoxic T-lymphocyte-associated protein 4 (CTLA-4) and programmed death ligand 1 (PD-1). Upon binding to their respective ligands, these molecules transmit inhibitory signals to T cells and attenuate T-cell activation. The immune system relies on these checkpoints to regulate inflammation and limit the risk of autoimmune disease. Many tumor types can circumvent T-cell-mediated destruction by taking advantage of these inhibitory pathways. Blocking antibodies disrupting these receptor-ligand interactions can enable enhanced T-cell-mediated antitumor activity (**Figure 6**). This approach to immune therapy is referred to as checkpoint blockade. Unlike adoptive T-cell therapy, which relies upon the presence of cancer-specific antigens and requires *ex vivo* manipulations, checkpoint blockade is not

tumor specific and can be used as an off-the-shelf monoclonal antibody to treat a spectrum of malignancies.

a. CTLA-4 blockade

The coinhibitory receptor cytotoxic T-lymphocyte-associated antigen 4 (CTLA-4; also known as CD152) predominantly regulates T cells at the stage of initial activation (approximately 48 hours after T-cell activation) by competing with the CD28 costimulatory receptor for binding to CD80 (B7-1) and CD86 (B7-2), which are typically expressed by antigen-presenting cells such as dendritic cells. Since CTLA4 has a much higher overall affinity for CD80 and CD86, CTLA4 expression on the surface of T cells has been proposed as a method of dampening the activation of T cells by outcompeting CD28 for CD80 and CD86.

CTLA-4 binding to CD80 and CD86 has been shown to deliver inhibitory signals to the T cell, thus reducing T-cell activation. CTLA-4 was found to increase T cell motility and override the T cell receptor (TCR)-induced stop signal required for stable conjugate formation between T cells and antigen-presenting cells.[100] Moreover, accumulation of CTLA-4 at the immunological synapse appears to be proportional to the strength of the TCR signal, suggesting that cells receiving stronger stimuli are more susceptible to CTLA-4-mediated inhibition.[101]

CTLA-4 signaling has also been shown to reduce the production of both the growth factor IL-2 and cyclin D3, cyclin-dependent kinase (cdk)4, and cdk6, thus restricting T cell expansion.[102,103,104] The possibility is raised that blockade of inhibitory signals delivered by CTLA-4-B7 interactions might augment T cell responses to tumor cells and enhance antitumor immunity. Two fully humanized CTLA-4 antibodies, ipilimumab and

tremelimumab, began clinical testing in 2000. Initial testing was as a single agent in patients with advanced disease that were not responding to conventional therapy.[105] Both antibodies produced objective clinical responses in ~10% of patients with melanoma,[105,106] but immune-related toxicities involving various tissue sites were also observed in 25-30% of patients, including the skin (dermatitis) and the colon (colitis). While tissues that undergo rapid regeneration, such as the skin and colon are the most affected, while less rapidly regenerated tissues such as the lungs, liver and the pituitary and thyroid glands, are less frequently affected.[106]

Immune toxicities from anti-CTLA4 therapy are usually successfully mitigated by treatment with systemic steroids or tumor necrosis factor (TNF) blockers when systemic steroids are ineffective.[106] In a phase 3 study, ipilimumab, at a dose of 3 mg per kilogram of body weight, was administered with or without gp100 every 3 weeks for up to four treatments (induction). Ipilimumab (10.0 months), compared with gp100 alone (6.4 months), improved the overall survival of metastatic melanoma patients over those treated with the current standard of care chemotherapy (dacarbazine, temozolomide, fotemustine, carboplatin, or interleukin-2).[107] From the original treatment group a set of super-responders was identified, who are currently still alive. The immune-related adverse events that were most frequently observed were associated with the skin and gastrointestinal tract.[107] Nevertheless, these negative side effects were found to be reversible with appropriate treatment.[107] The effect of ipilimumab on long-term survival is more impressive than the mean survival: 18% of the ipilimumab-treated patients survived beyond two years (compared with 5% of patients receiving the gp100 peptide vaccine alone).[107] In 2011, the US Food and Drug Administration (FDA) approved the

CTLA-4 inhibitor, ipilimumab (Bristol-Myers Squibb), for use in treating advanced melanoma, marking the first checkpoint blocking antibody to be approved for clinical use.

b. Blockade of the PD1 pathway

Another immune-checkpoint receptor, programmed cell death protein-1 (PD1), has emerged as a promising immune checkpoint inhibitor of T cell function. PD-1 binds to its ligands on cancer cells: PD-L1 (also known as B7-H1 or CD274) and PD-L2 (also known as B7-DC or CD273), primarily within the tumor microenvironment.[108] A key finding was the strong association found between melanocyte expression of PD-L1 and the presence of tumor-infiltrating lymphocytes (TILs) in human melanocytic lesions.[109] The TILs were found to be associated with the local production of the inflammatory cytokine IFN-γ.[109] Therefore, it was hypothesized that the B7-H1/PD-1 pathway may represent an adaptive immune resistance mechanism of immune escape exerted by tumor cells in response to endogenous antitumor activity.[109]

Expression of PD-L1 as an adaptive response to endogenous antitumor immunity can occur because PD-L1 is induced on most tumor cells in response to interferons (IFNs)-predominantly IFNγ. Similarly to CTLA-4, PD1 is highly expressed on Treg cells, where it may enhance their proliferation in the presence of ligand. Many tumors are highly infiltrated with Treg cells that further suppress effector immune responses. Increased PD1 expression on CD8+ TILs may either reflect an anergic or exhausted state, as has been suggested by decreased cytokine production by PD1+ compared with PD1- melanoma TILs.[110] This translates into a major immune resistance mechanism within the tumor microenvironment.

Figure 6. Targeting immune checkpoints with CTLA-4 and PD-1 blocking antibodies in cancer immunotherapy.

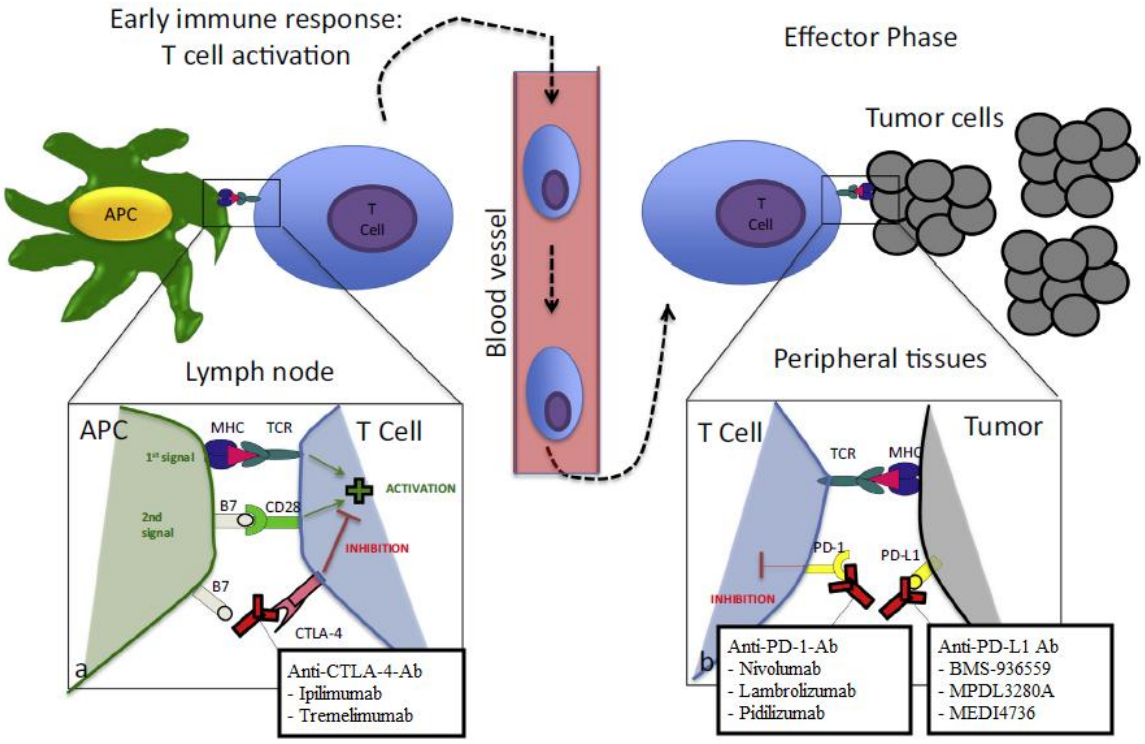

(a) Cytotoxic T-lymphocyte antigen 4 (CTLA-4) is up-regulated shortly after T-cell activation and negatively regulates T cells. Anti-CTLA-4 antibodies, such as ipilimumab and tremelimumab, enhance antitumor activity by blocking this inhibitory signal. (b) Programmed death 1 (PD-1) inhibitory receptor plays a more prominent role in modulating T cell activity in the peripheral tissues during the effector phase. PD-1 is expressed by T cells after antigen exposure, and its ligation with PD-L1 and PD-L2 results in negative regulation of T cells in the tumor microenvironment. Blockade with antibodies to PD-1 or PD-L1 (e.g., Nivolumab and MK-3475) results in the activation of T cells with specificity for the cancer. Figure adapted from Kyi et al.[111]

PD1 is more broadly expressed than CTLA4. The induction of PD1 expression of on other activated non‑T lymphocyte subsets, such as B cells and natural killer (NK) cells, and is believed to inhibit their lytic activity.[112] Therefore, PD1 blockade also probably enhances NK cell activity in tumors and tissues and may also enhance antibody production either indirectly or through direct effects on PD1+ B cells.[112]

Similar to the high expression of PD1 on TILs from many cancers, PD1 ligands are commonly upregulated on the tumor cell surface of many different human tumor types. On solid tumor cells, the major PD1 ligand that is expressed is PD-L1.[113,114] PD-L2 was also reported to be upregulated on cells from certain B cell lymphomas, such as primary mediastinal B cell lymphoma, follicular cell B cell lymphoma and Hodgkin's disease.[115] Taken together, the general findings of increased PD1 expression by TILs and the increased PD1 ligand expression by tumor cells has provided an important rationale for the capacity of antibody blockade of this pathway to enhance a patient's anti-tumor immune responses.

Recently, pembrolizumab (Merck) was approved by the FDA for previously treated advanced melanoma in September 2014.[116] Pembrolizumab has been assessed in a number of clinical trials. A phase I non-randomised trial enrolled 135 patients with advanced melanoma. The majority of participants (69%) had received previous systemic treatment, including chemotherapy, immunotherapy, or a BRAF inhibitor. Patients were given pembrolizumab 10 mg/kg every two or three weeks, or 2 mg/kg every three weeks. Across all doses, 38% of patients who could be evaluated had a confirmed response to treatment. The overall median progression-free survival among the 135 patients was longer than 7 months.[117] Immune-mediated adverse reactions included pneumonitis,

colitis, hepatitis and nephritis.[117] A randomised phase 3 trial compared pembrolizumab to ipilimumab. All enrolled patients had advanced melanoma but only 34% had been previously treated with systemic therapy. The response rate with Pembrolizumab at 10 mg/kg every two or three weeks was improved by 22% compared to ipilimumab, with fewer high-grade toxic events observed.[118]

D. Bispecific antibodies

An alternative non-genetic immunotherapy approach involves bispecific T cell engagers (BiTEs), by joining two different antigen-binding sites in a single molecule to recruit cytotoxic T lymphocytes (CTLs) to recognize MHC non-restricted tumor antigens.[119,50] BiTEs are small bispecific antibodies construct that can transiently link target cell antigens with any cytotoxic T cells by bridging to the invariant CD3 epsilon subunit of the T cell receptor (**Figure 7**). Potentially all pre-existing cytotoxic T cells in a patient can be engaged by this approach, of which effector memory T cells seem to make the dominant contribution to redirected target cell lysis. Therefore, the engagement of T cells with the help of BiTEs may not be impacted to the same extent by the tumor escape mechanism. BiTE antibodies have demonstrated efficacy in hematologic malignancies, both pre-clinically and clinically. Blinatumomab (antiCD3/CD19 BiTE), which has shown dramatic clinical efficacy in the treatment of patients with relapsed or refractory B-non-Hodgkin's lymphoma (NHL) and B-ALL, was approved recently (December 2014)[120] and represents a breakthrough for BiTE technology with potential applications for other targeting cancer therapy.

Blinatumomab is a 55-kDa fusion protein composed of two single-chain antibodies (scFvs) (**Figure 7**). Fusion is achieved by recombinant DNA technology using respective

cDNAs encoding the four variable domains and three linker sequences. The short, non-immunogenic linker sequence of 5 amino acids is used to recombinantly link the two scFvs in tandem. The short linker may allow the two scFvs a high degree of rotational flexibility since simultaneous binding to two epitopes positioned on cell membranes of two separate cells is required. The equilibrium dissociation constants (Kd) of blinatumomab for CD19 and CD3 are ~1nM, and ~100 nM, respectively.[121] At clinically relevant serum levels ranging from 0.5 to 3 ng/ml ($0.9–5.6\times10^{-11}$M), only very small amounts of blinatumomab are expected to be bound by T or target cells.[121]

Redirected lysis by blinatumomab and other BiTE antibodies such as MT110 (anti EpCAM/CD3 BiTE) is dependent on formation of a cytolytic synapse, allowing discharge of toxic proteins that are normally stored inside secretory vesicles of cytotoxic T cells.[122] These vesicles contain the pore-forming protein, perforin, which assembles in a calcium-dependent fashion in the target cell membrane[123] In addition, they also release a cocktail of granzymes, which are proteases capable of hydrolyzing multiple cytoplasmic proteins. Damage of the target cell membrane was evident from nuclear uptake of propidium iodide and the release of the cytosolic enzyme adenylate kinase.[122] Granzyme B activated programmed cell death was observed for the targeted cancer cells by observing membrane blebbing, cleavage of procaspases 3 and 7, fragmentation of nuclear DNA and cleavage of the caspase substrate poly(ADP ribose) polymerase (PARP).[122] The mode of action of blinatumomab and all other BiTE antibodies is summarized in **Figure 8**.

Key features of BiTE antibodies include the ability to redirect target cell lysis via T-cells at low concentrations (EC_{50} values ranging from 0.1 to 50 pmol/L (2-1,000 pg/mL)),

the ability to activate T-cells to kill in the presence of target cells, and the ability to allow T-cells to serially lyse target cells.[50] More than ten different antigens have been targeted by BiTEs including CD19,[124] EpCAM,[122] Her2/neu,[125] EGFR,[126] carcinoembryonic antigen (CEA),[127] CD33,[128] EphA2,[129] and Melanoma-associated chondroitin sulfate proteoglycan (MCSP or HMW-MAA).[130]

To assess the efficacy of BiTE antibodies, xenograft models were established in non-obese diabetic/severe combined immunodeficiency (NOD/SCID) mice supplemented with resting human T cells.[131] Other xenograft animal models were based on immunocompetent mice and patient cancer tissue, and human cancer cell lines. In addition, models prepared with syngeneic murine cancer cell lines producing lung metastases, orthotopic, or subcutaneous tumors have been investigated. Tested BiTE antibodies were either human- or murine-specific, or had a dual species specificity, referred to as "hybrid BiTE antibody".[50]

Blinatumomab was first administered as a short-term intravenous infusion in patients with non-Hodgkin's lymphoma.[121] However, neurologic adverse events (AEs), cytokine release syndrome, and infections were observed in patients in the absence of objective responses, which prevented continuous exposure to the drug.[121] This may have been due to the relatively short half-life of blinatumomab (~2h). Therefore, the next trial administered blinatumomab as a continuous intravenous infusion (civ) over 4–8 weeks via an implanted port system and a portable minipump. Most patients in this phase 1 study had stage III or stage IV NHL with exhibiting mainly mantle cell lymphoma (MCL), follicular lymphoma (FL), and diffuse large B cell lymphoma (DLBCL). In all patients treated at a dose level of 5 $\mu g/m^2/d$ and higher, a rapid and long-lasting

eradication of B cells from peripheral blood has been observed. Partial and complete tumor regressions were first observed at a dose level of 15 μg/m^2/day, and all seven patients treated at a dose level of 60 μg/m^2/day experienced a tumor regression. Blinatumomab also led to clearance of tumor cells from bone marrow and liver.[132] At all dose levels, the disappearance of peripheral blood CD8+ and CD4+ T cells was seen with the early loss (first few hours) from the peripheral blood (PB) after treatment initiation. T cell counts returned to baseline levels within 1-2 days, suggesting a redistribution phenomenon rather than elimination.[132] A detailed analysis of T cell subpopulations indicated that CD4+ and CD8+ effector memory T cells with CD45RA-/CCR7- phenotype primarily expanded, whereas counts of CD8+ T cells with phenotypes of naïve, central memory, and CD45RA+ effector memory T cells remained more or less constant.[132] The most common AEs during the study were flu-like symptoms (eg. pyrexia, fatigue, and headache), weight increase, and weight decrease. Step-dose escalation and corticosteroid premedication were instituted to minimize the incidence and severity of AEs, particularly cytokine release syndrome (CRS) and neurologic events. Patients had increased serum levels of certain inflammatory cytokines, such as IL-10 and IL-6 upon start of infusion. All cytokine increases were transient and normalized within days under the continued dosing of the BiTE. At the target dose of 60 μg/m^2/d, the overall response rates were 75 and 55% for indolent lymphoma and DLBCL, respectively, resulting in the continued development of blinatumomab in a broad range of B-cell malignancies.

Figure 7. Generation of Blinatumomab.

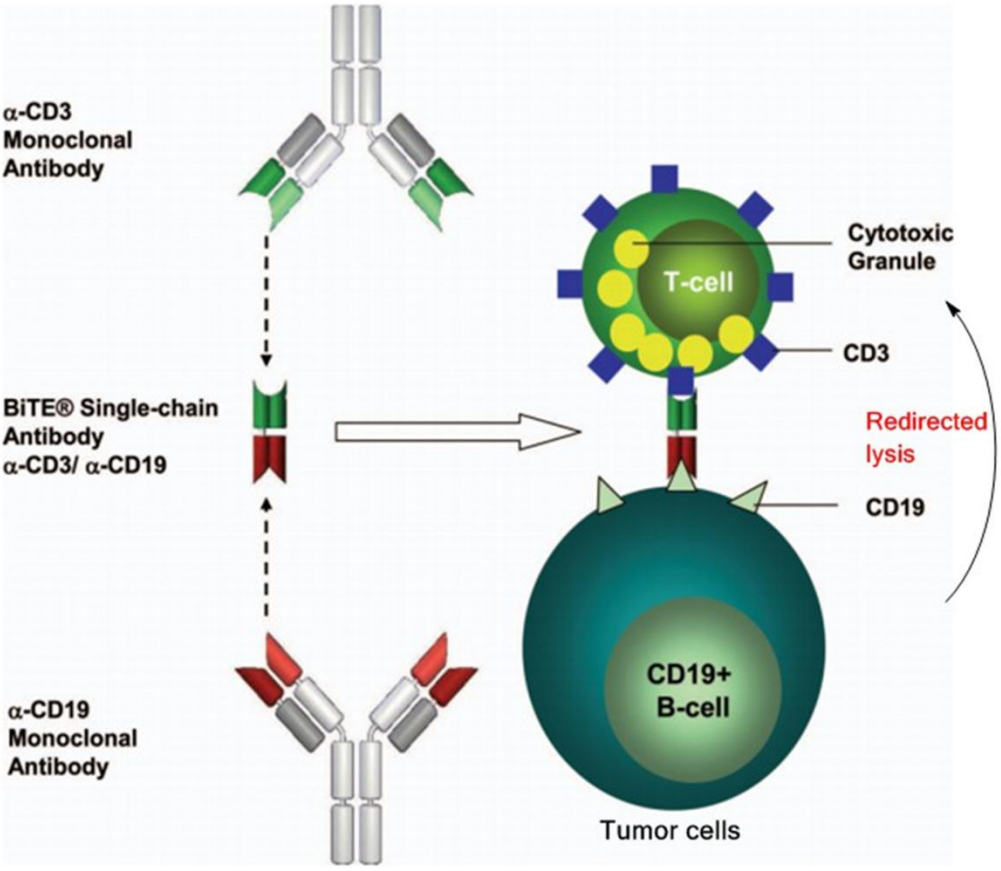

Blinatumomab, a bispecific single-chain antibody construct with dual specificity for CD19 and CD3, is the front runner of the BiTE (Bispecific T-cell engaging) antibody class. Figure adapted from Nagorsen et al.[133]

Figure 8. The mechanism of action of Blinatumomab.

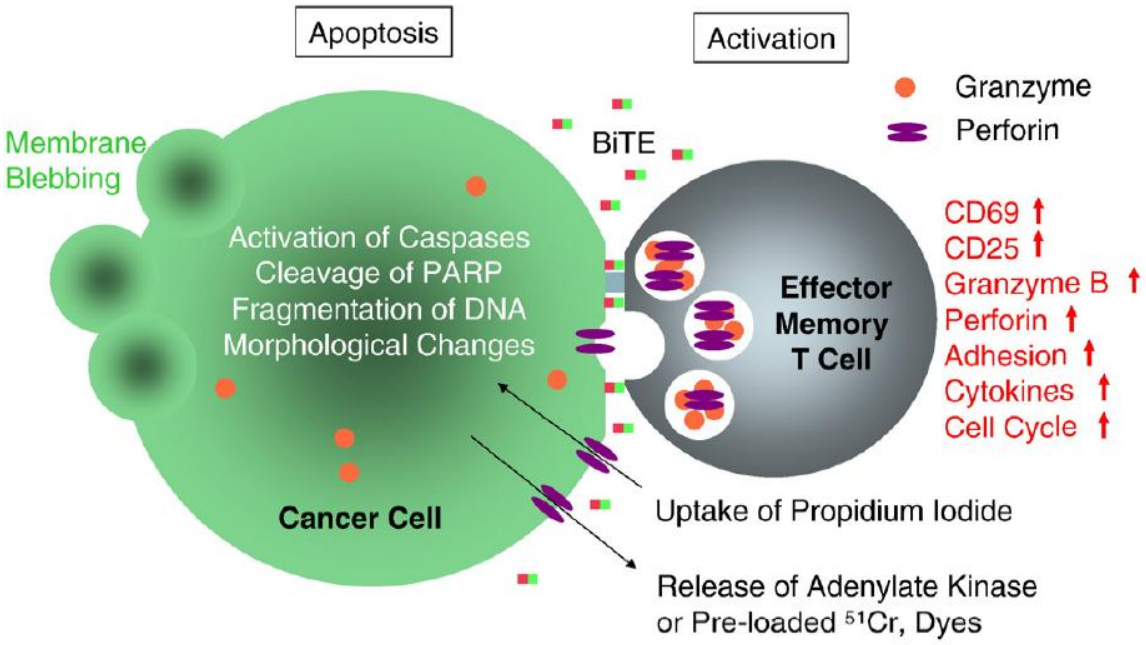

Blinatumomab and other BiTE antibodies transiently induce a cytolytic synapse between a cytotoxic T cell and the cancer target cell. Granules containing granzymes and the pore-forming protein perforin fuse with the T cell membrane and discharge their toxic content leading to the death of the target cell. Figure 8 is reprinted from ref 121 with permission. Copyright 2012 Elsevier Inc.[121]

III. **Summary and thesis goal**

Chemically self-assembled DHFR nanorings (CSANs) provide a diverse and flexible approach for engineering multivalent recombinant antibodies for targeted drug delivery, such as small molecules, toxins and nucleic acids. In this thesis, we are trying to explore their applications as the platform for delivery of vaccine adjuvants and for redirecting immune cells specificity for cancer immunotherapy. The first goal of this project was to direct the formation of heterodimer of bispecific CSANs. We have synthesized a MTX analog for the purpose of modulating DHFR-MTX interactions to favor the formation of DHFR heterodimers. The binding affinities of this MTX analog with either wild type DHFR or several DHFR mutants were determined. The second project was to evaluate the ability of bispecific CSANs for redirecting human T cells specificity against tumor cells. Finally, to explore the potential of $DHFR^2$ based CSANs as vaccines displaying multivalent antigens and adjuvants, we prepared CSANs assembled with the bisMTX-CpG oligonucleotides, and determined their *in vivo* immune responses in a mice model.

Chapter Two: Design of asymmetric dimerizer

I. Introduction

A. Chemically induced dimerization (CID) system

Cellular activities are in part activated by polypeptide hormones, cytokines, growth factors, or growth inhibitors to their cell surface receptors, including protein tyrosine kinase receptors (eg. EGF receptor),[134,135] cytokine receptors (GH receptor bound to JAK kinases),[136] antigen receptors (TCR),[137] trimeric receptors (TNF receptor),[138] and serine/threonine kinase receptors (TGF-β receptor).[139] Those receptors and several components in the intracellular signal transduction pathways are often regulated by ligand-induced dimerization or oligomerization. Diverse physical and biological outcomes can be achieved through protein dimerization strategies.[140] Dimerization of cell surface receptors can bring them into proximity with one another, resulting in the activation of intracellular signaling pathways, such as the TGF-β receptor or the EGF receptor.[141] Heterodimerization of proteins is a common mechanism for regulating cellular functions. Bcl-2, a death repressor molecule, can be neutralized by heterodimerizing with a Bax molecule *in vivo*. Bcl-2 homodimers favor survival whereas Bax homodimers favor death, therefore they compete for one another via heterodimers to precisely regulate the balance of proteins.[142] Furthermore different heterodimers may have distinct DNA-binding specificities and affinity.[143]

Chemically induced dimerization (CID) is the controlled assembly of proteins with a number of classes of dimerizers that can bind to two proteins simultaneously and bring them in close proximity.[144] CIDs have been developed to manipulate cell receptor signal transduction, and gene transcription.[145] Several CID systems have been investigated (**Table 1**). Homodimerization represents the dimerization of two identical proteins

whereas heterodimerization represents the linkage of two different molecules (**Figure 1A**). The first reported synthetic dimerizer FK1012 is a cell permeable bivalent derivative of an immunosuppressive drug FK506, which can tightly bind to its protein target FKBP.[146] FK1012 can successfully induce the dimerization of FKBP12 domains of a chimeric Src-ζ-FKBP12 receptor, which contains the intracellular domain of the T-cell receptor (ζ chain), and initiate the endogenous signal transduction cascade (**Figure 1C**).[146] Alternatively, a dihydrofolate reductase (DHFR) and methotrexate (MTX) CID system has been developed for the controlled assembly of stable and homogeneous protein polygons, or nanorings.[147]

Table 1. Chemically induced dimerization systems.

Target protein(s)		Dimerizer ligand	Reference
FKBP	FKBP	FK1012	[146] and [148]
FKBP	CAN	FK506	[148]
FKBP	CyP	FK506-CsA	[149]
FKBP	FRB	Rapamycin	[148] and [150]
GyrB	GyrB	Coumermycin	[151]
DHFR	DHFR	BisMTX	[152]

FKBP, FK506-binding-protein 12; CNA, calcineurin A; CsA, cyclosporin A; CyP, cyclophilin; FRB, FKBP-rapamycin binding domain of FKBP-rapamycin-associated protein; GyrB, B subunit of bacterial DNA gyrase.

Table adapted from Kopytek et al.[152]

Figure 1. Overview of established CID systems.

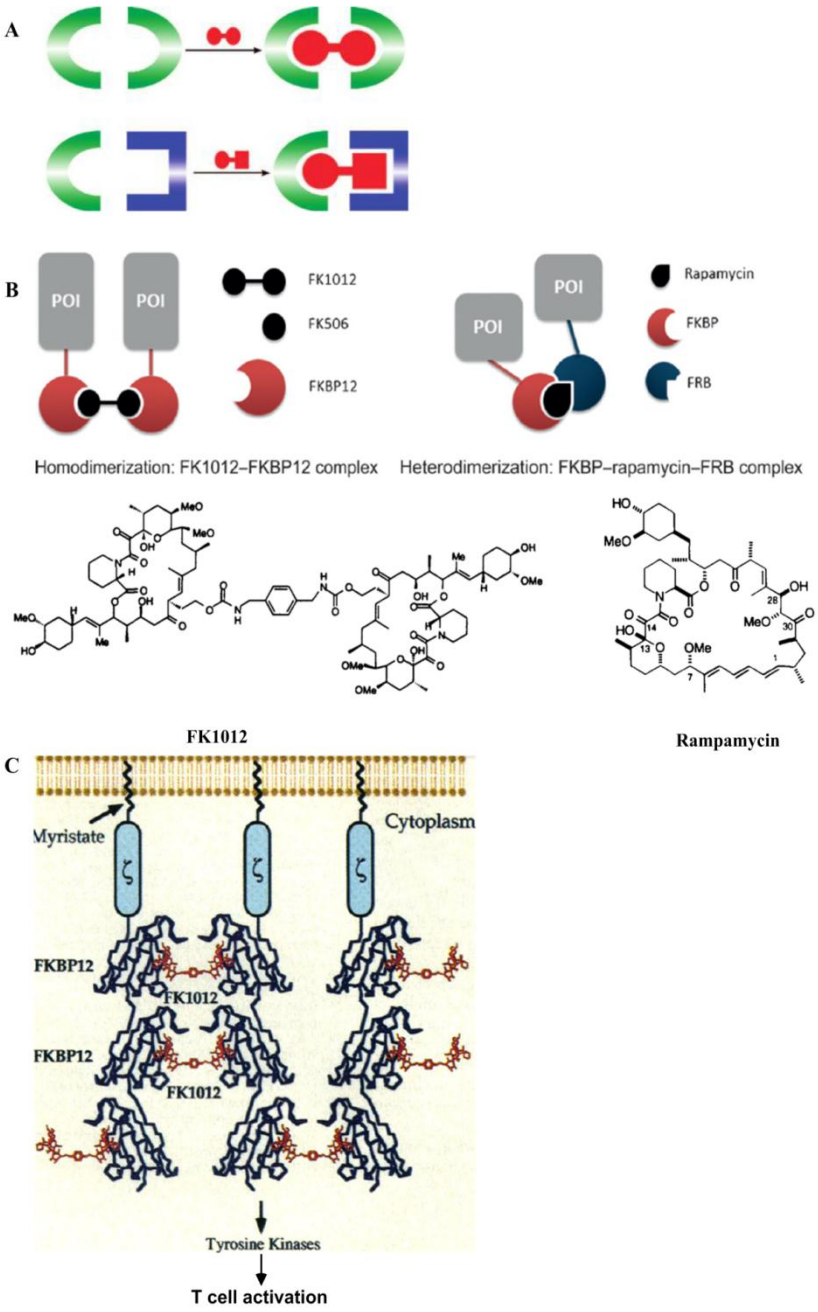

Scheme A indicates chemically induced dimerization of two identical proteins to form a homodimer (green) in the presence of a symmetric dimerizer (red) and two different proteins to form a heterodimer (green and blue) induced by an asymmetric dimerizer (red).[144] In scheme B, a synthetic small molecule, FK1012 can dimerize two proteins (FKBP) whereas rapamycin can mediate heterodimerization of FKBP and the FKBP-rapamycin-binding (FRB) domain of the mammalian target of rapamycin (mTOR).[153] C. Model for intracellular activation of Src-ζ-FKBP12 receptor by FK1012 and subsequent signaling. Figure adapted from Spencer et al.[146]

B. Introduction of DHFR-MTX

Dihydrofolate reductase (DHFR) catalyzes the NADPH-dependent reduction of dihydrofolate to tetrahydrofolate and is a key enzyme involved in thymidine biosynthesis or DNA synthesis. It has been used extensively as a drug target for the treatment of various forms of cancer, rheumatic diseases and bacterial infections.[154] The folate antagonists or DHFR inhibitors belong to an important class of therapeutic compounds. For example, trimethoprim and pyrimethamine are used as potent inhibitors of bacterial and protozoal DHFRs, but have little activity against mammalian cells. Methotrexate is used frequently as an anticancer drug and as an anti-inflammatory and immunosuppressive agent for the treatment of rheumatoid arthritis.[154]

MTX is a folate analog that binds DHFR about 10^8 times more strongly than dihydrofolate itself[155] with a dissociation constant (K_D) of ~0.6 nM for *E. coli*.[156] The crystal structure of binary complex DHFR and MTX has been determined to 1.7 Å resolution (PDB:4DFR).[155,157] Inspired by the design of other CID systems, Wagner and coworkers noted that although *E.coli* DHFR (ecDHFR) and methotrexate are monomeric in solution, they were crystalized in a dimeric form with C_2-symmetry.[158] The glutamate-γ-carboxyl tail of MTX is directly pointed toward its cognate and is sterically uncrowded. From molecular modeling result, a 9 to 12 carbon linker was found to be sufficient to bridge the 9 Å gap between the carboxylates without significantly perturbing the ligand orientation. To support this hypothesis, Kopytek and coworkers reported the synthesis of a MTX dimer (bisMTX) linked by 10 methylenes and 2 oxygens (12 atoms) to partially dimerize ecDHFR.[159] Wagner and coworkers synthesized a bisMTX bridged by methylene-based linker (12 atoms) and confirmed this ligand can induce dimerization of

ecDHFR up to 97% at a dimerizer: protein concentration ratio of 0.5:1, which further proved that the dimerization was stoichiometric (i.e., 2 equiv of enzyme dimerized per equivalent of bisMTX added).[158] The linker between the two MTX molecules was later optimized to a shorter 9-carbon linker, which was successfully co-crystalized with ecDHFR.[160] The crystal structure was shown in **Figure 2**.

To explore the application of DHFR-MTX CID system, Wagner and coworkers designed a set of DHFR fusion proteins with varying inter-domain linker lengths (1 to 13 amino acids) and found that bisMTX induced the self-assembly of a DHFR-DHFR fusion protein ($DHFR^2$).[147] Based on macrocyclization theory, ring formation is highly favored over linear counterparts, since the high affinity of DHFR for bisMTX would facilitate and enhance intramolecular effective molarity.[147,161] Instead of forming linear oligomers, highly stable cyclic protein nanorings with diameters ranging from 8 to 30 nm could be rapidly and easily prepared from 2 to 8 $DHFR^2$ monomers.[147] The protein nanoring size was found to be highly dependent on the length and composition of the peptide linker between $DHFR^2$. When the linker was 13 amino acids, dimer formation was mainly observed with smaller quantities of trimer, tetramer, and pentamer after incubation with bisMTX. In contrast, octamer formation was highly favored when the peptide linker was a single glycine. The cyclic structure was characterized by static and dynamic light scattering, and visualized by transmission electron microscope (TEM). The images observed by TEM (**Figure 3**) showed that the circular rings were remarkably homogeneous, with no apparent linear fragments, fractured, or displaced toroids present. The observed toroids range from 20 to 28 nm in outer diamer, corresponding to oligomers of 6-9 subunits.[147] Like other CID methods, $DHFR^2$-bisMTX system is able to

allow reversible MTX induced DHFR dimerization by the monomeric DHFR inhibitor trimethoprim.[162]

C. Ligand induced heterodimerization

Changes in the subcellular localization of signaling proteins and cellular gene expression in the nucleus are induced by extracellular growth and differentiation factors through a series of protein associations. During the propagation of a signal, association of distinct proteins in close proximity is necessary for cellular signaling pathways.[149] One of the approaches to generate selective protein heterodimers is ligand directed chemically induced dimerization. The first example of an asymmetric dimerizer incorporated the natural product rapamycin, which mediates heterodimerization of FKBP and the FKBP-rapamycin-binding (FRB) domain of the mammalian kinase target of rapamycin (mTOR), rendering TORC1 enzymatically inactive (Figure 1B), thus inhibiting cell growth and proliferation. As shown in **Figure 1B**, rapamycin directs heterodimerization of FKBP and FRB and has a high affinity (Kd < 1 nM) for FRB when bound to FKBP12, and is highly specific for the FRB domain of mTOR.

Figure 2. Crystal structure of DHFR in binary complex with MTX and bisMTX. [155,160]

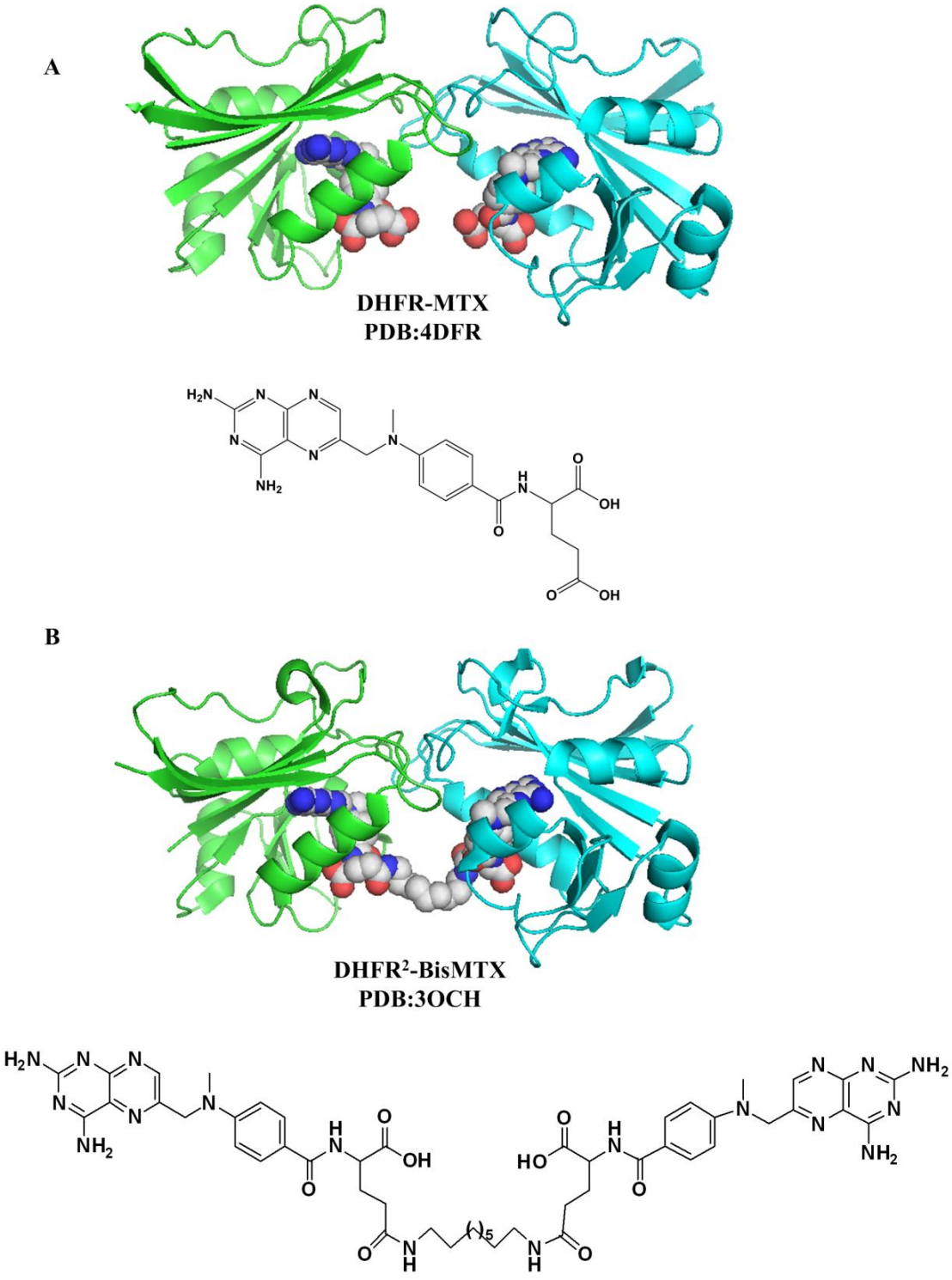

MTX (A) and bisMTX (B). Two methotrexate molecules are linked with a 9-carbon linker. [155,160]

Figure 3. Protein nanoring structure. [144]

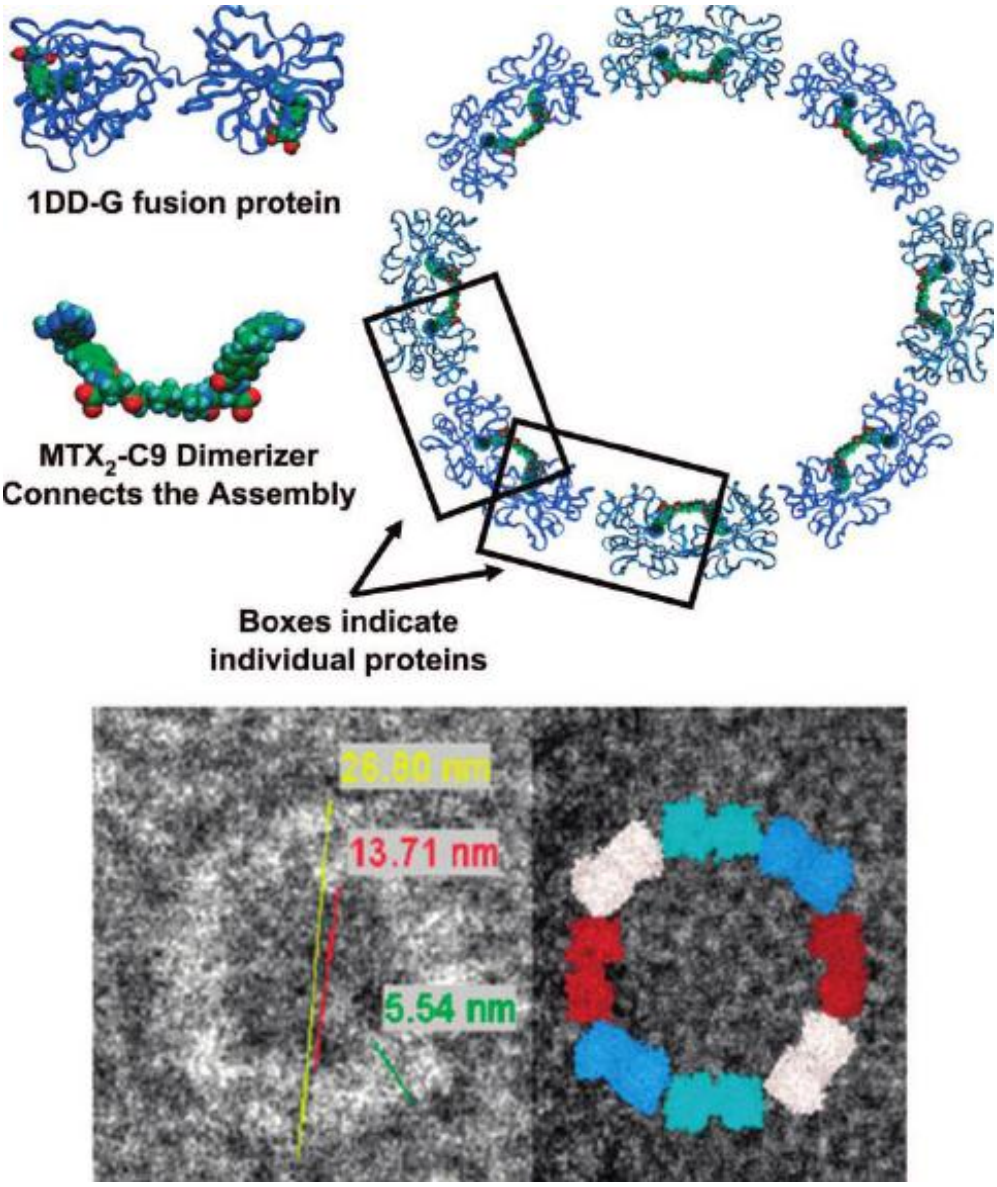

Upper panel, schematic of protein nanoring structure and assembly; lower panel, TEM of DHFR nanorings.[144]

Chemical modification of rapamycin at the surface contacting FRB alleviates the binding affinity. However, mutation of the FRB at this site can accommodate the "bumped" rapamycin analog (rapalog), which was functionalized at C16 and C20, restoring the dimerizing interactions. A triple mutant FRB capable of binding the rapalog with nanomolar affinity was identified. These FRB-rapalog partners permited the selective control of the biological activity of the FRB fusion proteins (**Figure 4**).[163] Binding of FRB and rapalog was assessed by rapalog-dependent cellular compartmentation of a single target protein GSK-3β, which regulates multiple intracellular signaling pathways. GSK-3β was observed both in the cytoplasm and nucleus in the absence of drug (**Figure 4A**). The analog, C20-Marap, binds efficiently to FRB (KTF), which was fused to a nuclear localization sequence (NLS), therefore induced the localization of GSK-3β to the nucleus due to dimerization of the GSK-3β -FKBP target (**Figure 4C**). Whereas, C16-BSRap induced the dimerization of the FRB (TLW) mutant, which was fused to a nuclear export sequence (NES), therefore, GSK-3β-FKBP was rapidly localized to the cytoplasm (**Figure 4B**).

Figure 4. Orthogonal control of GSK-3 β subcellular localization with specific rapalogs.

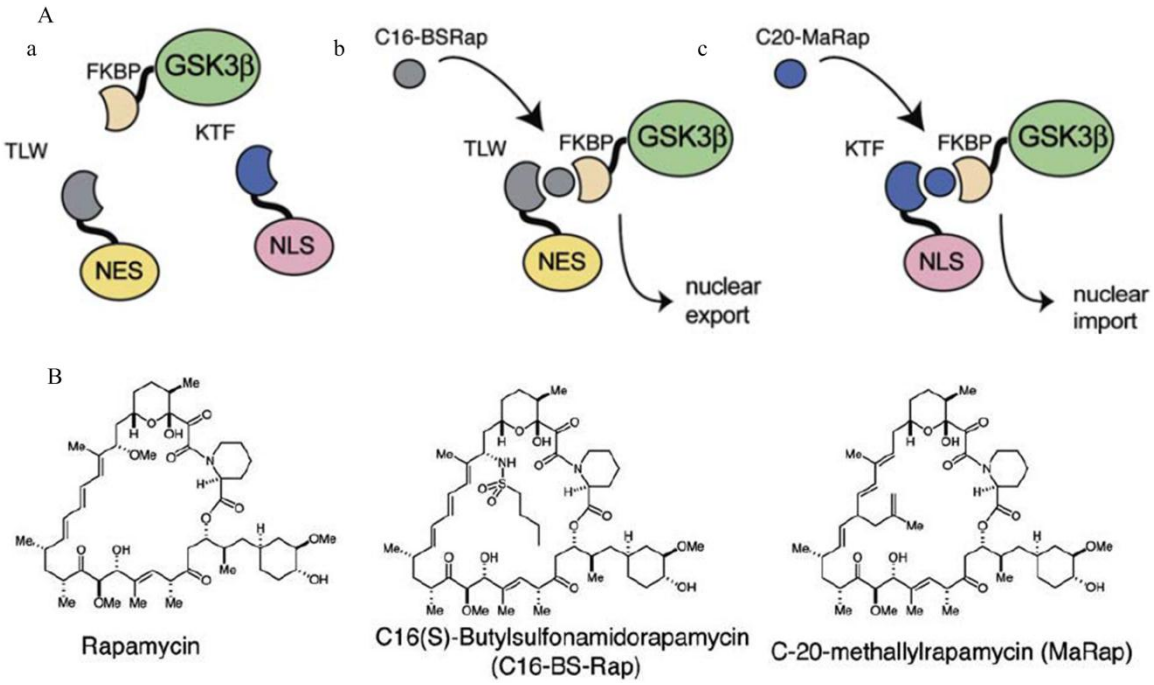

FKBP-GSK-3β -GFP is coexpressed with FRB(TLW)-NES and FRB(KTF)-NLS. In panel A, GFP is visualized in transiently transfected COS1 cells without stimulation where GSK-3β is localized to both cell compartments (a) or with 1 hr stimulation with (b) 10 nM C16-BSrap, (c) 10 nM C20-Marap. Illustrations beneath each figure depict the drug-selective recruitment of either TLW-exp or KTF-imp to FKBP-GSK-3 β to direct nuclear import or export. Structures of Rapamycin, C16-BSrap and C20-Marap are shown in panel B. Figure adapted from Bayle et al.[163]

Bertozzi and coworkers applied the CID concept to studies of glycobiology. Glycosyltransferases, localizes in Golgi and comprises separate catalytic (Cat) and localization (Loc) domains that are both required for fucose transferring and selectin ligand synthesis, therefore playing an important role in the immune system. Genes encoding fucosyltransferase 7 Loc and Cat domains were fused separately to FKBP or the DHFR gene. Trimethoprim (Tmp) conjugate (Tmp-SLF, **Figure 5B**) is capable of dimerizing a bacterial dihydrofolate reductase (DHFR) with FKBP. In the presence of Tmp-SLF, mammalian cells expressing corresponding chimeric proteins were detected with anti-selectin antibodies. Figure adapted from Czlapinski et al.[164]

Figure 5. Conditional activation of a Golgi glycosyltransferase using a CID.

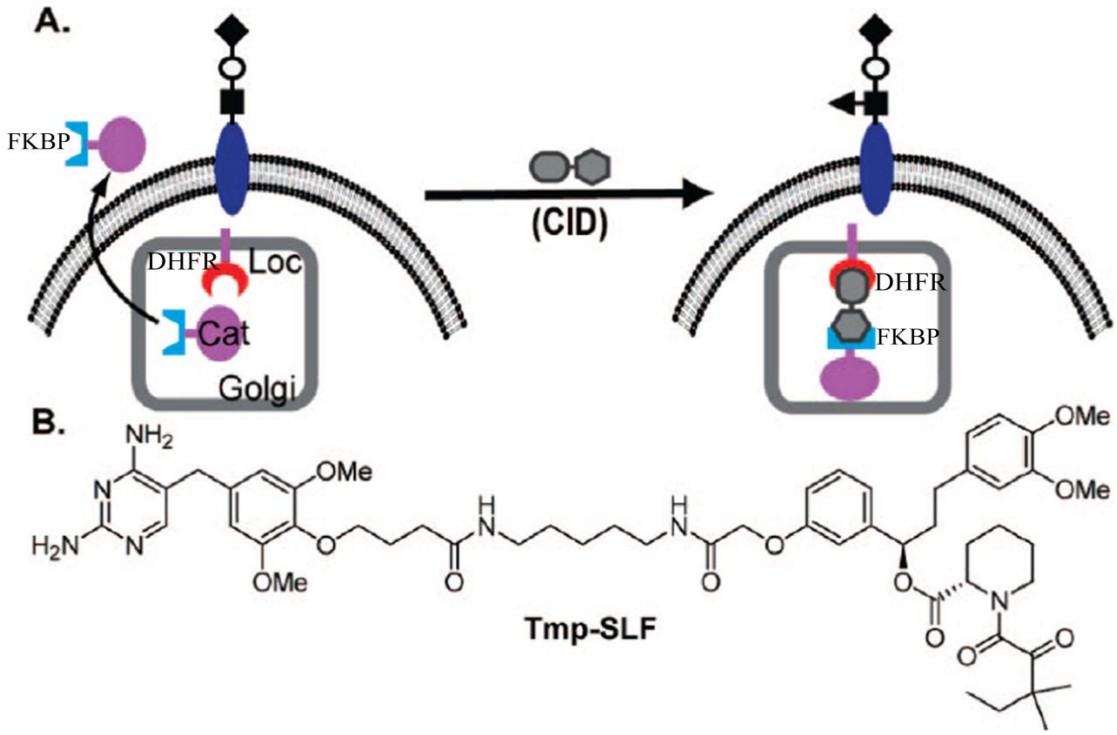

(A) The membrane-associated Loc and soluble Cat domains are separated and fused to small molecule binding proteins. In the absence of the CID, the Cat domain has no mechanism for Golgi retention and is secreted from the cell. In the presence of the CID, the Cat domain associates with the Loc domain and is therefore retained in the Golgi compartment where it can act on substrates. In this depiction, the glycosyltransferase is fucosyltransferase 7, which adds fucose to a glycan substrate forming sialyl Lewis x. Monosaccharide symbols: (♦), sialic acid; (O), galactose; (■), GlcNAc; (▲), fucose. (B) Tmp-SLF. Figure adapted from Czlapinski et al.[164]

D. Ligand directed chemically self-assembled DHFR nanorings (CSANs)

Our group has employed the power of chemically induced protein dimerization to develop a method to produce chemically self-assembled nanorings (CSANs). We have shown that two ecDHFR ($DHFR^2$) fused to an antiCD3 single chain antibody (scFv) can be engineered to spontaneously self-assemble upon the addition of the chemical dimerizer, bisMTX, into either highly stable bivalent or octavalent synthetic antibody CSANs. Depending on the length of the amino acid linker between two DHFRs, when the linker is 13 amino acids, bivalent antibodies antiCD3 CSANs that bind to the T-cell antigen CD3 epsilon of the human T-cell receptor can be prepared.[165] Similarly, several antibodies scFv-$DHFR^2$ fusion proteins were prepared such as anti-αvβ3, antiCD22, antiEpCam and antiEGFR-$DHFR^2$. When the linker between two DHFRs was 13 amino acids in length, dimer formation was mainly observed. In theory, equal proportion of two $DHFR^2$ linked by 13 amino acids and fused to two different antibodies should theoretically produce a stochastic mixture of dimeric nanorings with approximately 50% of the rings being bispecific and 25% of each homodimer. If the $DFHR^2$ contained only a single glycine amino acid linker, the stochastically >99% of the rings would be bispecific.[166] However, the nanorings would be composed of a stochastic mixture of both specificities, since there is no preference formation of one DHFR dimer pair over another.[166] To have more control over the dimerization state, a MTX analog was synthesized and the binding affinities of this MTX analog with either wild type DHFR or several DHFR mutants were determined. These data provide insights into the design of CSANs by controlled heterodimerization in the future.

Figure 6. Statistical distribution of bivalent CSANs.

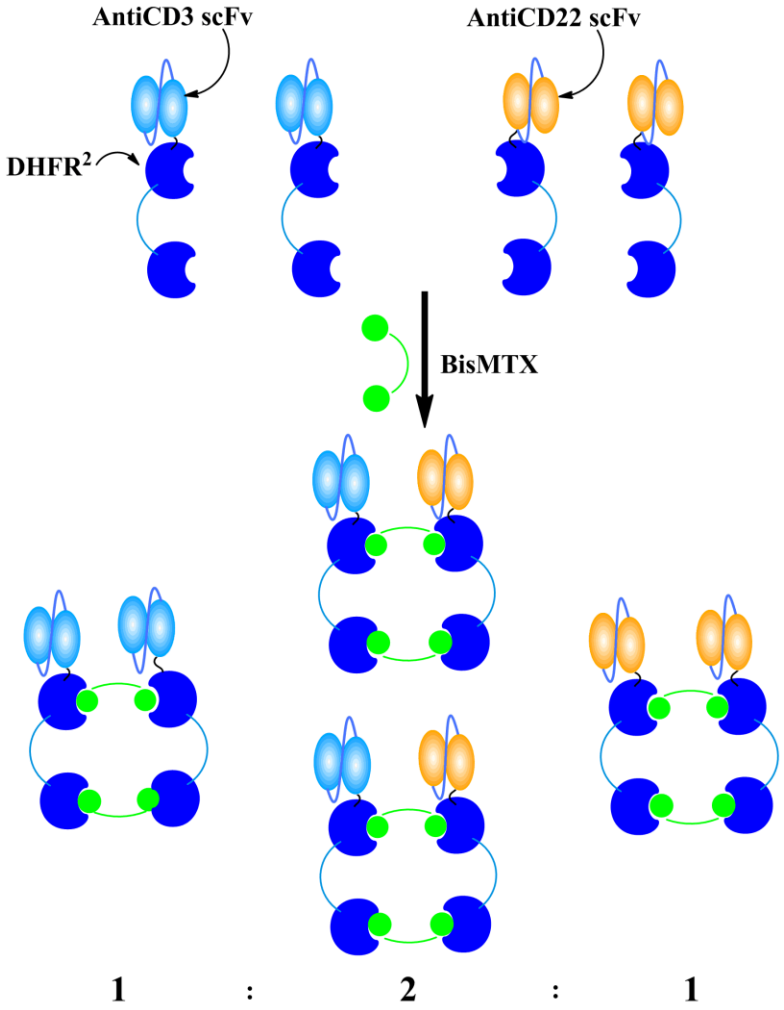

Wild type 13DHFR^2 (13DD) proteins fused with two scFvs are mixed with bisMTX, a stoichiometric mixture of homodimer antiCD3 CSANs: heterodimer bispecific CSANs: homodimer antiCD22 CSANs (1:2:1) is obtained.

In wild type *E. coli* DHFR, the cationic ammonium from guanidinium ($RNHC(NH_2)^{2+}$) at Arginine 57 (R57) forms salt bridge or ion pair with anionic α-carboxylate ($RCOO^-$) of MTX. This binding is tight and very specific (**Figure 7A**). Our hypothesis was to create a unique DHFR-MTX interaction by reversing the ion pair. We proposed to substitute the α-carboxylate of MTX, with a guanidino group from Arg-57, while using site directed mutagenesis the active site arginine with either aspartic acid or serine. The R57D mutation would potentially reverse the electrostatic interactions, while the serine would maintain hydrogen bonding interactions (**Figure 7B, 7C**).

Figure 7. Reversing side chain of DHFR and bisMTX.

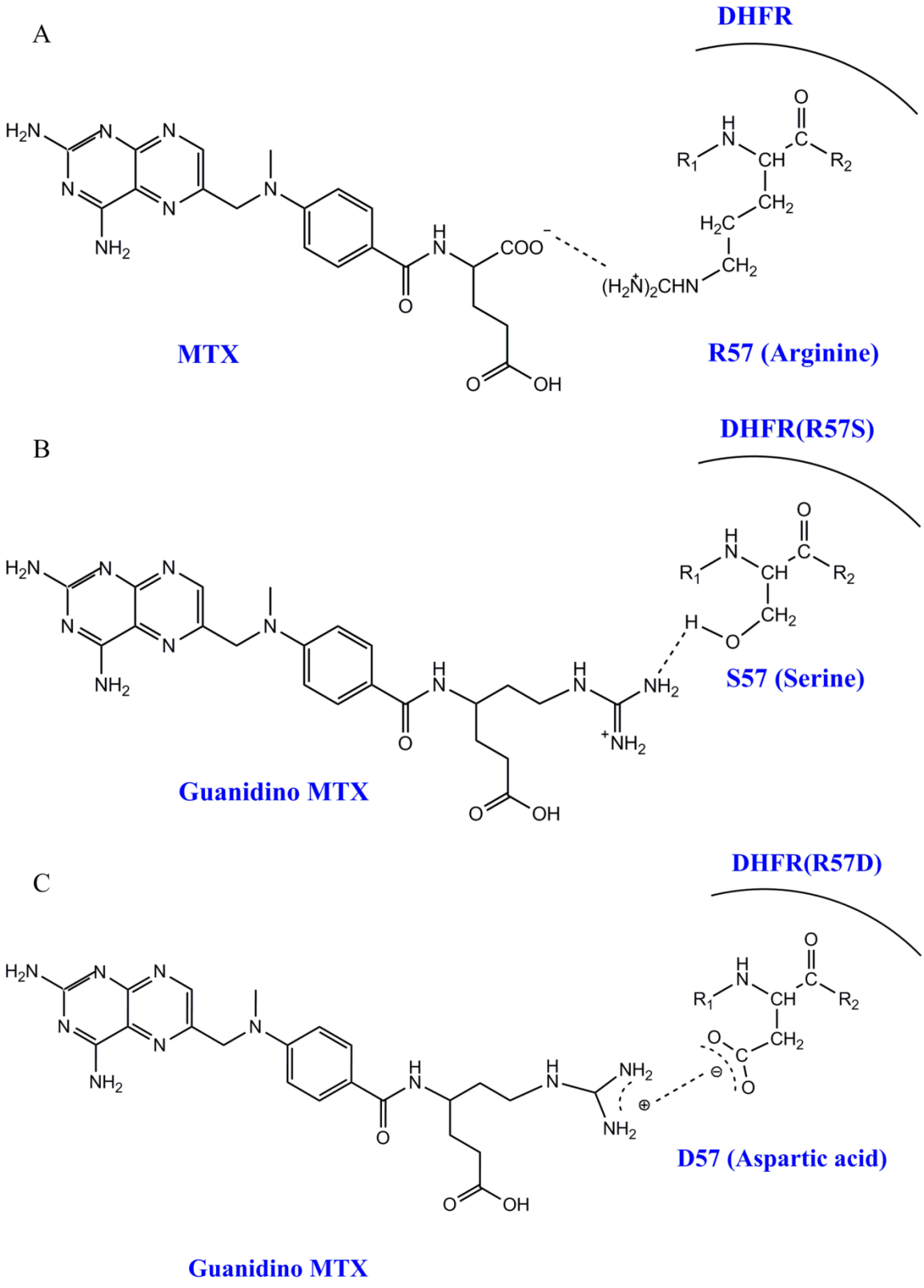

Figure 8. Hypothesis of ligand directed heterodimerization.

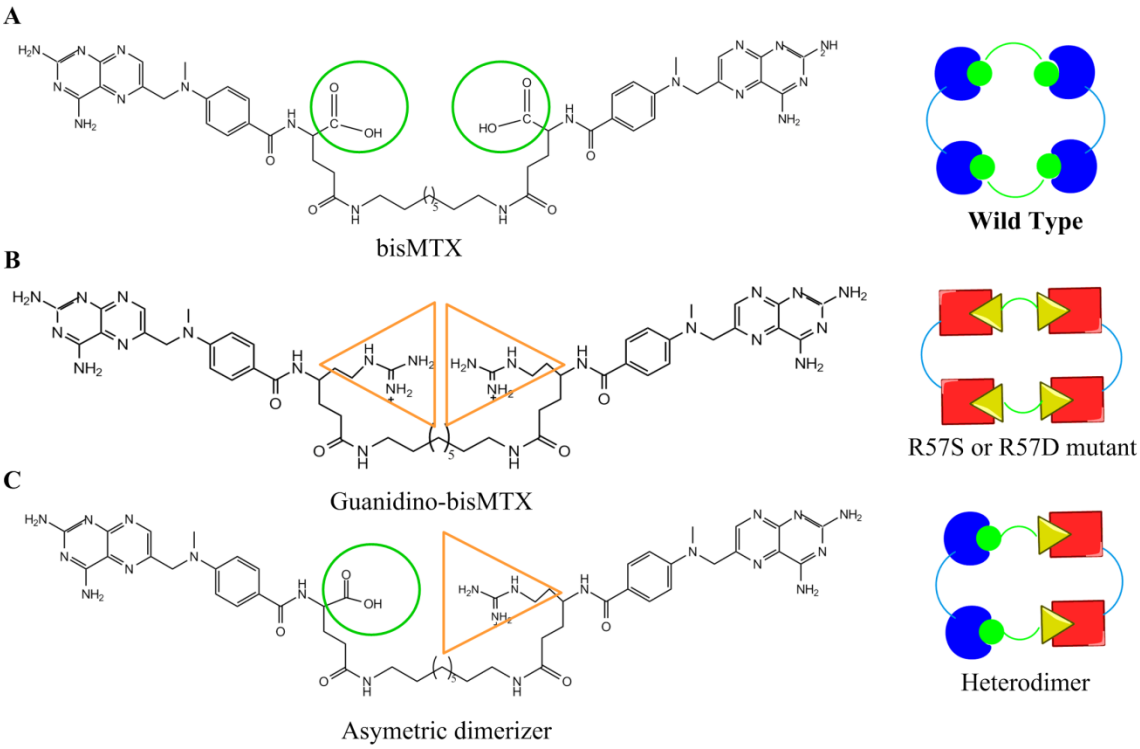

(A)When bisMTX (green) is mixed with wild type 13DHFR[2] (13DD, blue), it induces the dimerization of 13DD to form a homodimer. (B) When guanidine-bisMTX (yellow) is mixed with R57S or R57D (red), it forms a homodimer of 13DD (R57S or R57D). (C) If wild type (blue) and mutant 13DD (R57S or R57D, red) proteins are mixed with assymetric dimerizer (green and yellow), a heterodimer of wild type and mutant protein will be formed. Most importantly, the possibility of forming internal monomer would be much less.

II. Results and Discussion

A. Mutagenesis and protein preparation

Previously we have observed that the R57E mutant of DHFR has very low enzymatic activity and dose not dimerize with bisMTX. Since purification using MTX binding may not be suitable for altered folate binding affinity of DHFR mutants, the mutant enzymes were engineered to incorporate a His-tag so that they could be purified by Ni-affinity chromatography. Initially the monomer DHFR mutant plasmid was prepared by mutagenesis. Arginine 57 was mutated to either serine or aspartic acid. Six histadines were inserted into the C terminus of each DHFR mutant. All proteins were expressed as soluble proteins and purified by application to a Ni-column and elution with imidazole, followed by purification with a diethyl aminoethyl (DEAE) ion exchange column. The yield for R57D was approximately 15 mg per liter of Terrific Broth culture. The purity of protein was assayed by SDS-PAGE analysis. Surprisingly, R57S mutant could not be purified in either the soluble or insoluble fraction. Possibly due to the protein instability and misfolding, R57S mutant dose not bind well to Ni-column. Protein with high molecular weight was detected, whiles band corresponding to R57S monomer could hardly be visualized by SDS-PAGE gel (data not shown). Experimental conditions for cell culture, protein expression and purification need to be optimized in the future study to obtain good amount of purified R57S mutant for ligand-protein binding study.

Figure 9. SDS-PAGE characterization of DHFR (R57D).

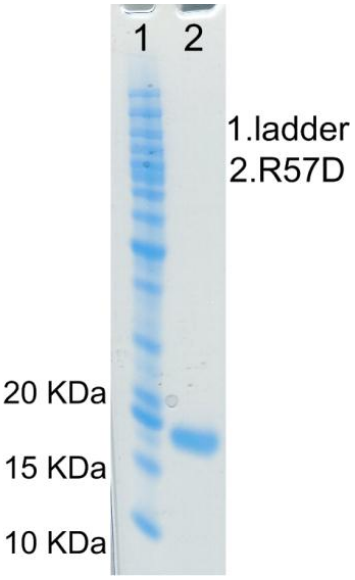

Pure protein shows single band at 18 KDa.

B. Analysis of the dissociation constant (Kd) of DHFR or R57D to ligands MTX or Guanidino-MTX.

The equilibrium dissociation constants (Kd) for protein and ligand binding were determined by the ligand-dependent quenching of intrinsic enzyme tryptophan fluorescence using fluorescence spectroscopy. As shown in **Figure 10**, the binding affinity of MTX for the R57D decreased by nearly 10 fold compared to the K_d for wild type DHFR from 14.62 $\pm$ 5.84 nM to 125.90 $\pm$ 24.84 nM respectively, thus not surprisingly indicating the importance of the interaction between the guanidino group of Arg-57 and the alpha carboxylate of MTX. Consistent with this result the Guanidino-MTX also exhibited a nearly 10 fold lower binding affinity for wild type DHFR (139.50 $\pm$ 36.59 nM) compared to DHFR-MTX (14.62 $\pm$ 5.84 nM). Unexpectedly, binding of Guanidino-MTX to the R57D mutant (K_d=125.0 $\pm$ 30.7 nM) was found to be close to its binding to wtDHFR (K_d = 139.50 $\pm$ 36.59 nM). Thus, while the alternative MTX analog, Guanidino-MTX, does have a decreased affinity for wtDHFR, it does not have an enhanced affinity for the R57D mutant over MTX.

Figure 10. Binding affinity of different proteins and ligands.

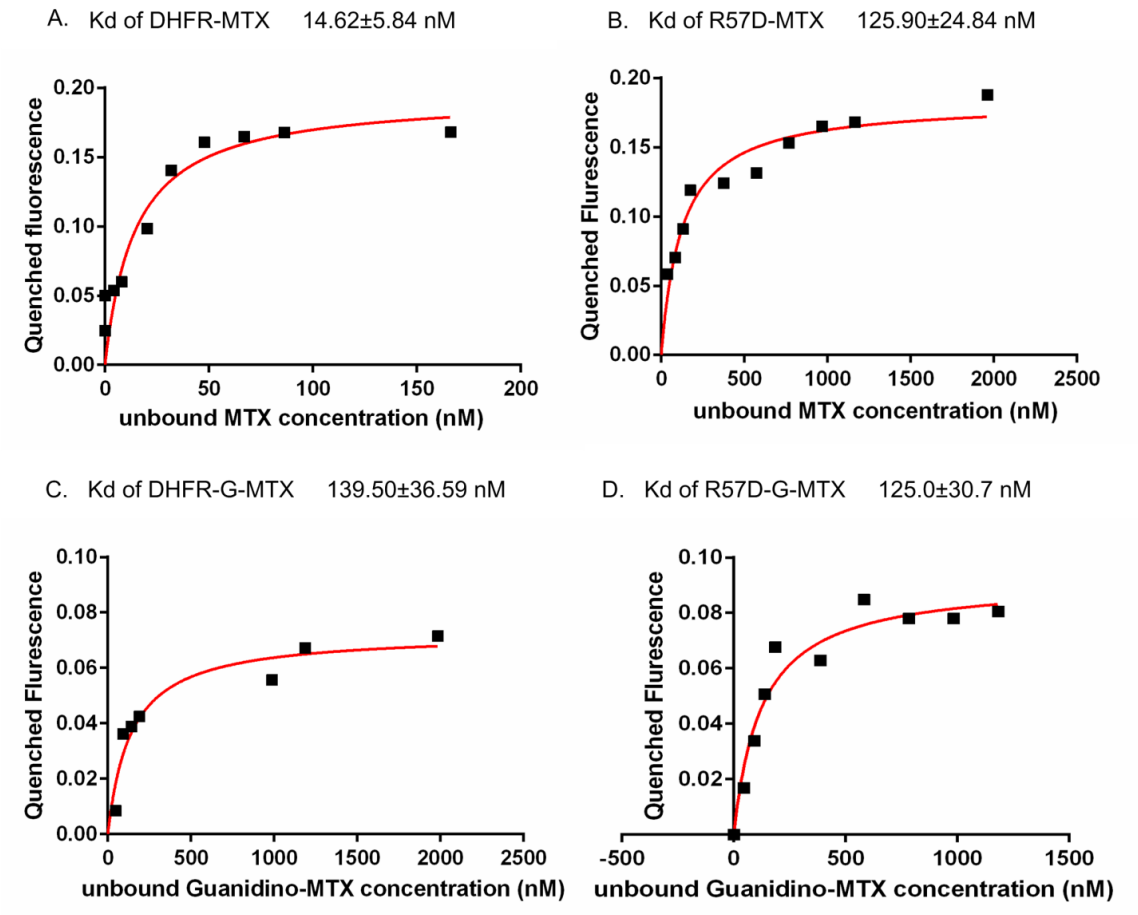

III. **Conclusion**

To achieve 100% of heterodimer formation of $DHFR^2$ for the purpose of engineering bispecific antibodies, monomer DHFR mutants and MTX analog guanidino-MTX were prepared. The ion pair of R57 DHFR with MTX was reversed, by removing the arginine guanidine group and placing it on MTX, then reducing the size of the R57 residue, such that the active site could accommodate the insertion of the extended guanidine group. The binding affinities of wild type DHFR or R57D with MTX or guanidine-MTX were determined. However, high binding affinity of guanidine-MTX with R57D has not been observed. This is possibly due to the steric interactions between the guanidine group with the residues at DHFR active site. It is also likely that the hydrophobic environment around Arg-57 increases the pKa of the substituted aspartate to such an extent that it is not deprotonated at neutral pH and thus unable to form an ion pair with Guanidino-MTX. A systematic mutational analysis of the inner sphere residues surrounding the Arg-57 will need to be carried out to further improve the binding of Guanidino-MTX to DHFR and thus provide a potential alternative DHFR ligand interaction that could be used for heterodimerization.

IV. Materials and Methods

A. Protein expression and purification

BL 21(DE3) competent E.coli expression cells were transformed with plasmid wtDHFR or R57D DHFR. Colonies were inoculated into 100 mL TB media containing 100 μg/mL ampicillin at 37 ˚C with shaking at 250 rpm overnight. One liter TB broth containing 100 μg/mL ampicillin was inoculated with 10 ml of the bacterial culture and grown for 3.5 hours till the cell OD_{600} reaches 0.6. Cells were then induced with 300 μM Isopropyl β-D-1-thiogalactopyrnoside (IPTG) and incubated for another 3 hours. Finally cells were pelleted by centrifugation at 7500 rpm for 15 min at 4 ˚C and the cell pellet was stored at -80 ˚C until use. The cells were lysed via a 30 min incubation at room temperature in lysis buffer (10 mM KH_2PO_4, 100 μM EDTA, 1 mM DTT, 1 mg/mL Lysozyme, pH 8.0) containing protease inhibitor and 8×15 seconds sonication. The crude lysate was then centrifuged at 40,000g for 40 min at 4 ˚C.

For wild type DHFR, the lysate was dialyzed against 2 L equilibration buffer (10 mM KH_2PO_4, 0.1 mM EDTA, 0.5 M KCl, 0.5 mM DTT, pH 6.0) overnight at 4 ˚C, then loaded onto a MTX agarose column. The bound protein was washed with a high salt buffer (50 mM KH_2PO_4, 1 mM EDTA, 1 M KCl, 1 mM DTT, pH 6.0) until the absorbance of A280 and A260 of the eluate is < 0.05, at which point the DHFR protein was eluted with folate elution buffer (50 mM KH_2PO_4, 1 mM EDTA, 1 M KCl, 5 mM folic acid, 1 mM DTT, pH 9.0). Fractions containing DHFR activity were pooled and dialyzed with DEAE equilibration buffer (10 mM Tris, 1 mM EDTA, 1 mM DTT, pH 7.2) overnight at 4 ˚C. The protein was loaded onto DEAE ion-exchange column and eluted with a gradient of 0~40 % buffer B (10 mM Tris, 1 mM EDTA, 0.5 M KCl, 1 mM

DTT, pH 7.2) over 300 minutes and then 40 ~ 100 % buffer B over the next 420 minutes. DEAE buffer A is the same as the equilibration buffer.

For DHFR (R57D), the lysate was dialyzed against 2 L equilibration buffer overnight at 4 ˚C, then loaded onto a Ni column. DHFR-Histag was eluted with elution buffer. Fractions were analyzed by SDS-PAGE gel, pure fractions were concentrated to 1mg/mL by Amicon centrifugal ultrafiltration devices (10KDa cutoff) and dialyzed with PBS buffer. Final protein concentration was determined by Bradford protein assay.

B. DHFR activity assay

DHF and NADPH stock were prepared in MTEN buffer (50 mM MES, 25 mM Tris, 0.1 M NaCl, 25 mM ethanolamine, pH 7.0) and the concentrations were estimated spectrophotometrically using the reagent's extinction coefficients at 280 and 340 nm, respectively. NADPH solution to a final concentration of 100 μM, and a DHFR sample were mixed to a final volume of 1 mL (MTEN buffer) minus the necessary volume of DHF. After 2 min of incubation, a baseline reading at 340 nm was taken to verify zero activity. DHF was then added from a concentrated master stock to a final concentration of 50 μM, the sample was mixed, and the absorbance was read at 340 nm for 1 minute. The rate of absorbance decline corresponds to Vo in μM/min and was calculated with the known extinction coefficient for the DHFR catalyzed reaction, 11,300 $M^{-1}cm^{-1}$.

C. Fluorescence Titrations

The dissociation constants (K_D) were determined by fluorescence titration employing a fluorescence spectrofluorimeter. The formation of the enzyme-ligand complex was followed by measuring the quenching of the tryptophan fluorescence of the enzyme upon addition of microliter volumes of a concentrated ligand stock solution.[167]

DHFR or R57D was diluted to a final concentration of 200 nM in 1 ml PBS buffer and baseline fluorescence reading was taken, scanning emission from 300 to 400 nM with excitation at 290 nm. Serial additions of ligands were performed. The emission at 340 nm was recorded. Data were fitted using the one-site binding (hyperbola) equation $Y = B_{MAX}*X/(K_{D(APP)} + X)$ [where B_{MAX} is the maximum extent of quenching and $K_{D(APP)}$ is the apparent dissociation constant] by nonlinear regression using GraphPad Prism 5.0 software.

Chapter Three: Prosthetic Antigen Receptors

I. Introduction

A. Prosthetic Antigen Receptors

Malignancies of B cell, such as B-acute lymphoblastic leukemia (B-ALL) or B non-Hodgkin lymphoma (B-NHL) origin are a heterogeneous group of hematological neoplasms occurring in blood, lymph nodes and bone marrow, which frequently disseminate throughout the body. Traditional treatments for B-cell malignancies have relied upon combination chemotherapy, which is usually complemented with radiation therapy and/or hematopoietic stem cell transplantation (HSCT), and monoclonal antibody (mAb) based therapeutics such as the chimeric antiCD20 antibody, rituximab.[168] Although they have significant clinical antitumor efficacy, most patients ultimately relapse and succumb to their disease, creating the need for improved therapies.[169]

The potential to harness T cells for the elimination of tumor cells is one of the most compelling concepts in anti-cancer immunotherapy development. Nevertheless, tumors have developed a number of mechanisms to evade T-cell immunosurveillance.[170,171] One approach to overcome the impotence of the immune system regarding cancer cells is to re-engineer T-cells with targeting molecules that are difficult for cancer cells to defend against.[172,173,174,175] For example, T-cells engineered to express antiCD19 CARs, have been shown to clinically eradicate B-cell leukemias.[176,177] Nevertheless, the preparation of the engineered cells is time consuming, costly and of variable efficiency, while the potential long-term risks of gene transfer methods on the expression of oncogenes and tumor-suppressor genes and of long lived engineered T-cells to target normal tissues are major concerns.[178,179] Consequently, an attractive alternative to CARs would be the development of prosthetic antigen receptors (PARs) that could stably (days) and

reversibly bind to the CD3 ε subunit of the T-cell-receptor/CD3 complex, while allowing targeting to a cancer cell surface receptor (**Figure 1**).

We have previously demonstrated that in the presence of the chemical dimerizer bisMTX, DHFR-DHFR ($DHFR^2$) and DHFR-DHFR-antiCD3 ($DHFR^2$-antiCD3) fusion proteins can spontaneously assemble into a range of chemically self-assembled nanorings (CSANs) whose size varies depending on the length and composition of the linker peptide between the DHFRs.[180,160,181,182] If the linker is a single glycine, we observed that rings containing 7 to 10 $DHFR^2$ fusion proteins with an average ring size composed of 8 monomers.[160,182] Therefore, the mixing of an equal proportion of two $DHFR^2$ linked by a single glycine and fused to two different antibodies should theoretically produce a stochastic mixture of CSANs that are approximately 99% bispecific (**Figure 1**). Consequently, we prepared fusion proteins of $DHFR^2$ linked by a single glycine either tethered to an antiCD3 scFv ($DHFR^2$-antiCD3, 1DDantiCD3) or a scFv targeting CD22 ($DHFR^2$-anti CD22, 1DDantiCD22), an antigen widely expressed on B-leukemias or lymphomas.

Figure 1. Prosthetic Antigen receptor (PAR)-T cells.

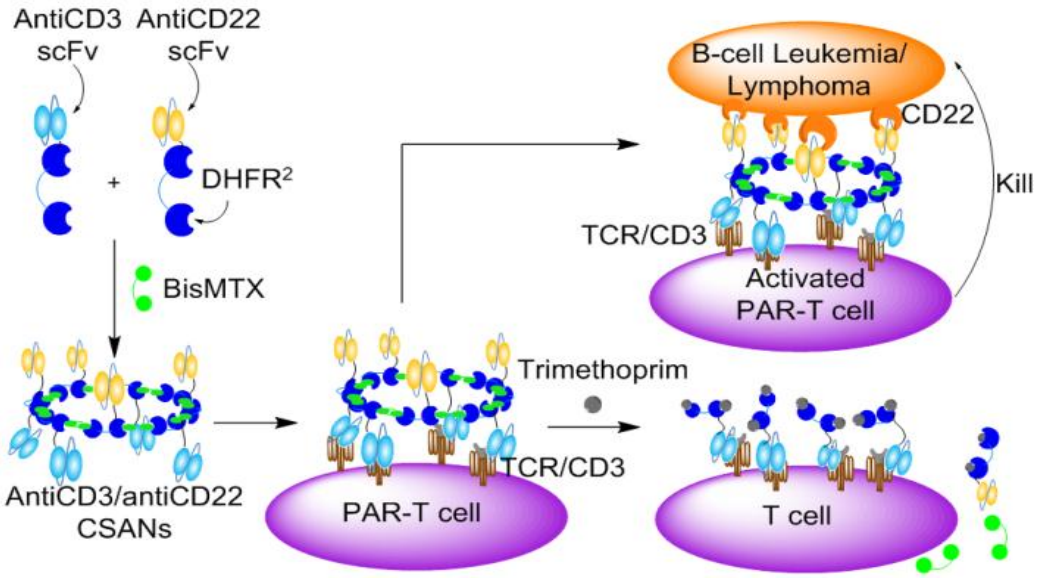

The mixing of an equal proportion of two $DHFR^2$ linked by a single glycine and fused to two different antibodies, antiCD3 scFv (blue) and antiCD22 scFv (yellow), should theoretically produce a stochastic mixture of CSANs induced by bisMTX (green). T cells armed with bispecific CSANs can generate prosthetic antigen receptors (PARs) T cells (PAR-T cells, purple) allowing targeting to cancer cells (orange). Trimethoprim (gray), a non-toxic FDA approved competitive inhibitor of DHFR, carries out disassembly of the bispecific antibody nanorings and allows cells to disengage.

B. CD22

B-lymphoblasts express CD20 in about 50% of cases, CD19 in more than 90% of cases, and CD22 in more than 80% of cases.[183] These markers are compelling targets for immunotherapy, because their expression is restricted to B cell lineage and clinical tolerance for B cell depletion is high using modern supportive care. CD22, also called Sialic acid-binding Ig-like lectin 2 (Siglec-2) or B-lymphocyte cell adhesion molecule (BL-CAM), is a member of the immunoglobulin superfamily that regulates B-cell activation and interaction with T cells, [183,184] which is expressed on the surface of mature B lymphocytes but is lost on plasma cells, early progenitor B cells, and hematopoietic stem cells.[185] CD22 has a tissue distribution that is similar to CD19.[186] Compared to CD20, CD22 is detected at a lower copy number than CD20 on normal B cells (~30,000 CD22 vs 100,000-150,000 CD20 molecules/cell).[185] Therefore it is an attractive target for cell-directed therapies.[121]

In this chapter, we first determined the binding affinity of engineered antiCD22 CSANs to CD22+ B lymphoma cells by comparison with those for the parental monoclonal antibody followed by investigations of their internalization by these cells using confocal microscopy. In addition, we studied the activation of T cells by cytokine profiling, immunophenotyping and T cell functional assays *in vitro* after treatment with bispecific antiCD3/CD22 CSANs. In the presence of target B lymphoma cells, cytolytic efficacy of redirected T cells was also determined. Finally, we assessed the ability of trimethoprim, a non-toxic FDA approved competitive inhibitor of DHFR to carry out disassembly of the bispecific antibody nanorings.

II. Results and discussion

A. Characterization of antibody purity and dimerization by SEC

The purity of antibody fusion proteins 1DDantiCD22 was firstly characterized by SDS-PAGE (**Figure 2A**). Purified antibodies 1DDantiCD3 and 1DDantiCD22, were incubated for 1 hour with bisMTX (1:1:2.2 equiv), and the assembled proteins were analyzed by size-exclusion chromatography (SEC; **Figure 2B**). Octavalent bispecific antiCD3/antiCD22 CSANs were eluted in a broad peak centered at 18.5 min with almost 100% oligomerization of 1DDantiCD3 and 1DDantiCD22 monomers eluted at 28.5 min. The bispecific CSANs have a similar retention time to the antiCD3 CSANs which were previously analyzed by SEC[160], indicating that they have similar hydrodynamic radius. Again, the major nanoring species formed were octamers.[160] The hydrodynamic radius of purified bispecific antiCD3/antiCD22 CSANs was found to be 16.06 ± 0.01 nm by dynamic light scattering (DLS) which is (**Figure 2**C).

Figure 2. Characterization of self-assembled antibodies.

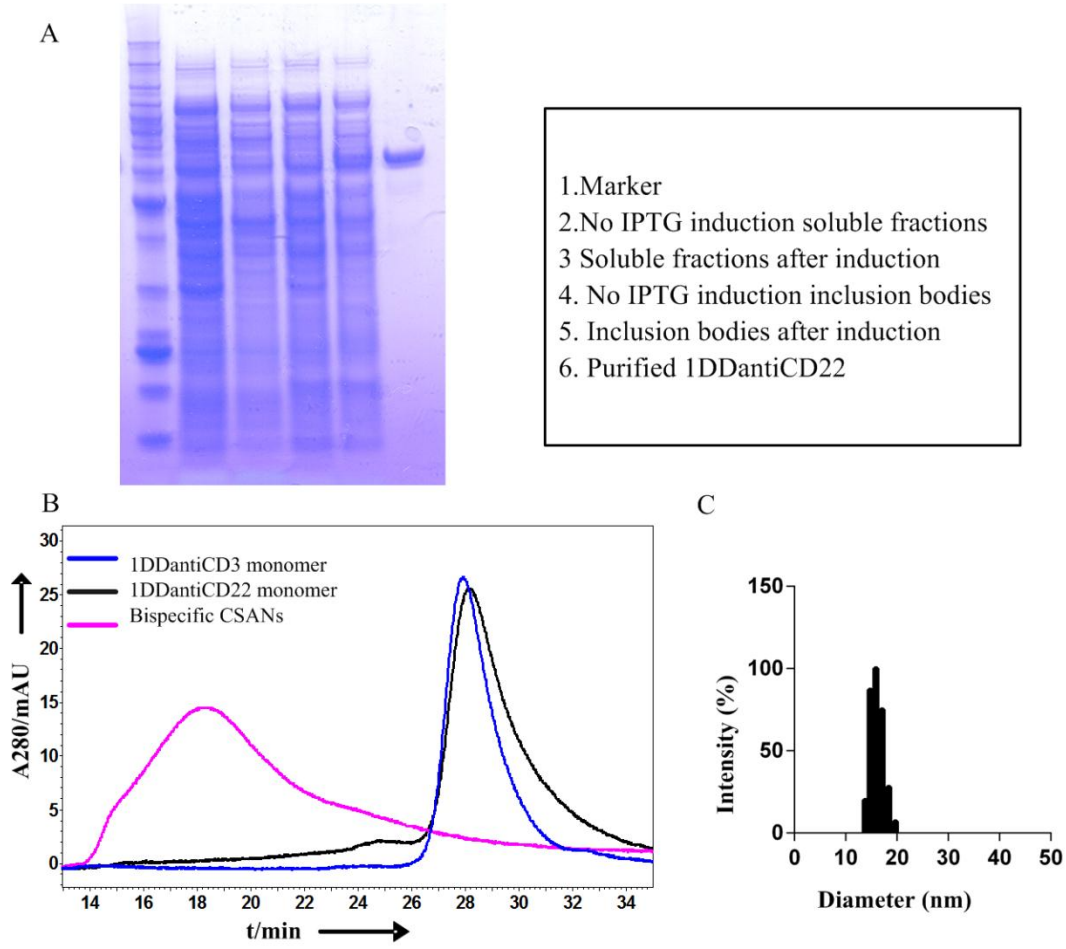

(A) SDS-PAGE for DHFR^{2}antiCD22 fusion protein expressed in Rosetta cells. (B) Characterization of the purified antibodies and antibodies dimerization by SEC. The assembly of bispecific CSANs was characterized by size exclusion chromatography. Blue curve: DHFR^{2}antiCD3 monomer (1DDantiCD3); Black curve: DHFR^2 antiCD22 monomer (1DDantiCD22); Purple curve: bispecific CSANs. (C) The hydrodynamic size of bispecific CSANs was measured by dynamic light scattering.

B. Characterization of binding affinities of 1DDantiCD22 and antiCD22 CSANs

To determine quantitatively the binding affinity of the monovalent or octavalent DHFR^{2}antiCD22 to the CD22 positive B lymphoma Raji cells, the dissociation constant was evaluated in a flow cytometric competitive binding assay. Binding of non-labeled antibodies to Raji cells was competed with a sub-saturated amount of FITC labeled mAb antiCD22 RFB-4, followed by quantitation of the fluorescence intensities of cell bound FITC labeled RFB-4 by flow cytometry (**Figure 3**). The lower binding affinity of the monomer 1DDantiCD22 (K_d=104.81 $\pm$ 0.5 nM) compared with the parental monoclonal antibody RFB-4 (K_d =1.05 $\pm$ 0.4 nM) is likely due to the transition from mAb to the single chain format in tandem with DHFR^2. Compared with the monomer 1DDantiCD22 (K_d =104.81 $\pm$ 0.5 nM), the multivalent antiCD22 CSANs were found to have a lower K_d value of 68.77 $\pm$ 0.5 nM.

C. Cell-internalization studies of self-assembled antibodies

Since antiCD22 scFvs and immunotoxins undergo receptor mediated endocytosis,[187] we tested the ability of antiCD22 CSANs prepared with fluorescein-labeled bisMTX (FITC-bisMTX)[181] to be internalized by CD22+ Daudi cells by confocal fluorescence microscopy. Consistent with receptor dependent endocytosis, green punctates could easily be observed by Daudi cells incubated at 37 ℃ with the fluorescent labeled antiCD22 CSANs, indicating internalization, while membrane bound green fluorescence was observed for incubations at 4 ℃ (**Figure 4**).

Figure 3. Characterization of binding affinities of antibodies by FACS competitive binding assay.

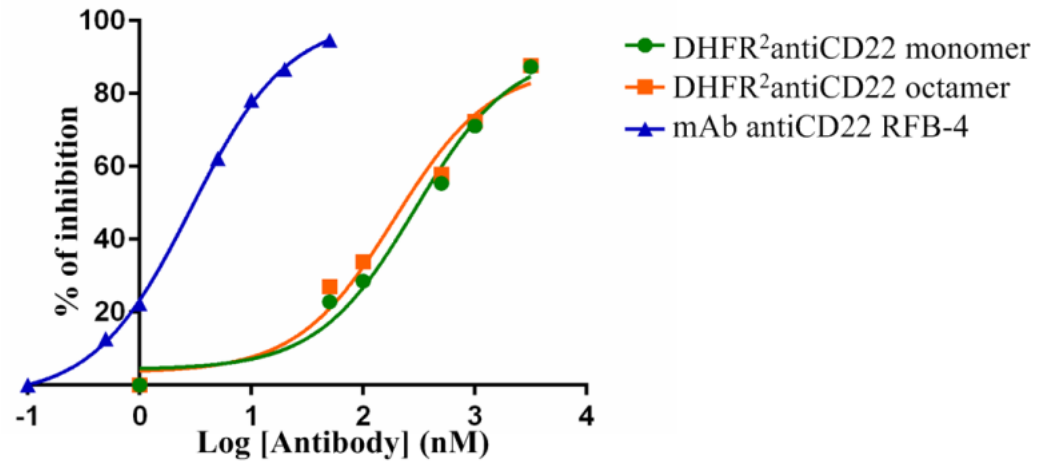

Flow cytometric competitive binding assay was applied to determine the disassociation constant of 1DDantiCD22 monomer (green dots), 1DDantiCD22 octamer (orange squares) and mAb RFB-4 (blue triangles) to CD22 positive B lymphoma Raji cells.

Figure 4. Cell internalization studies of self-assembled antibodies.

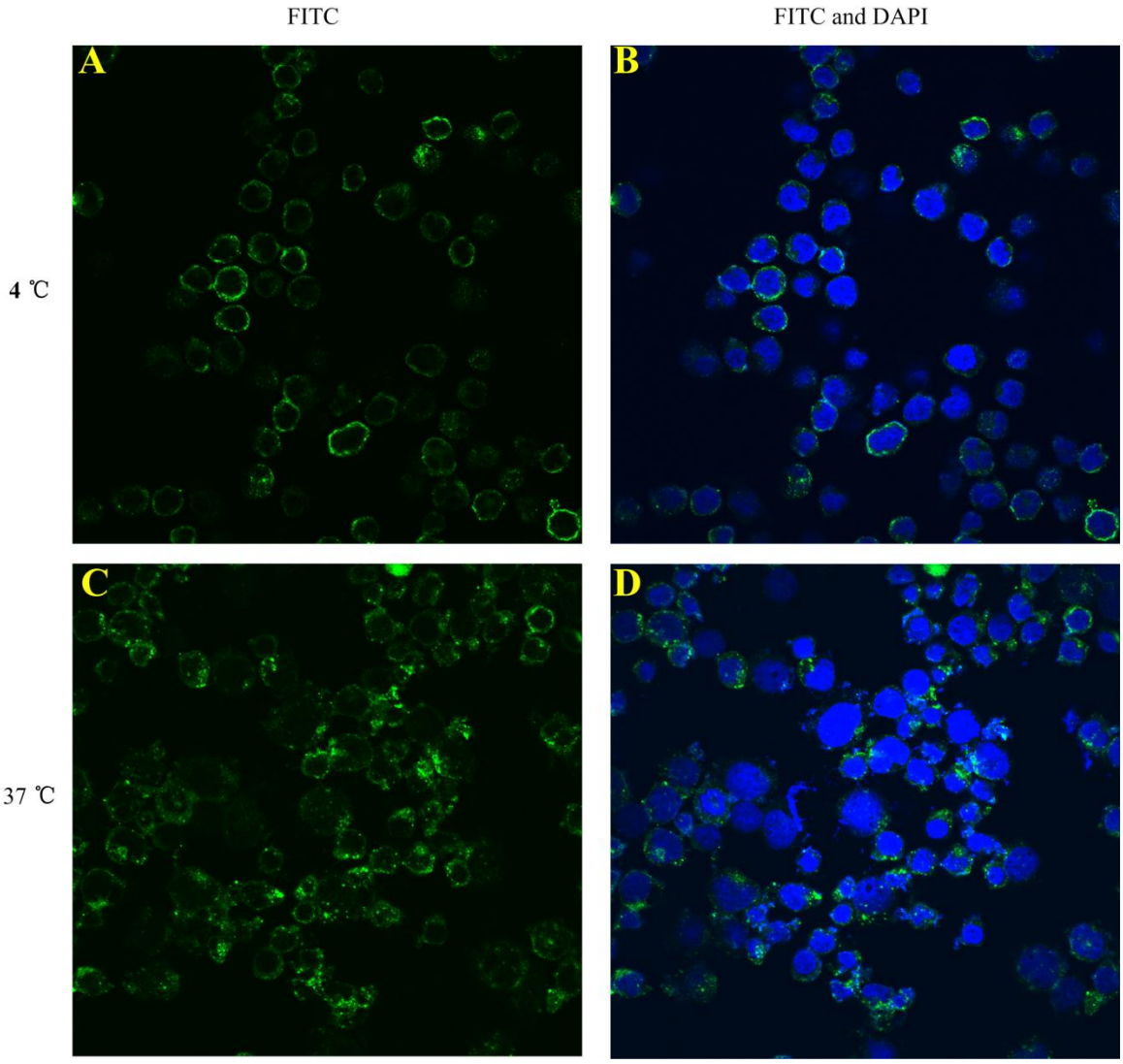

Fluorescence confocal microscopy images showing (A) Daudi cells incubated with antiCD22 CSANs assembled by FITC-bisMTX at 4 ℃. (B) Overlaid with DAPI labeling the cell nucleus at 4 ℃. (C) Daudi cells incubated with $DHFR^2$antiCD22 assembled by FITC-bisMTX at 37 ℃. (D) Overlaid with DAPI labeling the cell nucleus at 37 ℃.

D. Binding specificity studies

To confirm that the bispecific CSANs maintained the binding specificity and selectivity of the monospecific CSANs, FACS analysis was carried out with PBMCs (CD3+) and Raji cells (CD22+). Both antiCD3 and antiCD3/antiCD22 CSANs were found to bind to a similar extent to PBMCs, while no significant binding of antiCD22 CSANs was observed. Similarly, both antiCD22 and antiCD3/antiCD22 CSANs were found to bind to a similar extent to Raji cells, while no significant binding of antiCD3 CSANs could be detected (**Figure 5**).

E. Characterization of the stabilities of bispecific CSANs

Unlike monovalent bispecific antibodies, multivalent bispecific CSANs might be expected to have high avidity and thus exhibit stable binding to cells. Previously, we have demonstrated that antiCD3 CSANs bind to the surfaces of PBMCs and are not significantly internalized.[160] Having demonstrated that both monospecific and bispecific CSANs were stable for greater than 72 h at 37˚C in PBS (data not shown), we investigated the stability of the bispecific CSANs on PBMCs in complete RPMI at 37 ˚C. To assess the binding of the CSANs to T-cells, with a flow cytometric competitive binding assay, we determined the ability of antiCD3/ant-CD22 CSANs to compete with the FITC labeled parental antibody UCHT-1 for binding to CD3 receptors on PBMCs. After incubating the PBMCs with antiCD3/antiCD22 CSANs and washing the cells, we found that greater than 85% of the potential binding of UCHT-1 could be blocked over three days. (**Figure 6A**) A small loss in the ability of the antiCD3/antiCD22 CSANs to block UCHT-1 binding could be observed from day four to five, which may indicate the effects of cell division and thus dilution of the bispecific CSANs. In addition, the

antiCD3/antiCD22 CSANs were found to have a significantly greater ability to block UCHT-1 binding than the $DHFR^2$antiCD3 monomer. Therefore, the bispecific CSANs bind cell surface CD3 and remain largely intact on the surface of T-cells.

One of the distinct advantages of our bispecific CSANs over other bispecific antibodies is the potential to initiate disassembly by the addition of the competitive inhibitor and FDA approved drug, trimethoprim.[160,180,181] Previously, we have demonstrated that incubation with trimethoprim results in the disassembly of antiCD3 CSANs prepared with FITC-bisMTX, which can be monitored by the loss of FITC fluorescence.[181] Consequently, we investigated the disassembly of antiCD3/antiCD22 CSANs prepared with FITC-bisMTX bound to PBMCs in the presence of variable concentrations of trimethoprim for 1 h at 37 ˚C (**Figure 6B**). By monitoring the decrease of mean fluorescence intensity of FITC on PBMCs using flow cytometry, the IC_{50} of trimethoprim was determined to be 1.18± 1.1 μM, which is well below the plasma concentration of 5 μM typically found after a typical clinical oral dose of trimethoprim.[188]

Figure 5. Characterization of binding specificity of self-assembled antibodies.

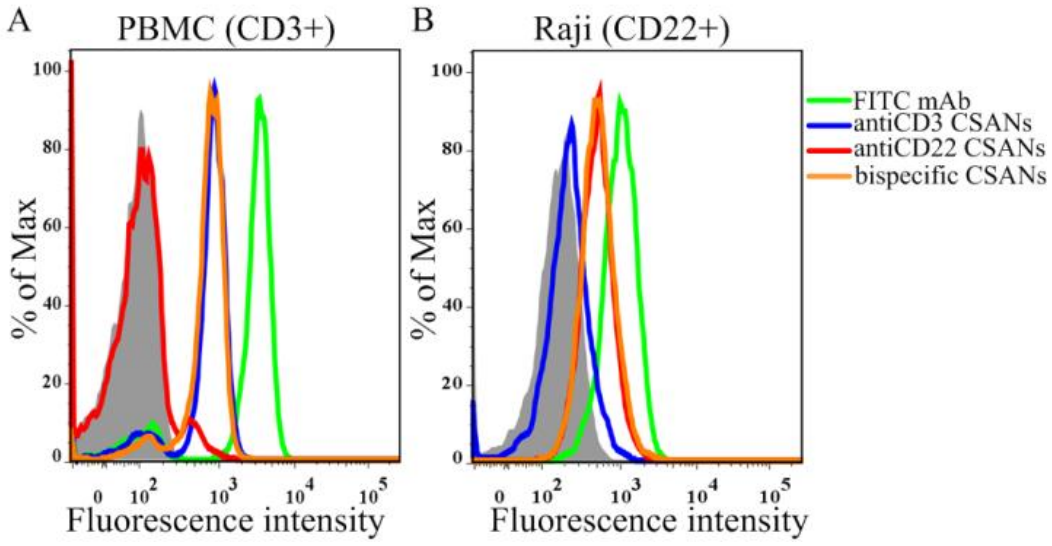

Flow cytometry based binding assay of monospecific antiCD3 CSANs (blue), antiCD22 CSANs (red) and bispecific CSANs (orange) to PBMCs (A) and CD22 positive Raji cells (B). Positive controls: FITC-antiCD3 mAb UCHT-1 (green) (A) and FITC-antiCD22 mAb RFB4 (green) (B).

Figure 6. Characterization of the stabilities of self-assembled antibodies.

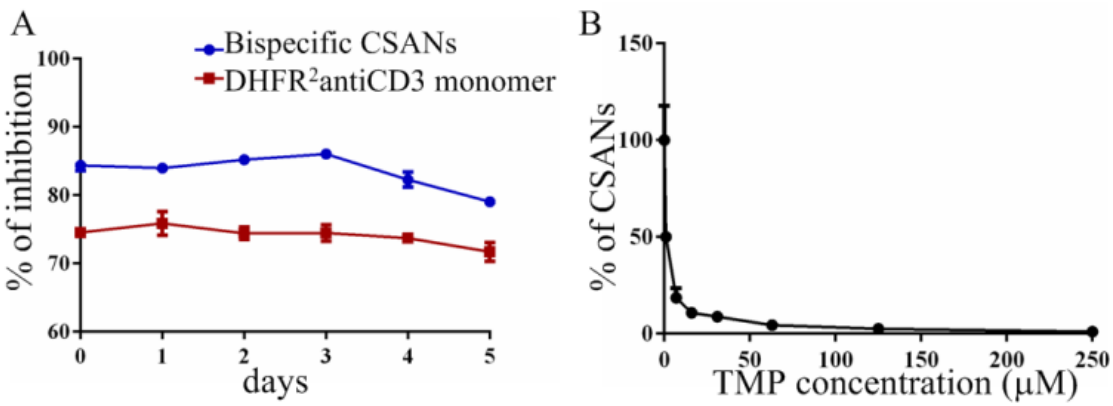

(A) Time course study of the stability of bispecific CSANs (blue) and 1DDantiCD3 monomer (red) on PBMC cells. (B)The disassembly of bispecific CSANs by trimethoprim.

F. T cell activation studies

a. Cell surface markers upregulation studies

To determine the ability of antiCD3/antiCD22 CSANs to activate T-cells, we investigated their ability to upregulate the early activation marker, CD69, and the late activation marker, CD25 (IL-2R).[189] As can be seen in **Figure 7A**, incubation of PBMCs with either media or $DHFR^2$ (1DD) octamer resulted in insignificant expression of CD69 by CD4+ or CD8+ cells, regardless of the presence of the target cells. In contrast, both antiCD3 CSANs and antiCD3/antiCD22 CSANs enhance CD69 expression to similar levels with or without incubation with Raji cells. Similar to the results observed for CD69, appreciable increases in the expression of CD25 (**Figure 7B**) were only observed in the presence of either antiCD3 CSANs or antiCD3/antiCD22 CSANs. However, a much greater increase (5- to 7-fold) in CD25 expression was observed in the presence of Raji cells when compared to incubations in their absence. When a set of similar experiments was carried out with UCHT-1 F(ab')2, compared to the antiCD3 CSANs and antiCD3/antiCD22 CSANs, only a modest level of CD69 and CD25 expression with or without Raji cells was observed. Thus, the multivalent CSANs are able to facilitate the pre-activation of CD4+ and CD8+ T cells to greater extent than bivalent antiCD3 UCHT-1 F(ab')2.

Figure 7. Expression of CD 25 and CD 69 on PBMCs.

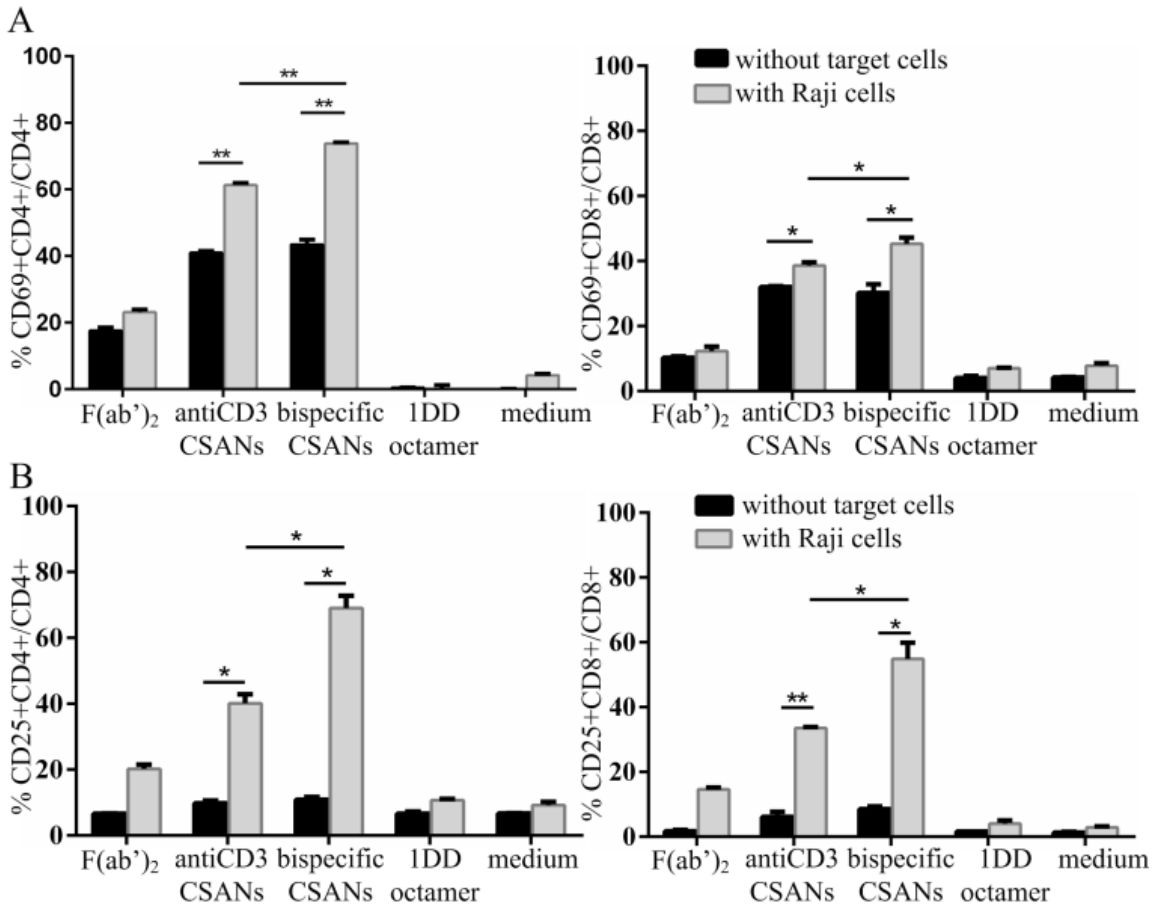

Un-stimulated PBMCs were co-cultured with different treatments in the presence or absence of CD22+ Raji cells for 24 h. The expression of the activation markers CD69 (A) and CD25 (B) on CD8+ T cells or CD4+ T cells were analyzed by flow cytometry. Data were obtained from one donor and are representative of data from three donors. * $P<0.05$ or ** $P<0.005$ with respect to in the absence of Raji cells or with antiCD3 CSANs treatment.

To further investigate the specificity of the activation of T-cells by antiCD3 CSANs and antiCD3/antiCD22 CSANs, we determined the ability of purified CD4+ and CD8+ T cells to undergo activation in the presence of the Raji (CD22+, MHCI+) and K562 (CD22-, MHCI-) cell lines (**Figure 8**). Consistent with our results with PBMCs, activation of the CD4 and CD8 cells was observed to a similar extent after treatment with either antiCD3 CSANs or antiCD3/antiCD22 CSANs. Only a modest increase in the expression of CD69 by CD8+ T cells in the presence of Raji cells was observed. In contrast, no significant difference was detected in the presence of K562 cells relative to no cells. Again, similar to the results with PBMCs a significant increase was observed in CD25 expression for CD4+ and CD8+ T cells in the presence of Raji cells relative to K562 cells and no cells.

b. Degranulation marker upregulation studies

The presence of cytotoxic granules and evidence of de-granulation is a hallmark of cytotoxic CD8+ T cells activation. The level of degranulation can be assessed by determining the amount of the degranulation marker CD107a on the surface of CD8+ cells. Similar to our findings for CD69 and CD25 (**Figure 9**), treatment of CD8 cells with either antiCD3 CSANs or antiCD3/antiCD22 CSANs resulted in increased expression of CD107a, with a modest increase found for the bispecific over antiCD3 CSANs in the presence of Raji cells.

c. Cytokine release determination

A hall mark of T-cells activation and their interaction with targeted cells is the production of the pro-inflammatory cytokines, IL-2 and IFN-γ. The cell media concentration of IL-2 or IFN- γ was determined by ELISA.

Figure 8. Expression of CD25 and CD69 on redirected CD4+ and CD8+ T cells.

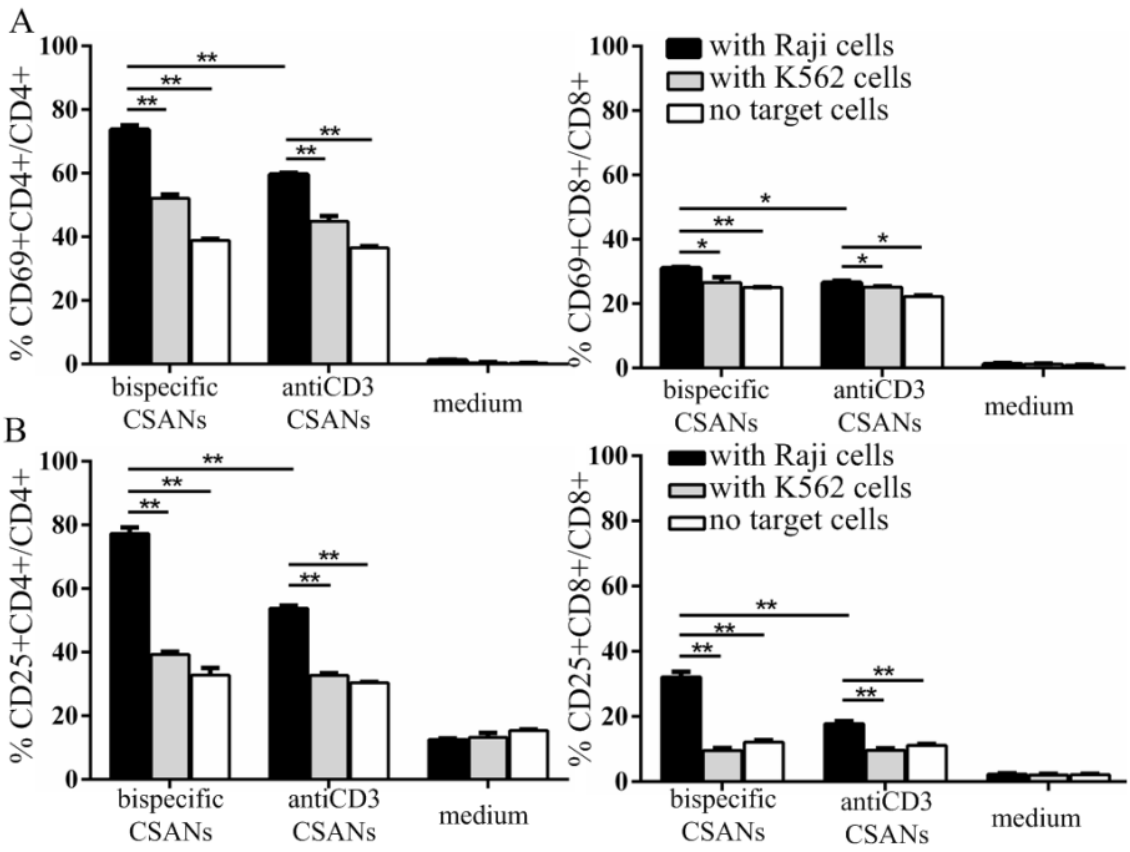

Unstimulated CD4+ or CD8+ T cells were co-cultured with different treatments in the presence or absence of CD22 positive Raji cells or CD22 negative K562 cells for 24 h. The expression of the activation markers CD69 and CD25 on CD8+ T cells (A) or CD4+ T cells (B) was analyzed by flow cytometry. * $P<0.05$ or ** $P<0.005$ with respect to in the absence of Raji cells or with antiCD3 CSANs treatment. Student t test to compare mean ± SD of two groups was used.

Figure 9. Degranulation of CD8+ T cells after cross-linkage with CD22+ Raji cells via bispecific CSANs.

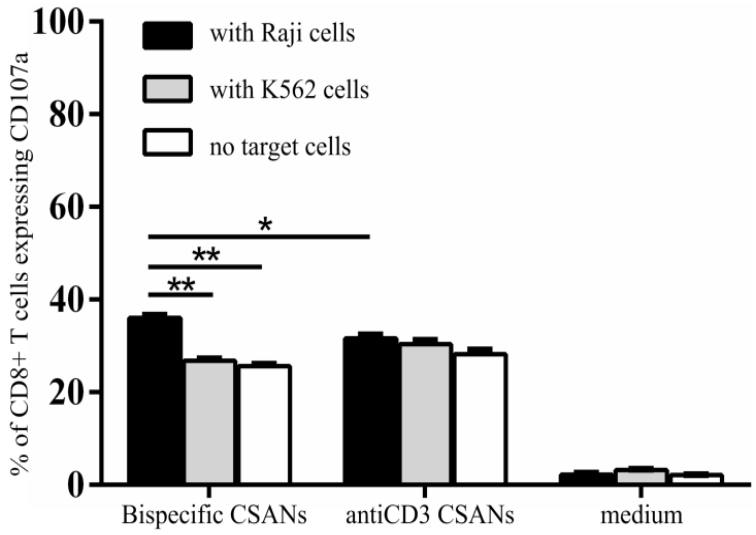

Unstimulated CD8+ T cells were cultured with CD22 positive Raji cells or CD22 negative K562 cells in the presence or absence of antiCD3 CSANs or bispecific CSANs. After 5 h of incubation, the degranulation marker CD107a was analyzed on CD8+ T cell surface. All samples contain APC/antiCD107a mAbs. Data were obtained from one donor and are representative of data from three donors. * $P<0.05$ or ** $P<0.005$ with respect to in the absence of Raji cells or with antiCD3 CSANs treatment.

As can be seen in **Figure 10A**, treatment Raji cells with PBMCs bound to antiCD3 CSANs resulted in a 2-fold increase in the amount of secreted IL-2, when compared to treatment with either antiCD22 CSANs or media control, while in the presence of antiCD3/antiCD22 CSANs a greater than 8- fold increase in IL-2 production was observed relative to the same controls. When compared to incubations with K562 (CD22-) cells or no target cells, a greater than 13- fold increase in IL-2 production was observed. Interestingly, no difference in IL-2 production was observed for PBMCs treated with either antiCD22 CSANs or media, whether in the presence of Raji cells or not, indicating that the CSANs do not inherently lead to T-cell activation. The increase in the IL-2 were found to be consistent with an even greater effect found for both antiCD3/antiCD22 CSANs and antiCD3 CSANs on IFN- γ production (**Figure 10B**). IFN- γ production was only observed when the PBMCs were incubated with antiCD3/antiCD22 CSANs and antiCD3 CSANs in the presence of Raji cells, with a greater than 2- fold increase observed for the bispecific over the antiCD3 CSANs. Taken together, these results demonstrate that the bispecific CSANs were able to selectively redirect T-cells to CD22+ Raji cells. The observed enhanced ability of T-cells functionalized with antiCD3 CSANs to release cytokine production in the presence of Raji cells is likely due to their known expression of MHC-I. The inability of the antiCD3 CSANs to induce cytokine expression by PBMCs in the presence of K562 cells (CD22-, MHCI-) is consistent with this conclusion.

To further assess the role of MHCI expression by Raji cells on the induction of cytokine release by T cells treated with antiCD3/antiCD22 CSANs, purified CD8+ T cells were co-cultured with Raji cells which were pretreated with either the parental mAb

antiCD22 or antiMHC-I in the presence of anti-bodies treatment. As can be seen in **Figure 11**, treatment with antiCD22 mAb reduced the level of IFN-γ production to the same level observed for treatment with antiCD3 CSANs. Treatment with antiMHCI further reduced the level of IFN-γ by CD8+ T cells incubated with antiCD3/antiCD22 CSANs by 50% and by 60% for CD8+ T cells treated with antiCD3 CSANs. Further studies demonstrated that the inclusion of excess amounts of the $DHFR^2$ octamer (**Figure 12**), which does not contain either of the antiCD22 or antiCD3 scFvs, did not affect the production of IFN-γ by PBMCs functionalized with antiCD3 CSANs in the presence of Raji cells. Thus, consistent with our prior results, PBMCs treated with antiCD3 CSANs appear able to induce IFN-γ production in the presence of Raji cells because of their ability to engage MHCI on Raji cells, thus augmenting the effect observed for the bispecific CSANs.

d. Cell cytotoxicity studies

Given the effects of the antiCD3/antiCD22 CSANs on cytokine production, we determined the ability of activated PBMCs to target and carry out the lysis of Raji cells. We first determined the concentration dependence of the bispecific CSANs on cell lysis and found that maximal killing was observed at a concentration of antiCD3/antiCD22 CSANs of 100 to 200 nM (**Figure 13A**). Choosing a concentration of 200 nM (**Figure 13B**), we then varied the effector/tumor cell ratios from 1.25:1 to 20:1 and measured the degree of cell lysis after 24 h. In each case the presence of the bispecific CSANs enhanced cell killing at least 2- fold greater than activated PBMCs alone. These results are consistent with the enhanced level of cytokine production induced by antiCD3/antiCD22 CSANs, relative to antiCD3 CSANs.

Figure 10. Effects of self-assembled antibodies on the cytokine production by PBMCs.

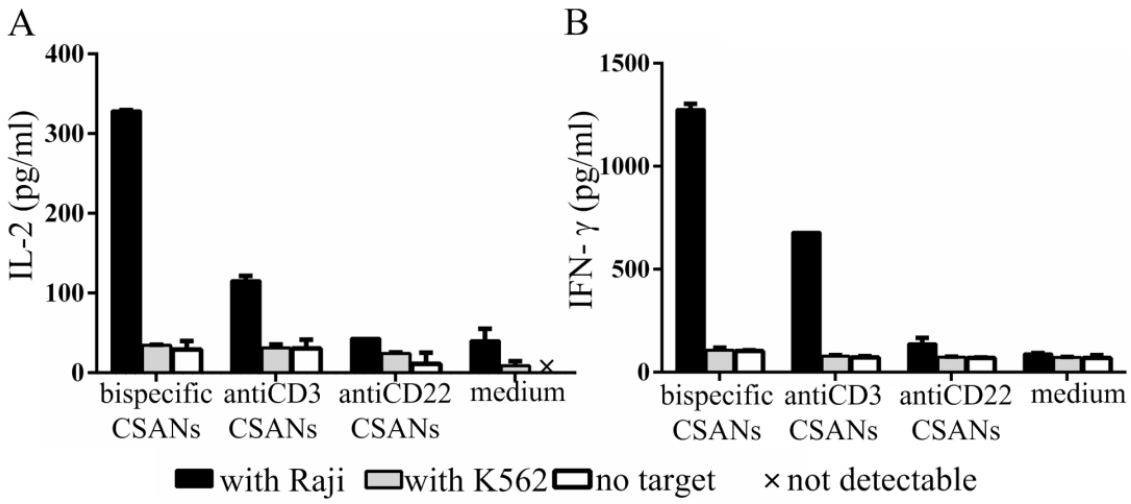

Effects of CSANs on the cytokine production of IL-2 (A) and IFN-γ (B) by PBMCs. Tumor cells Raji or K562 cells and PBMC cells were co-cultured in the presence of different CSANs treatments (E:T=10:1).

Figure 11. IFN- γ release from CD8+ T cells.

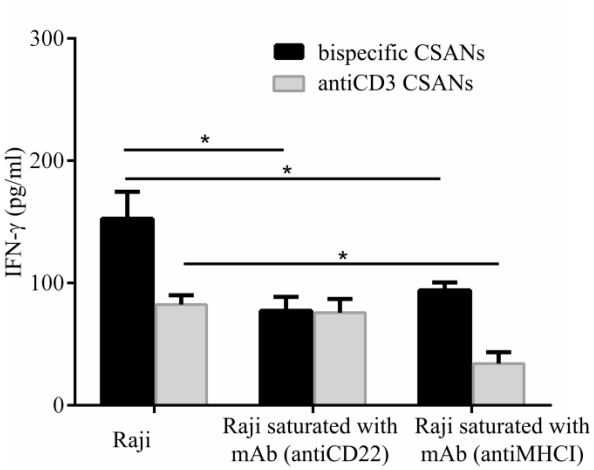

Purified CD8+ T cells were coincubated with either antiCD3 or bispecific CSANs in the presence of target Raji cells. For this study, Raji cells were presaturated with either antiCD22 mAb or antiMHCI mAb. After 24 h incubation, the IFN- γ release in the supernatant was quantified by ELISA. Data were obtained from one donor and are representative of data from two donors. * $P<0.05$ or ** $P<0.005$ with respect to Raji cells presaturated with mAb.

Figure 12. IFN-γ release indicating $DHFR^2$ octamer do not block the interaction between T and Raji cells.

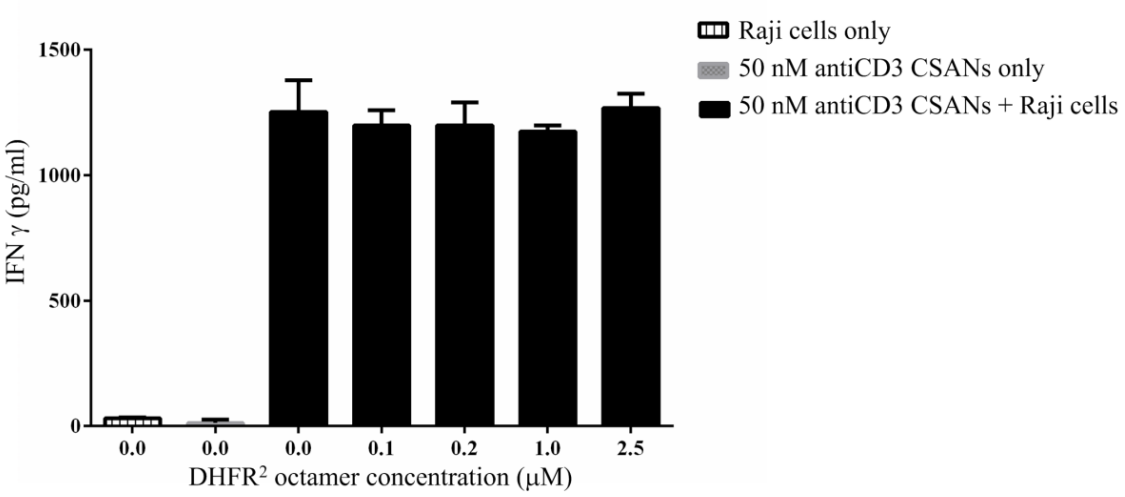

Unactivated PBMCs were incubated with 50 nM of antiCD3 CSANs together with different concentrations of $DHFR^2$. After 24 h incubation, the IFN-γ release was determined in the cell culture supernatant.

Figure 13. Killing capacity of bispecfic CSANs functionalized T cells.

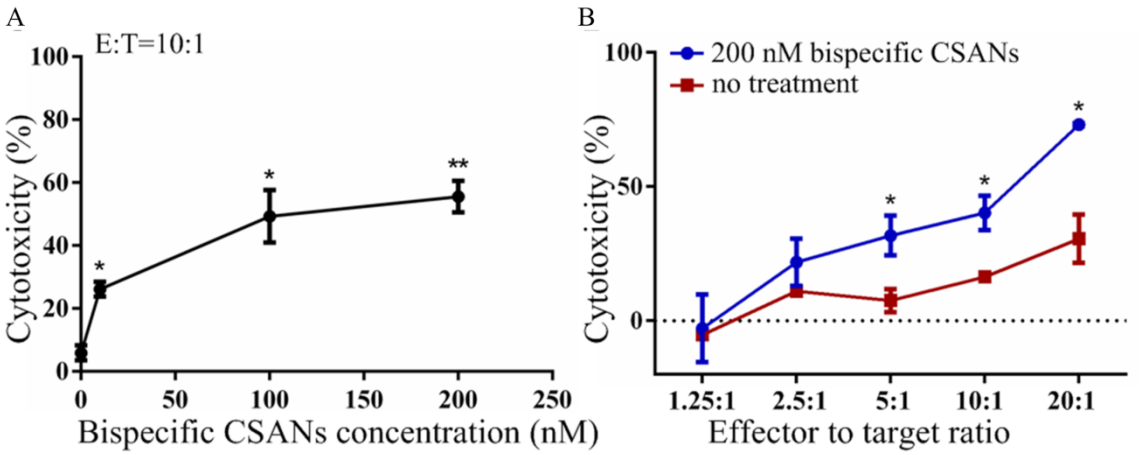

(A) Pre-activated T cells were incubated with variable concentrations of bispecific CSANs at E:T ratio 10:1. (B) Killing capacity of T cells against Raji cells in the presence of 200 nM bispecific CSANs at different E:T ratios.*P<0.05 or ** P<0.005 with respect to in the absence of treatment.

III. **Discussion**

In summary, we have demonstrated that antiCD3 bispecific CSANs can stably bind, but not fully activate T-cells. Once engaged with their target, however, cytokine release is rapidly enhanced and the modified T-cells have an enhanced ability to initiate targeted cytotoxicity. The cytotoxicity induced by bispecific CSANs armed T cells on B lymphoma Raji cells increased by 13% compared to the cytotoxicity of antiCD22 CAR-T cells when E:T ratio is 20:1.[185] Thus, bispecific CSANs can be viewed as prosthetic antigen receptors (PARs) whose presence on the cells can be easily removed by a non-toxic FDA approved drug, trimethoprim. The results of ongoing studies comparing the ability of PARs to serve as a potential, non-genetic compliment to CARs will be reported in due course.

IV. Materials and methods

A. Construction of p1DD13CD22 Plasmid

To prepare the DHFR^{2}antiCD22 fusion protein (1DDantiCD22), we firstly constructed the p13DDantiCD22 plasmid from the p13DD13CD3.2 plasmid template previously made in our lab. The gene for antiCD22 scFv was amplified by PCR from pUM22 plasmid with primers having a 5'- XbaI (TCTAGA) site and 3'- SacI site (GAGCTC). The PCR product and the p13DD13CD3.2 plasmid were double digested, purified and then ligated to form the p13DD13CD22. The p13DD13CD22 plasmid encodes a fusion protein containing a cysteine free ecDHFR coupled by a 13 amino acid linker (GLGGGGGLVPRGT) to a second cysteine-free ecDHFR, followed by a second 13 amino acid linker, containing the XbaI restriction site, to the VH and VL regions of antiCD22 (scFv) gene, and finally a SacI restriction site. Plasmid p1DD13CD22 was obtained by shortening the first linker from 13 amino acids to 1 amino acid (G) by mutagenesis. The primers used for the deletion were forward 5′-GGAGCGGCGGGGCATGATCAGTCTGATTGCGGCGCTAGCGGTAG-3′ and reverse 5′-CAGACTGATCATGCCCCGCCGCTCCAGAATCTCAAAGCTATAGC-3′. DNA sequencing analysis (University of Minnesota, Biomedical Genomics Center) was used to confirm the gene was correct in sequence and had been cloned in frame.

B. Protein expression, refolding, and purification

1DDantiCD22 protein was expressed, refolded, and purified by our previously reported method.[180,160] Briefly, the protein was over expressed in the Escherichia coli strain Rosetta (DE3) (Millipore). The inclusion bodies were obtained by sonicating cells in lysis buffer, followed by refolding the protein with the sodium N-lauroyl-sarcosine

(SLS) air oxidation method. The refolded protein was purified by a FFQ column, a MTX affinity column and a size exclusion column.

C. Size exclusion chromatography

1DDantiCD3 and 1DDantiCD22 were incubated with dimerizer bisMTX-C9 at 1:1:2.2 ratios in P500 buffer (0.5M NaCl, 50mM KH_2PO_4, 1mM EDTA, pH 7) for 1 hour at room temperature. Then the protein solution was injected into a Superdex G200 size exclusion column (Amersham Biosciences, USA), eluted with P500 buffer and the relative peak sizes quantitated by absorbance at 280nm.

D. Dynamic light scattering

DLS measurements were performed on a Brookhaven 90Plus Particle Analyzer (Holtzville, NY) with a 35 mW red diode laser. Samples (1.5 mL) were measured at room temperature in suspensions of PBS at (1mg/mL).

E. Cell culture, isolation of PBMCs and T cell subpopulation

Human PBMCs were isolated from buffy coats of healthy donors blood sample by Ficoll density gradient centrifugation. Unactivated CD8+ or CD4+ T cells were isolated from PBMCs by positive selection using CD8+ or CD4+ T cell isolation kit (Invitrogen Life Technologies, Grand Island, NY). Pre-activated T cells were prepared according to the following protocol: PBMC 2×10^6 cells/well in 24 well plates were stimulated with 150 μl antiCD3/CD28 dynabeads and 50 U/mL of IL-2, 10 ng/mL of IL-7 and 50 μM β-mercaptoethanol for at least one week in complete RPMI 1640 medium (Lonza) supplemented with 10% (v/v) fetal bovine serum, L-glutamine (final concentration of 2mM) , Penicillin (100 units/mL), and Streptomycin (100 μg/mL) in a humidified

incubator with 5% CO_2 at 37 ˚C. Thereafter the medium was replaced with fresh complete RPMI medium. Those T cells were used as effector cells for cytotoxicity assay and termed as pre-activated T cells. Raji and Daudi (B lymphoma) and K562 (chronic myelogenous leukemia) cells were cultured in complete RPMI medium.

F. *In vitro* competitive binding assay to measure Kd of 1DDantiCD22

The Kd value of 1DDantiCD22 monomer and octamer were determined by our previously reported method.[180] After pre-mixing a dilution series of purified 1DDantiCD22 monomer or octamer with the subsaturating concentration of PE-labeled RFB-4 mAb, 5×10^6 Raji cells were incubated with antibodies mixture in PBS supplemented with 1% BSA and 0.1% sodium azide (FACS buffer) for 30 minutes at room temperature. The cells were then washed, and fluorescence intensities of cell bound PE-labeled antibodies were quantitated by FACS BD LSR II. Percentage of fluorescence inhibition was calculated by subtracting the mean fluorescence observed at given competitor concentration from 100% binding, which was defined as mean fluorescence observed in the absence of competition, then divided by 100% binding. Relative affinities were calculated from the corresponding IC_{50} values according to the equation: $K_D(I)=IC_{50}/(1+[PE\text{-}RFB4]/K_D(PE\text{-}RFB4))$, where I is the unlabeled inhibitor, [PE-RFB4] is the concentration of PE-RFB4 used in the competitive reaction, K_D(PE-RFB4) is the binding affinity of PE-RFB4, IC_{50} is the concentration of the inhibitor that yields 50% inhibition of binding. K_D(PE-RFB4) was determined as previously described by fitting mean fluorescences of cell bound PE labeled RFB4 observed at different concentrations of PE-RFB4 to the Lineweaver-Burk equation: $1/F=1/Fmax+(K_D/Fmax)(1/[PE\text{-}RFB4])$.

G. Cytotoxicity assay

Cytotoxicity was measured by levels of LDH (lactate dehydrogenase) release from lysed cells using CytoTox96® Non-Radioactive Cytotoxicity Assay kit (Promega). The appropriate number of pre-activated T cells, according to the requested effector (E) to target (T) cell (E/T) ratio as indicated in the respective experiment, were pipetted to each well of a round bottom 96-well plate and pre-treated with bispecific CSANs for 30 minutes at room temperature. Then 5×10^3 Raji cells were pipetted in. Complete RPMI medium was added up to 200 μl and the plate was incubated for 24 h under standard conditions.

For estimation of the maximum release, Raji cells without PBMCs were solubilized by lysis buffer (provided in the assay kit). The absorbance at 490 nm was recorded using a Synergy H1 Multi-Mode Reader (Biotek). The percent cytotoxicity was calculated as ((LDH release sample − SReffector − SRtarget)/(MRtarget− SRtarget)) × 100. SR: spontaneous release; MR:maximum release. All samples were measured as triplets. Statistical analysis of mean specific lysis was performed by Student's t-test. The p values < 0.05 were considered significant.

H. Fluorescence Confocal Microscopy

FITC-bisMTX and 1DDantiCD22 were mixed (1 μM) and added to 1×10^6 Daudi cells at either 4 or 37 ℃ for 1 h in RPMI medium. Cells were then pelleted by centrifugation (400g for 5 min). After being washed twice with PBS, cells were then fixed with a 4% paraformaldehyde solution for 10 min and washed thrice with PBS. Cells were incubated on Poly-Prep slides coated with poly-L-lysine (Sigma) at 4 or 37 ℃ for 30 min. Finally, cells were treated with ProLong Gold Antifade reagent with DAPI

(Invitrogen), and a coverslip was applied. After overnight incubation, images were taken within inner sections of the cells by sequential scanning using an Olympus FluoView 1000 BX2 upright fluorescence confocal microscope. Resulting images are the compression of three to five z-axis slices.

I. Flow cytometric analysis

For PBMC, pure CD4+ or CD8+ T cells analysis, single cell suspensions were stained with the following mAbs: APC-conjugated CD69 (BD Biosciences), PE/Cy7-conjugated CD25 (BD Biosciences), APC-conjugated anti-human CD107a (LAMP-1) (BD Biosciences), PE-conjugated anti-human CD8 (BD Biosciences), and FITC-conjugated anti-human CD4 (BD Biosciences). The cells were phenotypically acquired on the LSRII (BD Biosciences) and analyzed with FlowJo software (Tree Star, Inc.).

To test the specific binding of CSANs to Raji and PBMC cells, Raji cells and PBMC were treated with FITC-bisMTX dimerized 0.5 μM antiCD3 CSANs, antiCD22 CSANs or bispecific antiCD3/antiCD22 CSANs. As positive control, PBMC and Raji cells and were stained with either 10 nM FITC conjugated UCHT1 or FITC conjugated RFB4.

J. Activation assay with bispecific CSANs

In one well of a 48-well plate, 5×10^5 PBMCs were co-cultured with 5×10^4 Raji cells (CD22 positive) at a ratio of 10:1, in the presence or absence of 100 nM antiCD3 CSANs, bispecific antiCD3/antiCD22 CSANs, 100 nM $DHFR^2$(1DD) octamer, or 100nM UCHT-1 $F(ab)_2$ in a total volume of 400 μl RPMI 1640 medium, without additional cytokines for 24 h at 37 ℃. Pure CD4+ and CD8+ T cells were also analyzed for activation assay. As a negative control, CD4+ and CD8+ T cells were also incubated with K562 cells (CD22

negative) at a ratio of 10:1 in the presence of 100 nM antiCD3 CSANs or bispecific antiCD3/antiCD22 CSANs. All samples were analyzed as triplicates.

K. Degranulation assay

In one well of a 48 well plate, 6×10^5 pure CD8+ T cells were cocultured with 6×10^4 Raji cells or K562 cells in the presence of 100 nM antiCD3 or bispecific CSANs. In addition, 8 μl antiCD107a APC mAb (BD Biosciences) and complete RPMI 1640 were pipetted to each well (final volume of 400 μl). After 1 h of incubation at 37 ℃, 0.27 ul of BD GolgiStop (BD Biosciences) and 0.4 ul of BD GolgiPlug (BD Biosciences) were added. After an additional incubation of 4 h, cells were spun down and washed with ice-cold FACS buffer. Flow cytometry analysis was performed on a FACS BD LSR II (BD Biosciences). All samples were analyzed as triplicates.

L. Determination of cytokine concentration

In one well of a round bottom 96-well plate, 5×10^4 PBMC cells were co-cultured with Raji or K562 cells in the presence of 50 nM antiCD3 CSANs or bispecific antiCD3/antiCD22 CSANs for 24 h at 37 ℃. Complete RPMI medium was added to make final volume 200 μl. The amount of IL2 and IFN γ in the cell culture supernatant was quantified by OptEIA ELISA Sets (BD Biosciences), according to the manufactures protocol.

M. Competitive disassembly of bispecific antiCD3/antiCD22 CSANs

5×10^5 PBMC cells were incubated with 1 uM bispecific CSANs (pre-determined as the concentration of bispecific CSANs that saturate 5×10^5 PBMC cells in 100 μl medium) (one equivalent of 1DDantiCD3 and one equivalent of 1DDantiCD22 were

incubated with three equivalents of dimerizer FITC-bisMTX in Phosphate buffered saline (PBS) for 1 h to allow complete oligomerization) for 1 h at room temperature. Excess CSANs were washed away. Cells were then resuspended in different concentrations of trimethoprim and incubated for another 1 h at 37 ˚C. Cells were washed with PBS supplemented with 1% BSA and 0.1% sodium azide (FACS buffer) twice and counted by FACS BD LSR II.

N. Time course study of the stability of bispecific antiCD3/antiCD22 CSANs

5×10^5 PBMC cells were incubated with either 1 uM bispecific CSANs or 1 uM 1DDantiCD3 monomer for 1 hour at room temperature. Cells were then washed and plated in 48 well plates. On each day of the next following five days, cells with antibodies treatment were washed with FACS buffer and stained with saturation amount of FITC mAb antiCD3. To check the maximum fluorescence, the same number of cells were incubated with RPMI complete medium only and stained with saturation amount of FITC mAb antiCD3. This experiment was run in triplicates for each time point. Percentage of fluorescence inhibition was calculated by subtracting the mean fluorescence observed at given competitor concentration from 100% binding, which was defined as mean fluorescence observed in the absence of competition, then divided by 100% binding.

Chapter Four: Chemically Self-Assembling Protein Nanorings Prepared with CpG Chemical Dimerizers Elicit a Th-1 Type Immune Response

I. Introduction

In modern vaccination, protein antigen-based subunit vaccines have been explored as a safer alternative to traditional weakened or killed whole organism based vaccination strategies.[190,191] However, without an optimized delivery strategy and including adjuvants, those subunit vaccines weakly stimulate the immune system and induce both limited antibody response and minimal cellular immunity. To enhance the immunogenicity of an antigen and increase their efficacy, molecular adjuvants that act by immunopotentiation through innate immune receptor (eg. Toll-like receptors (TLRs)) can be added.

TLRs are pattern recognition receptors that trigger innate immunity, providing immediate protective responses against pathogens. Among the ten TLRs described in human,[192] TLR9 is triggered by CpG oligodeoxynucleotides (ODN) containing unmethylated CpG dinucleotides (referred to as CpG motifs) in a consensus of 5'-pur-pur-CpG-pyr-pyr-3'.[193] CpG is underrepresented (CpG suppression) and selectively methylated in vertebrate DNA, but is present at the expected frequency (1/16 bases) and unmethylated in bacterial DNA.[193,194] CpG ODNs have many effects on the innate immune system, including the direct stimulation of B cells to proliferate and secrete more immunoglobulin (Ig),[195] induction of rapid cellular activation and cytokine release including IL-12, TNF-α and IL-6 from antigen presentation cells (APCs) such as macrophages and dendritic cells (DCs).[195,196] The cytokines produced by APC stimulate natural killer (NK) cells to secrete interferon gamma (IFN-γ) for increased lytic activity. In addition, CpG ODNs enhance the generation of antigen-specific responses and the expression of co-stimulatory molecules.[197] Therefore, CpG ODNs have received a great

deal of attention as promising vaccine adjuvants against a range of diseases including infectious diseases, cancer and allergies.[198,199,200]

While CpG ODNs have potent immunostimulatory effect, the major limitations hindering their application include their rapid degradation, absorption and inefficient delivery to target cells or tissues.[201] Several strategies for enhancing the immune response using CpG ODNs have been reported, such as direct conjugating CpG ODN to protein antigens.[202,203] However, there are limitations associated with antigen-CpG ODN conjugates as a vaccine formulation: (i) the efficiency and number of conjugates is dependent on the chemical characteristics of the antigen; (ii) the antigenic epitopes may be altered during the conjugation process. Alternative delivery approaches have been explored, including co-encapsulation of CpG ODN with antigenic proteins or peptides in PLGA nanoparticles,[204,205] self-assembled virus like nanostructures,[206] non-covalent conjugation to streptavidin by biotinylation,[207] or conjugating CpG ODN on the surface of antigen containing nanoparticles.[208]

Here, we report an alternative one step preparation process to achieve the multivalent co-delivery of CpG and antigens without chemical conjugation. Previously we have demonstrated that in the presence of the chemical dimerizer bisMTX, two *E. coli* dihydrofolate reductase molecules ($DHFR^2$) that have been fused together through a peptide linker can spontaneously assemble into a range of chemically self-assembled nanorings (CSANs) whose size varies depending on the length and composition of the linker peptide between the DHFRs.[160,165,181,182] If the linker is a single glycine, we observed formation of rings containing 7 to 10 $DHFR^2$ (1DD) fusion proteins with an average ring diameter of 25-30 nm and height of 5 nm.[160,182] Further, bisMTX ligands

with a third arm functionalized with oligonucleotides (bisMTX-Oligo) have been developed as a method for the programmable self-assembly of antibody and small molecule oligonucleotide conjugates, as well as for the targeted delivery of antisense oligonucleotides.[209,210]

To explore the potential of $DHFR^2$ based CSANs to be used as vaccines by the multivalent display of an antigen and adjuvant, we prepared CSANs and CSANs assembled with the bisMTX dimerizer linked to CpG oligonucleotides (bisMTX-CpG) and compared their immune responses in mice.

II. Results and Discussion

A. Characterization of CpG CSANs

We have prepared a bisMTX molecule with a third arm containing a maleimide for reaction with thiol functionalized oligonucleotides[211] CpG 1826 and ODN 1982. $DHFR^2$ monomer (1DD) protein was incubated for 1 hour with either CpG 1826 trilinker or ODN 1982 trilinker (1:1.2 equiv), and the assembled proteins were analyzed by size-exclusion chromatography (**Figure 1**). Similar to CSANs previously prepared with bisMTX[182] or bisMTX-oligonucleotides,[25] CSANs prepared with either bisMTX-CpG 1826 or bisMTX-ODN 1982 eluted in a broad peak centered at 20 min (**Figure 1**) with almost 100% oligomerization of 1DD monomer (33.5 min). Incorporation of bisMTX into the CSANs was verified by the observance of the overlapping MTX absorbance at 305 nm. The hydrodynamic radius of purified CpG CSANs was determined by dynamic light scattering (**Figure 2 B**) was 9.84 ± 0.01 nm, which was found to be modestly lower than the value observed for CSANs 12.9 ± 0.01 nm, (**Figure 2 A**) prepared with bisMTX.

Figure 1. Characterization of self-assembled protein nanorings by SEC.

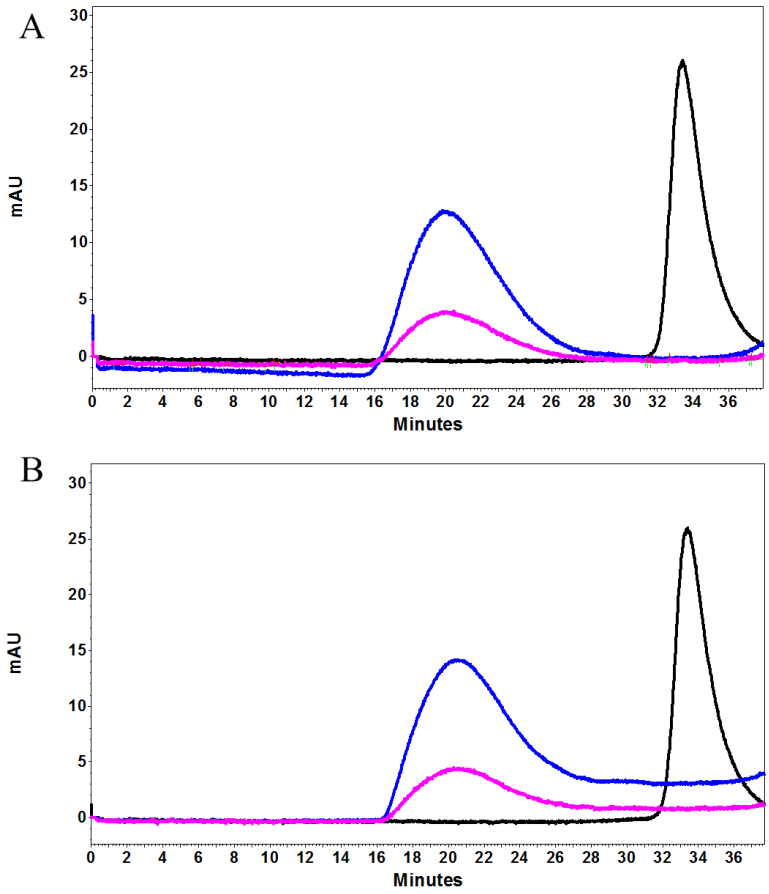

The assembly of CpG 1826 CSANs (A) and ODN 1982 CSANs (B) was characterized by size exclusion chromatography. Blue curve: A_{280} nm; Purple curve: A_{304} nm; Black curve: DHFR[2] monomer (1DD).

Figure 2. Characterization of self-assembled protein nanorings by dynamic light scattering.

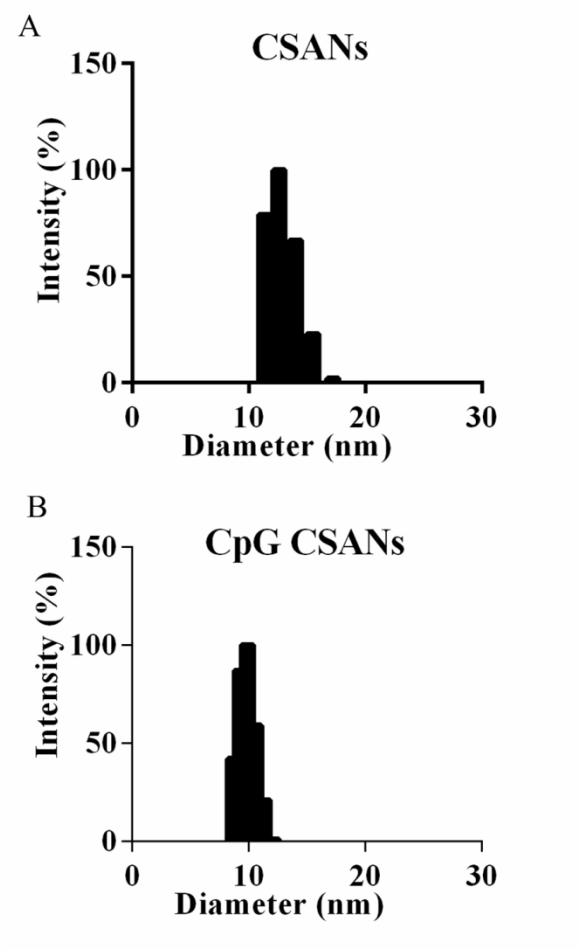

B. CpG CSANs and free CpG 1826 elicit similar level of immunomodulatory activity *in vitro*

To assess the *in vitro* immunomodulatory activity of the CpG-CSANs, CpG-CSANs were incubated with isolated splenocytes from three naive mice for 24 h. Their ability to induce expression of the co-stimulatory protein, CD86 (B7-2) and T-cell dependent antibody class switching and germinal center protein, CD40, on antigen presenting cells (APCs) was determined and compared to incubation with the $DHFR^2$ monomer (1DD), CSANs, CpG 1826, ODN CSANs or ODN 1982. As shown in **Figure 3**, both free CpG 1826 and CpG CSANs treated splenocytes upregulated CD86 (B7-2) ($P=0.19$) and CD40 ($P=0.94$) to similar levels. However, significant enhancement of CD86, but not CD40, expression over the control treated splenocytes was observed. Neither the $DHFR^2$ monomer nor the CSANs upregulated CD86 or CD40, compared to medium treated control cells, thus indicating that DHFR does not inherently activate splenocytes *in vitro*. In addition, induction of CD86 or CD40 was not observed for either the control oligonucleotide, ODN 1982, or conjugated form, ODN CSAN.

Figure 3. Upregulation of costimulatory molecules on the B cells surface is CpG dependent.

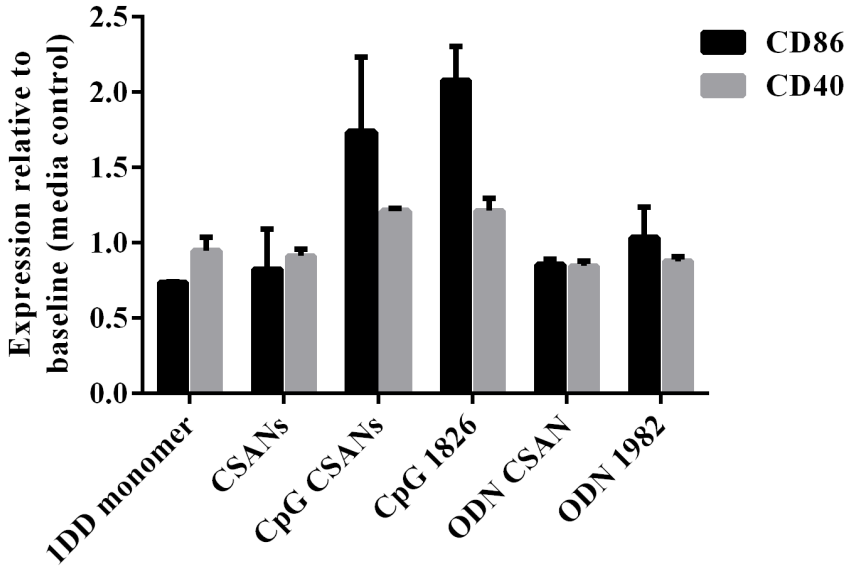

Flow cytometry was used to measure cell surface molecules expression on gated CD19+ B cells of naive BALB/c mice splenocytes after a 24 h incubation with 0.2 uM of either the $DHFR^2$ monomer, CSANs, CpG-CSANs, CpG 1826, ODN CSANs or ODN 1982. The relative mean fluorescence intensity (MFI) value was quantified and related to the MFI of expression levels on cells cultured in medium alone. Data are the average results from three mice.

To assess the effect of CpG-CSANs on cytokine release by splenocytes, the increase in the amount of IL-6, which leads to maturation of B cells, and TNF-α, which stimulates DC maturation and T-cell activation, was determined. CpG CSANs and CpG 1826 treated cells were found to release comparable amounts of IL-6, while no significant release of IL-6 was observed for cells treated with either ODN 1982 and ODN 1982 CSANs (**Figure 4**) or $DHFR^2$ monomer (1DD) and CSANs (data not shown). TNF-α release was not observable by treatment with either CpG-CSANs or the controls (Data not shown).

To further determine the ability of the CpG CSANs to activate APCs, mouse macrophage RAW 264.7 cells were incubated with variable concentrations of CpG CSANs and the corresponding control groups overnight. Significantly higher concentrations of IL-6 (**Figure 5A**) and TNF-α (**Figure 5B**) release was detected for cells treated with CpG 1826 and CpG CSANs than ODN 1982 and ODN 1982 CSANs. Neither IL-6 or TNF-α release was detected for RAW 264.7 cells treated with either $DHFR^2$ monomer or CSANs (data not shown), a finding which is consistent with complete removal of potentially contaminating lipopolysaccharide (LPS).[192]

Figure 4. CpG ODN induces cytokine release from naive BALB/c mice splenocytes.

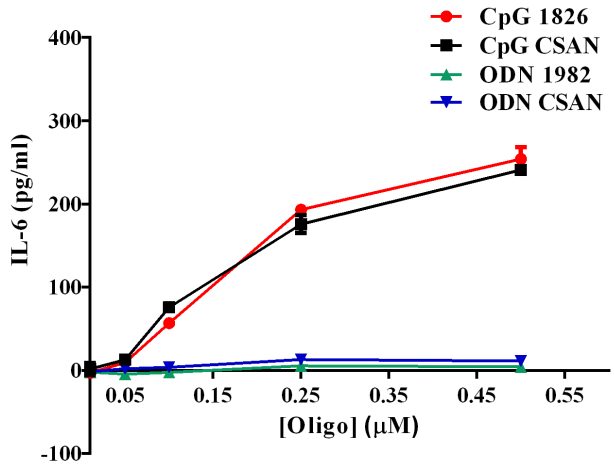

Mice splenocytes were isolated from naive mice and incubated with different concentrations of treatment and control groups overnight. The supernatants were probed for IL-6 release by ELISA. Data are the average of two mice donors. Points show mean ± SD.

Figure 5. CpG ODN induced cytokine release from RAW 264.7 cells.

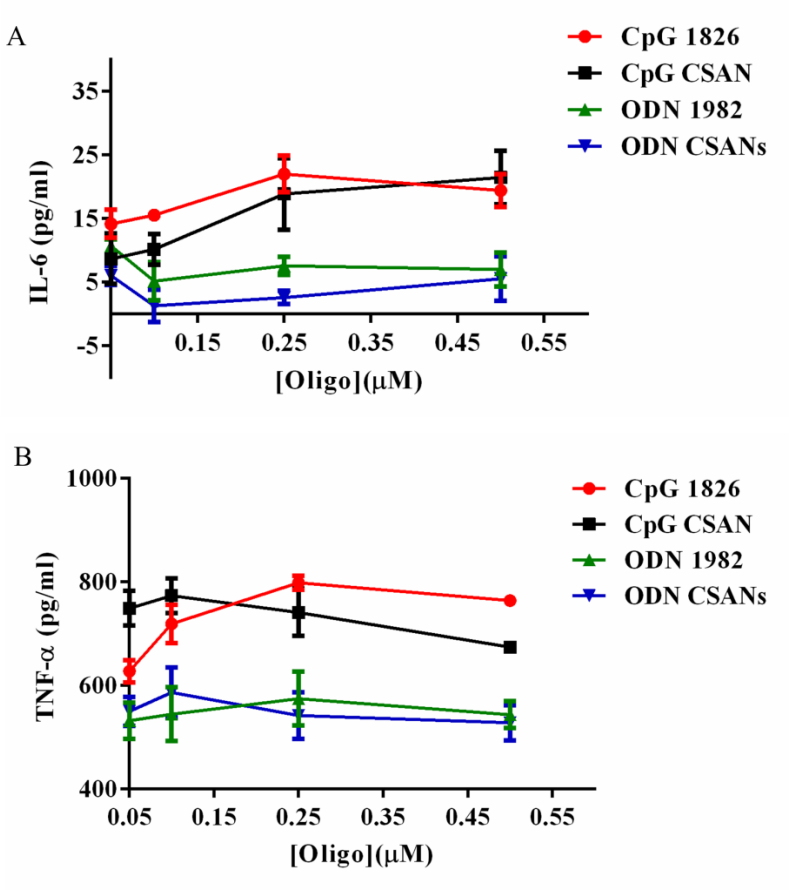

RAW 264.7 cells were incubated with treatments overnight. The supernatants were probed for IL-6 (A) and TNF-α(B) release. Points show mean ± SD.

C. Uptake of CSANs and CpG CSANs by RAW264.7 cells

The internalization of antigens by APCs, which triggers antigen presentation, is a key step in the generation of potent immune responses. To evaluate the uptake of CSANs and CpG CSANs by macrophages, RAW264.7 cells were incubated with FITC labeled CSANs or CpG CSANs for 1 h at 37 ˚C. The fluorescence intensity obtained by flow cytometry demonstrated that both the CSANs and CpG CSANs (**Figure 6A**) were taken up by the cells to the same extent. When cells were treated with CpG CSANs together with either CpG 1826 or control ODN 1982, the amount of CpG CSANs taken up by the RAW264.7 cells was modestly, but significantly reduced by 16% and 18%, respectively, while little effect was observed on the uptake of the CSANs (**Figure 6 B**).

Previously, it has been shown that nanoparticles displaying oligonucleotides are internalized by phagocytic cells through the Class A Scavenger Receptor (SRA).[212] SRA internalization of these particles has been shown to be inhibited by fucoidan or polyinosine (polyI).[213] After pre-incubation of the RAW264.7 cells with either fucoidan or polyinosine (polyI) the fluorescence of cells treated with CpG CSANs (**Figure 6A**) dramatically decreased by 73% and 85%, respectively. Whiles the fluorescence of cells treated with CSANS (**Figure 6B**) decreased by 68% and 79% respectively. Thus, although internalization of the CSANs and oligonucleotides is not self-exclusionary, the uptake of both, including CpG CSANs is dependent on SRA.

Figure 6. Cellular uptake of self-assembled protein nanorings.

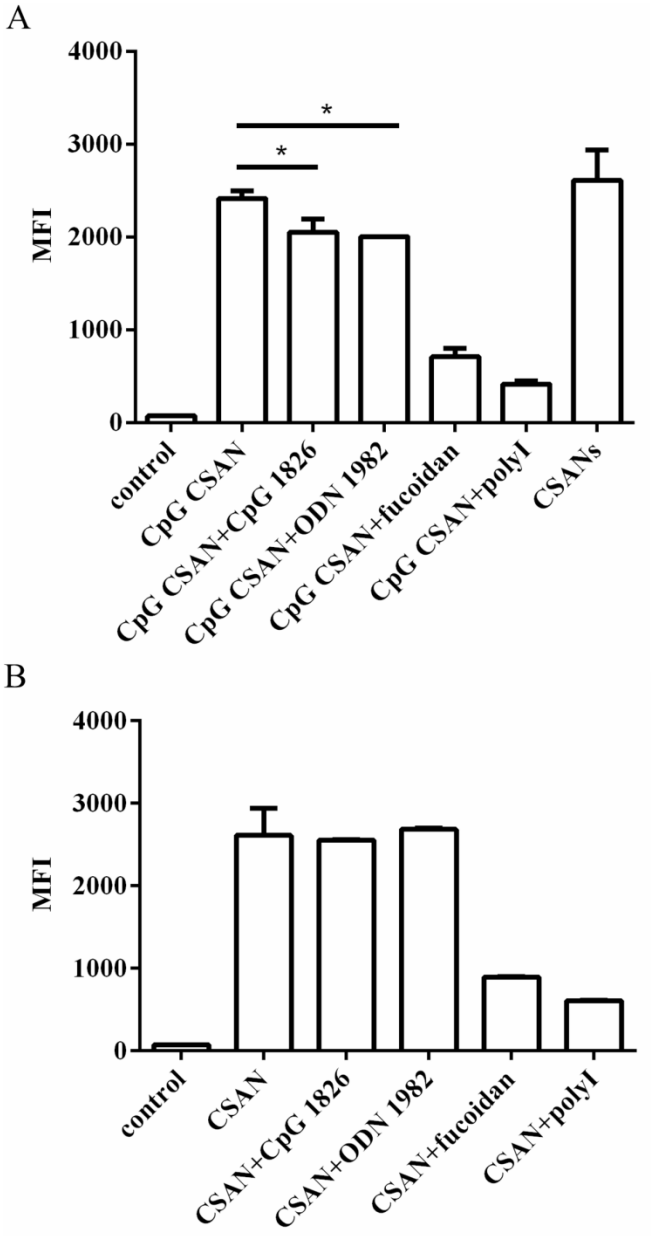

Cellular uptake of CpG CSANs (A) and CSANs (B) by RAW264.7 cells. The cells were incubated with FITC labeled proteins in the presence of either CpG 1826, ODN 1982, fucoidan or polyI. The uptake amount was measured by flow cytometry indicated by mean fluorescence intensity. Samples were run in triplicates.

D. CpG CSAN stimulate DHFR-specific Ig response

In response to the antigen challenge by CpG-CSANs, the amount of antibodies specific to DHFR (total IgG) were quantified by ELISA. As shown in **Figure 7**, mice immunized with CpG CSANs but not ODN 1982 CSANs elevated the levels of antigen-specific IgG gradually from day 13 to day 30. In contrast, no significant increase at day 13, 21 and 30 in the amount of IgG was observed for immunization with either the CSANs (P=0.4559) or the mixture of CSANs and free CpG 1826 (P=0.0754). In addition, inflammatory cytokines such as IL-6 and TNF-α were not detectable in the serum on day 30 both CpG-CSANs and control immunizations.

Previously, it has been shown that CpG ODN induced a strongly Th1-dominated response to vaccine, as measured by production of antigen-specific IgG2a antibody.[214] Examination of the IgG isotypes present in the plasma 30 days after immunization revealed that no significant IgG1 or IgG2a was induced by the CSANs, when compared to the PBS control and ODN CSANs (**Figure 8**). In contrast, unlike ODN CSANs or CSANs, CpG CSANs immunizations resulted in the generation of antigen specific IgG2a, but no significant amounts of IgG1(**Figure 8**).

Figure 7. CpG CSANs enhanced anti-DHFR IgG response in immunized mice.

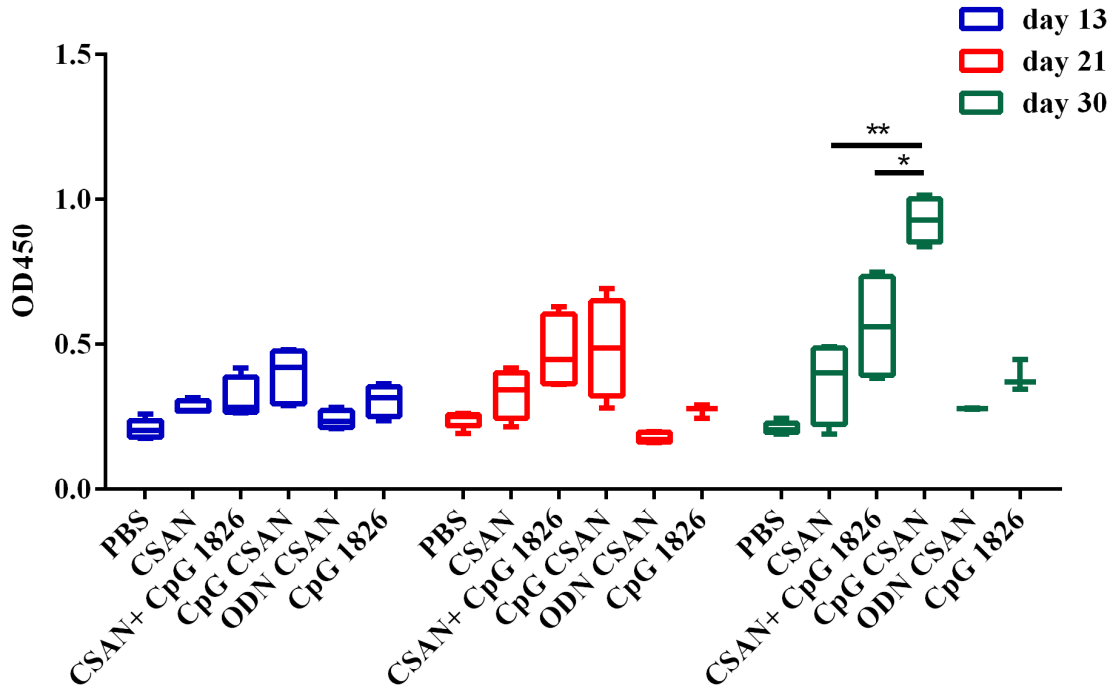

On day 13, 21 and 30 since the first immunization, sera were collected for estimation of anti-DHFR IgG antibodies by ELISA. Data were shown as absorbance values at 450 nm wavelength at appropriate dilutions. Each bar represents the mean value of absorbance value OD450 ± SD for each group (n=4). Values of $p < 0.05$ were considered significant and were indicated as follows: *$p < 0.05$; **$p < 0.01$. Statistical differences between the groups were determined by one-way ANOVA analysis and Student t test.

Figure 8. Concentrations of antigen-specific IgG1 and IgG2a antibodies on day 30 after immunization.

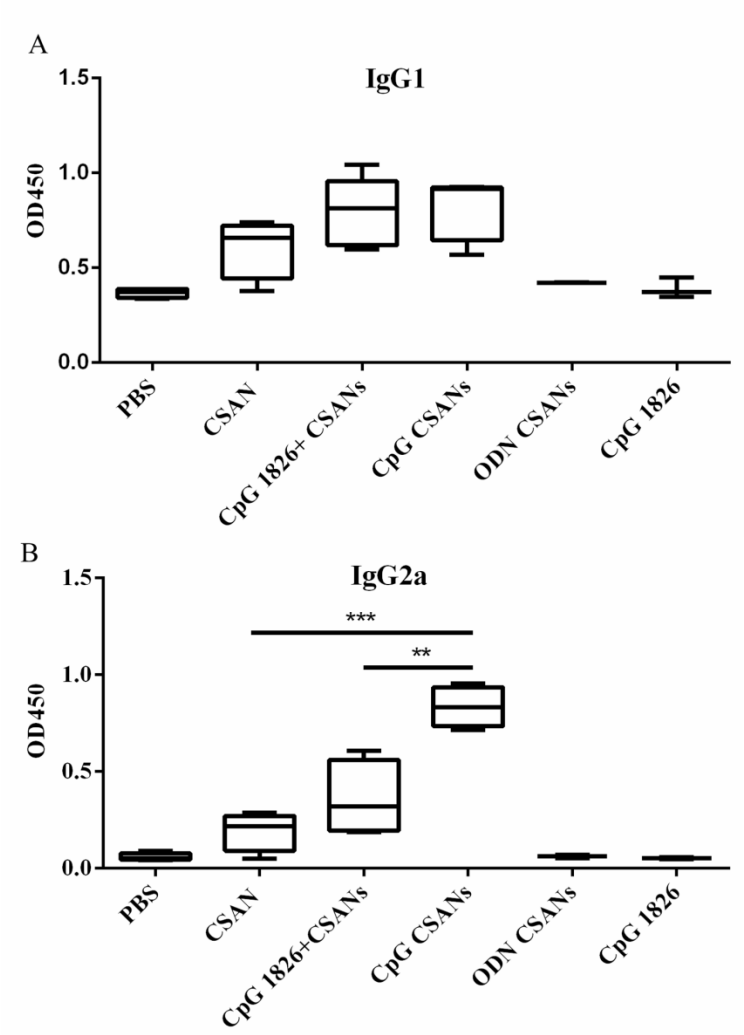

The levels of antigen-specific IgG1 (A) and IgG2a (B) antibodies were measured by ELISA. Data are shown as absorbance values at 450 nm wavelength at appropriate dilutions. Each bar represents the mean value of OD450±SD for each group (n=4). Values of $p < 0.05$ were considered significant and were indicated as follows: *$p < 0.05$; **$p < 0.01$; **$p < 0.001$. Statistical differences between the groups were determined by one-way ANOVA analysis and Student t test.

III. **Conclusion**

CSANs displaying ligands such as scFvs and peptides have been shown to target cells and tissues both *in vitro* and *in vivo*.[215] In this study we have examined the immunogenicity of CSANs prepared with bisMTX and $DHFR^2$ and found that, while they are easily taken up by APCs, they do not either elicit the release of inflammatory cytokines such as IL-6 and THF-α or activate B-cells resulting in the production of antigen specific IgG. CSANs that have been assembled with the chemical dimerizer, bisMTX-CpG are also internalized by APCs, but in contrast to CSANs, induce the production of IL-6 and TNF-α. Relative to CpG 1826 alone, the polyvalency of the CpG CSANs does not seem to have an observable effect on the amount of cytokine release. Similar to polyvalent VLPs, however, immunization of the mice with CpG CSANs resulted in a Th1 type response that is dominated by the polyvalent engagement with B-cell BCRs. Thus, the co-stimulation of B-cells by a polyvalent antigen and TLR9 agonist can lead to the production of IgG2a, one of the most potent antiviral and antibacterial antibodies. [216] The modularity of CSANs, which allows the site-specific incorporation of molecular adjuvants, as well as the recombinant engineering of $DHFR^2$ antigen fusion proteins, will allow us to explore the potential for this platform to serve as a vaccine strategy.

IV. Materials and Methods

A. Synthesis of Bis-MTX-Maleimide

The synthesis of BisMTX-maleimide was reported earlier.[209] BisMTX-NH_2 was mixed with 5 eq of N-succinimidyl 4-maleimidobutyrate and 1 eq of N, N,-diisopropylethylamine (DIPEA) in dimethyl formamide (DMF) and stirred at room temperature overnight. The product was then purified by HPLC using 0.1% TFA in water (solvent A) and 0.1% TFA in acetonitrile (solvent B) (RediSep Rf Gold 100 Å C18 Columns). Product peak was isolated using a gradient of 2% to 40% B. Relevant fractions were pooled and lyophilized prior to storage (yield 85 %). BisMTX-Maleimide was characterized LC-ESI-MS (Mw=1356).

B. LC-ESI-MS analysis of bis-MTX-maleimide

Completion of reaction and formation of products were purified by HPLC using 15 mM ammonium acetate (solvent A) and 100% acetonitrile (B) on Haisil C18 RP column (5 µm, 250 x 4.6 mm, Haggins Analytical Inc). Product peak was isolated using a gradient of 2% to 25% B. Relevant fractions were pooled and speedvac prior to storage or analysis. For LC-ESI-MS, Zorbax SB-C18 column (150 mm x 0.5 mm, 5 µm, Agilent Technologies, Inc.) was used. Sample was eluted with 15 mM ammonium acetate (A) and 100% acetonitrile (B) with gradient of 2 % B to 75 % B over 35 min. 1st channel is TIC (Total Ion Current), 2nd channel is UV302 nm (bisMTX) and 3nd channel is ionization pectra.

Figure 9. Scheme for the synthesis of bis-MTX-maleimide.

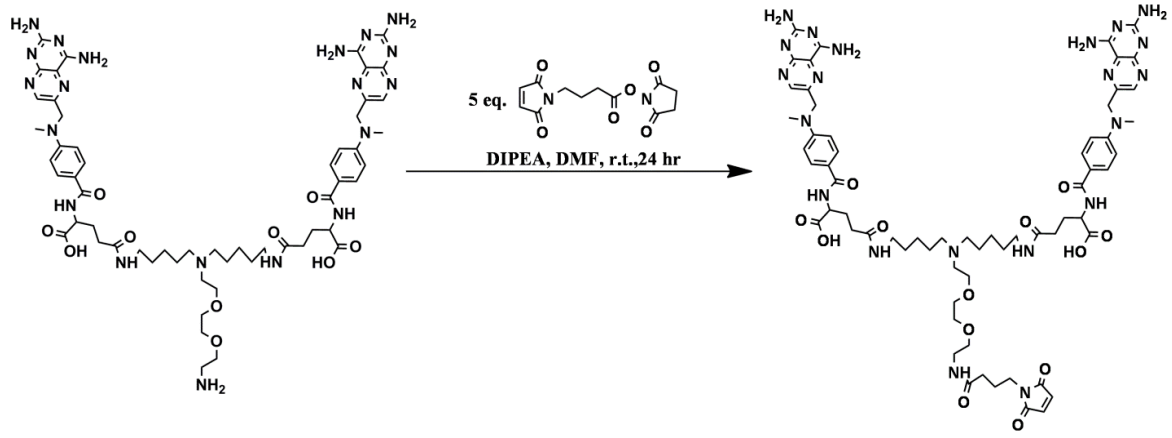

Figure 10. LC-ESI-MS of bis-MTX-maleimide

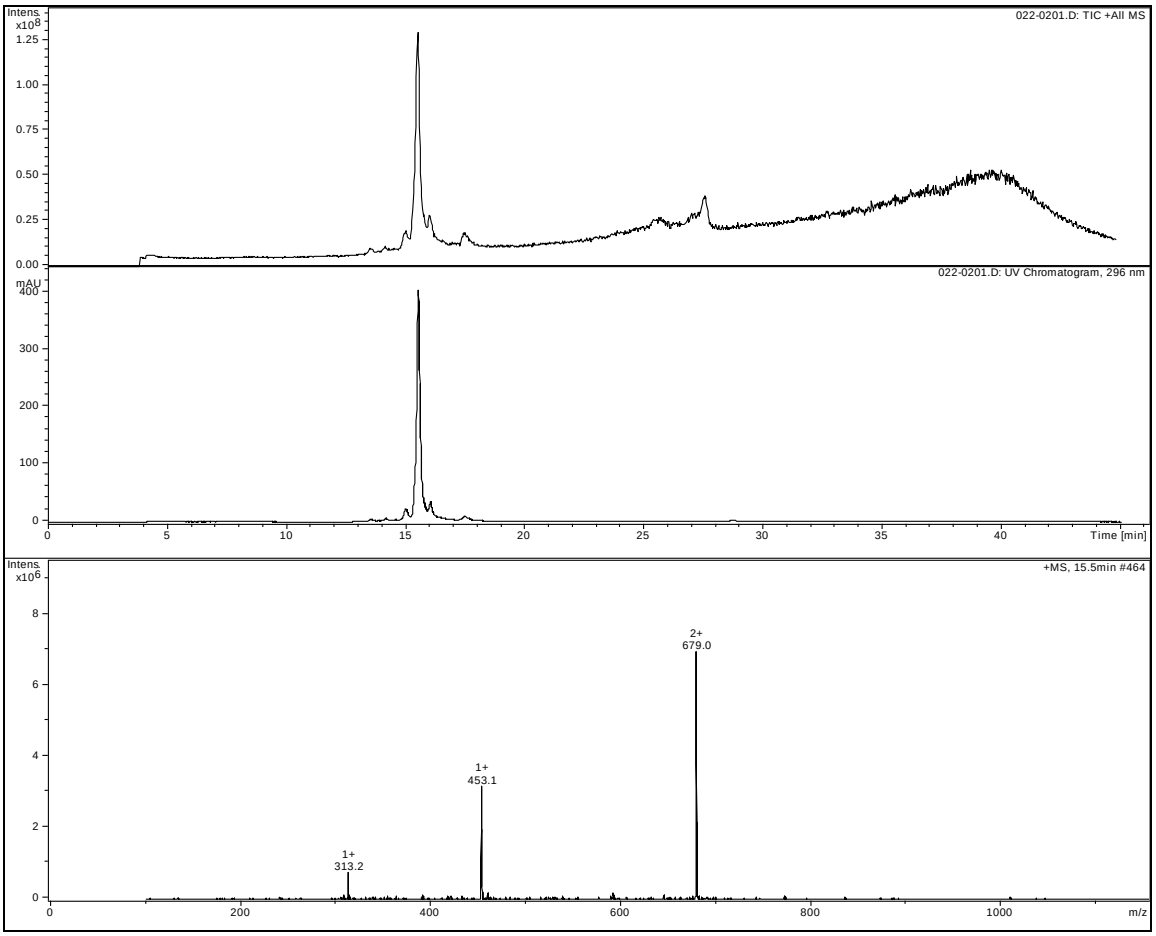

C. Synthesis of BisMTX-oligodeoxynucleotides (ODN-trilinker)

The thiol protected oligodeoxynucleotides ODN1826 (CpG, TCCATGACGTTCCTGACGTT), containing CpG motifs, and ODN1982 (CTRL, TCCAGGACTTCTCTCAGGTT) were purchased from IDT (Integrated DNA Technologies). ODN were phosphorothioate-modified to increase their resistance to nuclease degradation. Synthetic ODN were deprotected by 100 equivalent dithiothreitol (DTT) in TE Buffer (Tris 10 mM, EDTA 1 mM, pH 7.5) for 24 hr. DTT was removed by eluting the oligonucleotides through illustra NAP-10 columns (GE Healthcare Life science). Deprotected oligos were then magnetically stirred with 2.5 eq of BisMTX-maleimide in TE buffer for 24 hr at room temperature. Completion of reaction and formation of products were purified by HPLC using 15 mM ammonium acetate (solvent A) and 100% acetonitrile (B) on Haisil 100 Å C18 RP column (5 μm, 250 x 4.6 mm, Haggins Analytical Inc). Product peak was isolated using a gradient of 2% to 25% B. Relevant fractions were pooled and speedvac prior to storage or analysis. For LC-ESI-MS, Zorbax SB-C18 column (150 mm x 0.5 mm, 5 μm, Agilent Technologies, Inc.) was used. Sample was eluted with 15 mM ammonium acetate (A) and 100% acetonitrile (B) with gradient of 2 % B to 75 % B over 35 min. Traces for CpG1826 (5' TCCATGACGTTCCTGACGTT 3', m/z = 6519), ODN1982 (5' TCCAGGACTTCTCTCAGGTT 3', m/z = 6519) , BisMTX-CpG1826 (m/z = 7875) and BisMTX-ODN1982 (m/z = 7875) are given below in Fig (A), (B), (C), and (D) respectively. LPS content of ODN and ODN-trilinker was < 0.5 ng LPS/mg DNA, as measured by Limulus amebocyte assay (Thermos scientific).

Figure 11. Scheme for the synthesis of bisMTX-oligodeoxynucleotides.

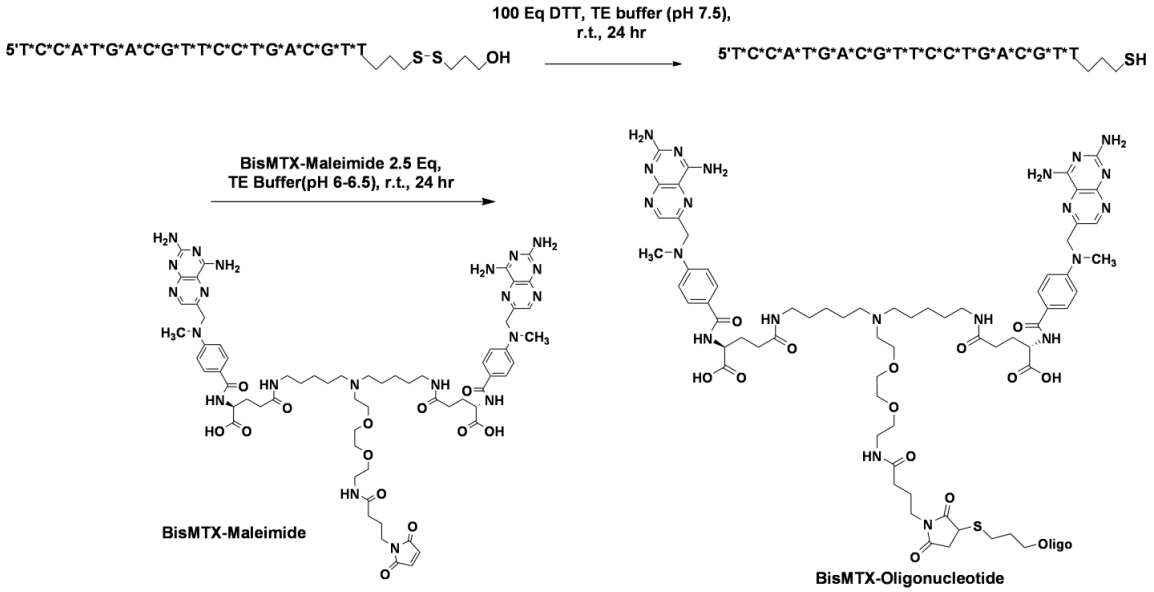

Figure 12. LC-ESI-MS Spectra of CpG 1826, ODN 1982, CpG1826-trilinker and ODN1982-trilinker .

(a) CpG 1826

Molecular Mass (Mr): 6516.7 Std. Deviation: 0.381192

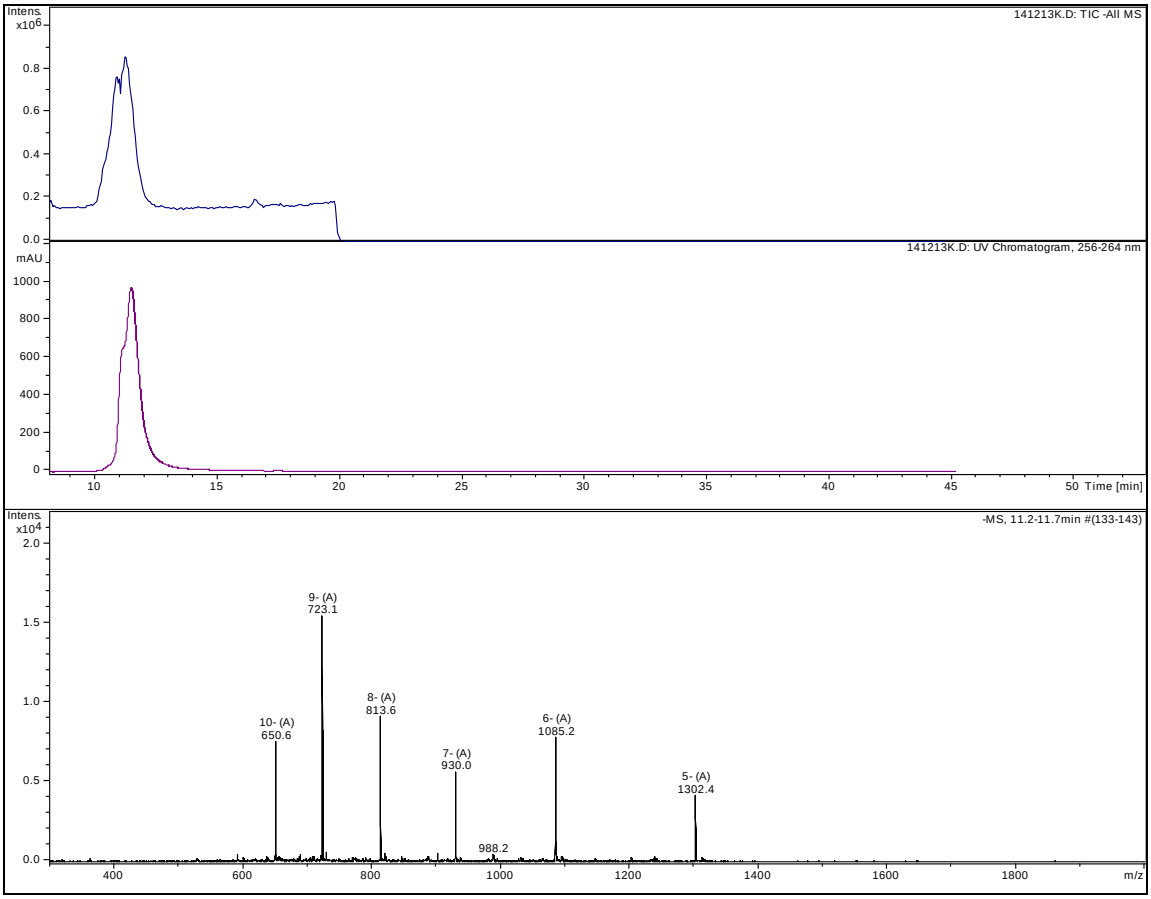

(b) ODN 1982

Molecular Mass (Mr): 6519.6 Std. Deviation: 0.585252

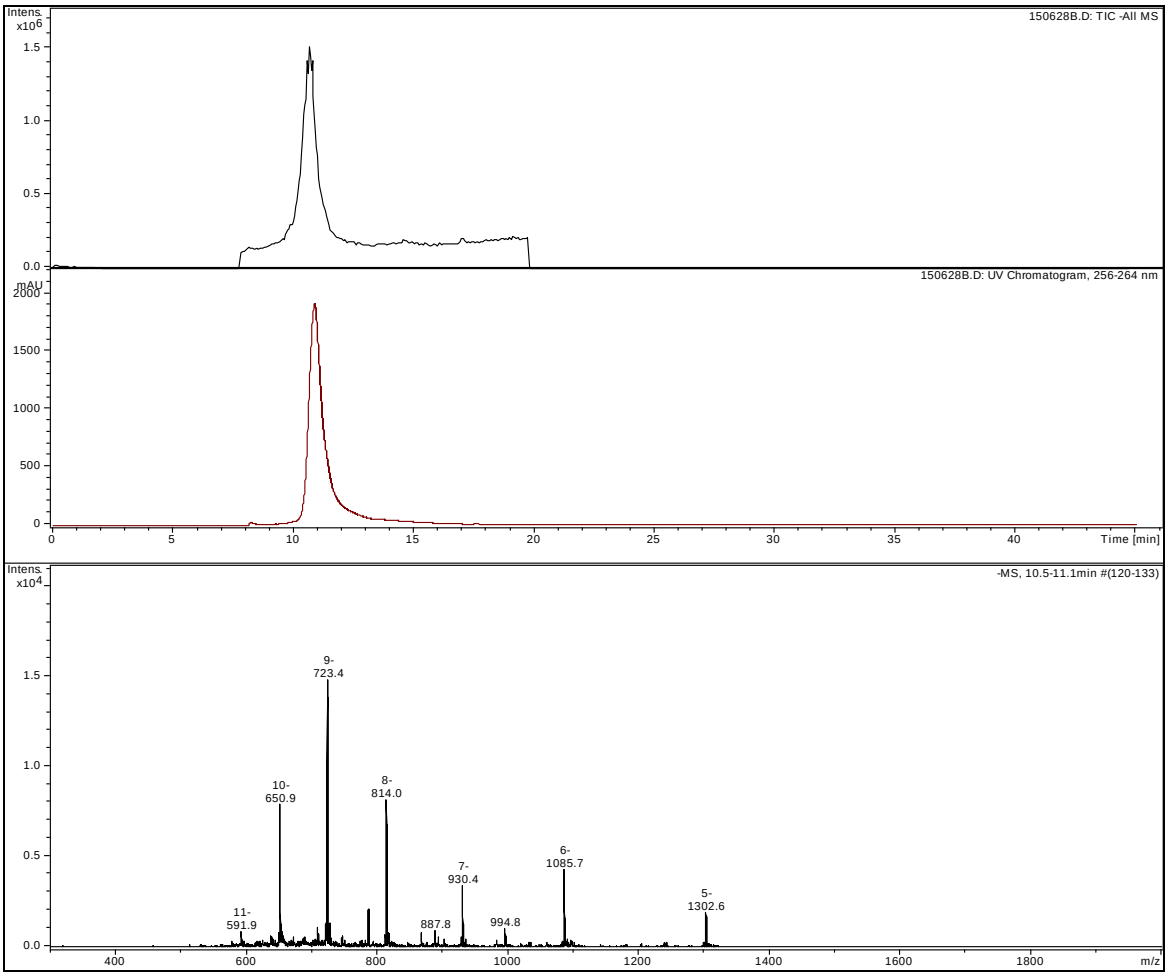

(c) CpG1826-trilinker

Molecular Mass ([M - H]-): 7875.0 Std. Deviation: 0.715329

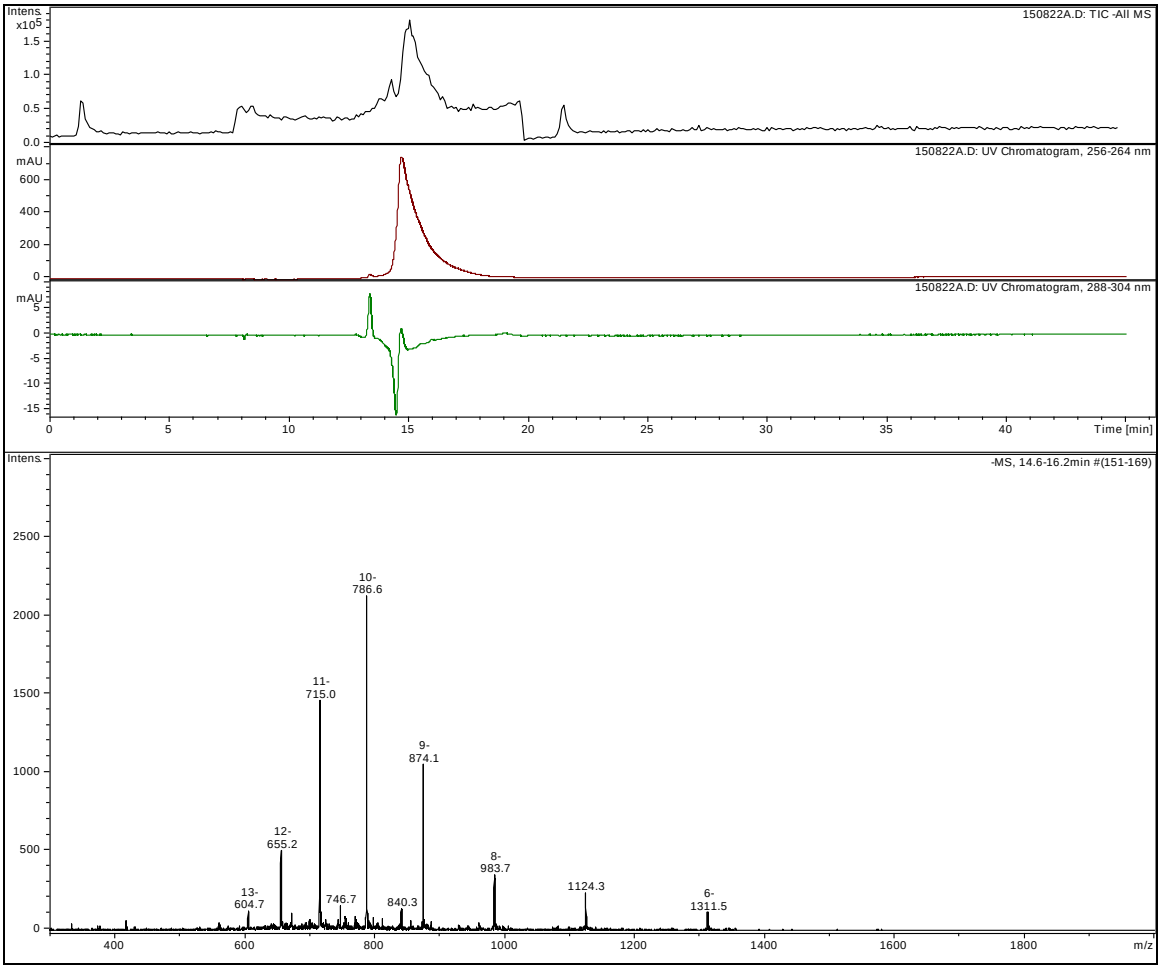

(d) ODN1982-trilinker

Molecular Mass ([M - H]-): 7875.7 Std. Deviation: 0.467962

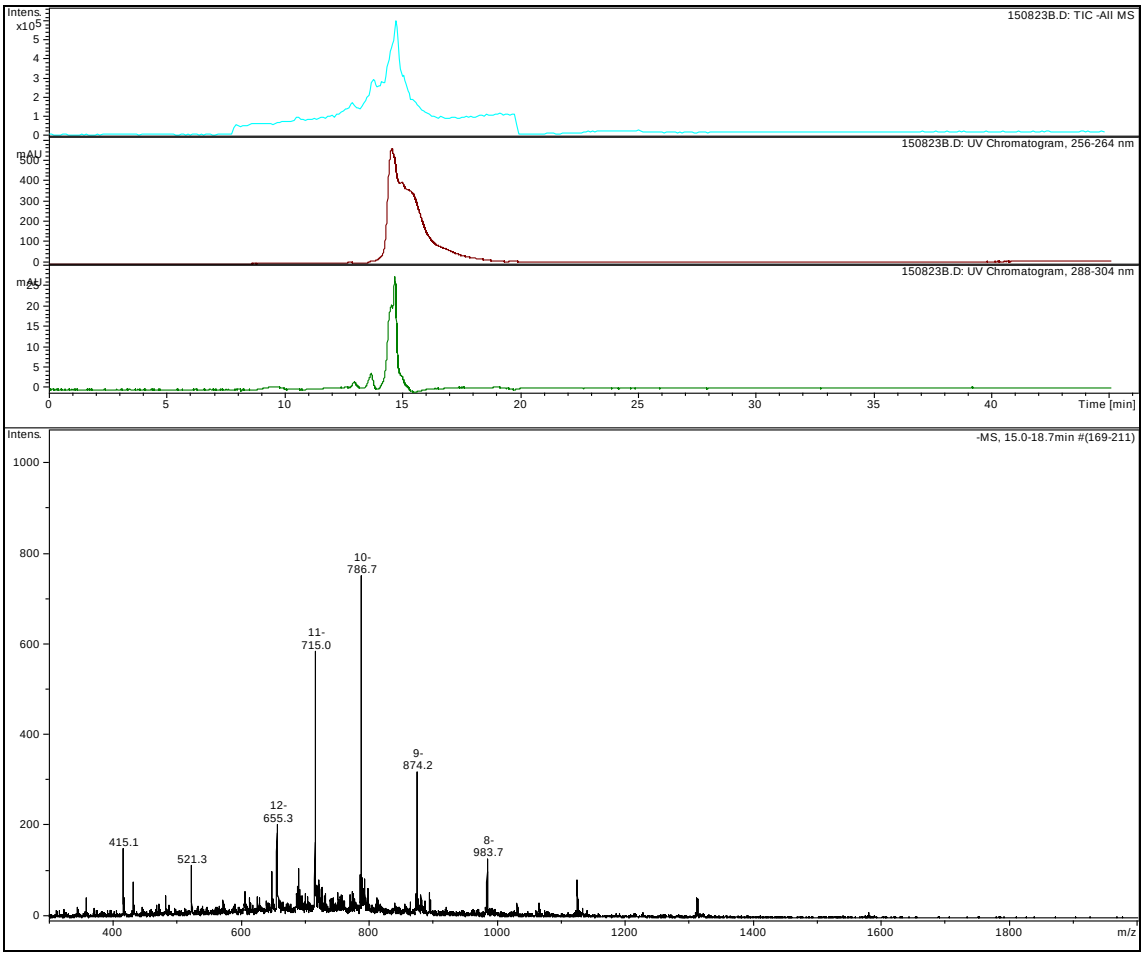

D. Protein Expression, Purification and endotoxin removal

ClearColi BL21(DE3) (Lucigen) cells were transformed with plasmid encoding DHFR-DHFR ($DHFR^2$, 1DD) with a glycine residue between the two DHFRs. Following cells membrane disruption, cell lysate containing soluble $DHFR^2$ protein was loaded onto methotrexate affinity column (20 ml resin) that was previously equilibrated with Buffer A (50mM KH_2PO_4, 1mM K_2EDTA, pH 6). Column was firstly washed with 50 column volumes of buffer A containing 0.1% Triton-114 (Sigma-Aldrich), and then washed with another 25 column volumes of buffer B (50mM KH_2PO_4, 1mM K_2EDTA, 1M KCl, pH 6) without detergent at 4 ˚C. Elution was achieved with Folate buffer (10mM K_2HPO_4, 0.1mM K_2EDTA, 1M KCl, 15mM Folate, pH 9). Fractions were dialyzed and further purified by diethyl aminoethyl (DEAE) ion exchange column. Pure protein was stored in 15% of glycerol at -80 ˚C and buffer exchanged with PBS containing 0.4 M NaCl before use. LPS content of protein (< 0.01 ng LPS/mg) was measured by Limulus amebocyte assay (Thermos scientific).

E. Size exclusion chromatography

1DD were incubated with dimerizer CpG1826-trilinker or ODN1982-trilinbker at 1:1.2 ratios in P500 buffer (0.5M NaCl, 50mM KH_2PO_4, 1mM EDTA, pH 7.0) for 1 hour at room temperature. Formation of multimeric nanostructures were analyzed by Size exclusion chromatography (SEC) using G200 gel filteration column (Superdex G200, GE Healthcare) and eluted at a flow rate of 0.5 ml/min with P500 buffer.

F. Dynamic light scattering

DLS measurements were performed on a Brook haven 90 Plus Particle Analyzer (Holtzville, NY) with a 35 mW red diode laser. Samples (1.5 mL) were measured at room temperature in suspensions of PBS at (1.5 mg/mL).

G. Mice and cell lines

Female BALB/c mice (7 weeks old), stock #01B05, were purchased from the National Cancer Institute (Frederick, MD, USA). All mice were housed under pathogen-free conditions at the AALAC-accredited University of Minnesota Animal Care Facility. All animal procedures were approved by the University of Minnesota Institutional Animal Care and Use Committee. Four mice per group were immunized intravenously with 30 μg (834.7 pmol) of CSANs with or without 834.7 pmol of free CpG oligos, CpG CSANs, CTRL CSAN or 834.7 pmol of free CpG oligos only in PBS in a total volume of 300 μl/animal. A booster injection with the same concentration and volume of vaccines was administered on day 14. Blood samples were taken on day0, 13, 21 and 30 by retro-orbital bleeding. Mice were sacrificed by cervical dislocation. Single cell suspension was prepared aseptically from the spleens. Mouse splenocytes were grown in RPMI media for FACS and in vitro activation assay.

H. In vitro activation cell activation

Freshly isolated spleen cells from naive mice were plated onto 96 well plates in 10^5 cells/well densities. Different concentrations of treatments were used to treat cells overnight at 37 ˚C in 5 % CO_2 humidified atmosphere.

I. Flow cytometry

Fluorescently labeled mAbs obtained were the following: anti-mouse CD40-PE-Cy5 (clone: 3/23) (BioLegend), anti-mouse CD40-APC (clone:3/23) (BD Biosciences), anti-mouse CD19 (clone:1D3), anti-mouse CD86 (clone:GL1). On day 30, spleen cells were isolated from each mice. Following red blood cell lysis, cells were stained with fluorescently labeled mAb, washed and then phenotypically acquired on the LSRII (BD Biosciences) and analyzed with FlowJo software (Tree Star, Inc.).

J. Macrophage RAW 264.7 cells activation

RAW 264.7 (murine macrophage) cells were plated onto 48 well plates in 10^5 cells/well densities the day before the treatment. The next day, supernatant was removed and different concentrations of treatment were added in the medium. After overnight incubation at 37 ˚C in 5 % CO_2 humidified atmosphere, cytokines (IL-6, TNF-α) were determined in the supernatant.

K. CSAN uptake study by RAW 264.7 cells

Either CSAN or $DHFR^2$ monomer was FITC labeled. CpG CSANs were prepared with 1:1.1 equivalent of $DHFR^2$ monomer and CpG-trilinker. 5×10^5 RAW cells were preincubated with either 10 μg of Fucoidan (Sigma) or 20 μg of polyinosinic acid (Sigma) for 30 minutes at 37 ˚C, then 0.5 μM of either CSAN or CpG CSAN were added in the cell culture with or without free CpG/nonCpG ODN. After another1 h incubation, cells were washed with FACS buffer and counted on the LSRII (BD Biosciences).

L. Measurement of DHFR-specific antibodies by ELISA.

Levels of antibodies binding to DHFR were measured by enzyme-linked immunosorbent assay (ELISA). Briefly, Maxisorp 96-well plates (Thermo scientific)

were coated first with $DHFR^2$ (1μg/well) in ELISA diluent (PBS containing 10% FBS) overnight at 4 ˚C. Following 1 h blocking with ELISA diluent, diluted sera (1:10) of immunized mice were transferred to the coated plates and incubated for 2 h at room temperature. Horseradish peroxidase-conjugated rabbit anti-mouse IgG-HRP (Sigma–Aldrich) diluted 1:80,000, or goat anti-mouse IgG1-HRP (Santa Cruz) diluted 1:4,000, or goat anti-mouse IgG2a-HRP (Santa Cruz) diluted 1:4,000, in the same diluent were incubated for 1 h at room temperature. The amount of bound peroxidase was visualized by incubation with tetramethylbenzidine and hydrogen peroxide (BD Bioscience). After 15 min, the reaction was stopped with 0.2 M H_2SO_4 and A_{450} was measured with a microplate reader (Biotek). Samples were measured in triplicates.

Bibliography

1. Coley, W. B., The treatment of malignant tumors by repeated inoculations of erysipelas. With a report of ten original cases. 1893. *Clin Orthop Relat Res* **1991,** (262), 3-11.

2. Bukowski, R. M.; Goodman, P.; Crawford, E. D.; Sergi, J. S.; Redman, B. G.; Whitehead, R. P., Phase II trial of high-dose intermittent interleukin-2 in metastatic renal cell carcinoma: a Southwest Oncology Group study. *J Natl Cancer Inst* **1990,** *82* (2), 143-6.

3. Schmidt, C., Immunology: Another shot at cancer. *Nature* **2015,** *527* (7578), S105-S107.

4. Ishii, H.; Tanaka, S.; Masuyama, K., Therapeutic strategy for cancer immunotherapy in head and neck cancer. *2015* **2015**.

5. Tuohy, V. K.; Jaini, R., Prophylactic cancer vaccination by targeting functional non-self. *Annals of Medicine* **2011,** *43* (5), 356-365.

6. Bijker, M. S.; Melief, C. J.; Offringa, R.; van der Burg, S. H., Design and development of synthetic peptide vaccines: past, present and future. *Expert Rev Vaccines* **2007,** *6* (4), 591-603.

7. Parkin, D. M., The global health burden of infection-associated cancers in the year 2002. *Int J Cancer* **2006,** *118* (12), 3030-44.

8. Dranoff, G.; Jaffee, E.; Lazenby, A.; Golumbek, P.; Levitsky, H.; Brose, K.; Jackson, V.; Hamada, H.; Pardoll, D.; Mulligan, R. C., Vaccination with irradiated tumor cells engineered to secrete murine granulocyte-macrophage colony-stimulating factor stimulates potent, specific, and long-lasting anti-tumor immunity. *Proc Natl Acad Sci U S A* **1993,** *90* (8), 3539-43.

9. Kantoff, P. W.; Higano, C. S.; Shore, N. D.; Berger, E. R.; Small, E. J.; Penson, D. F.; Redfern, C. H.; Ferrari, A. C.; Dreicer, R.; Sims, R. B.; Xu, Y.; Frohlich, M. W.; Schellhammer, P. F., Sipuleucel-T Immunotherapy for Castration-Resistant Prostate Cancer. *New England Journal of Medicine* **2010,** *363* (5), 411-422.

10. Walter, S.; Weinschenk, T.; Stenzl, A.; Zdrojowy, R.; Pluzanska, A.; Szczylik, C.; Staehler, M.; Brugger, W.; Dietrich, P.-Y.; Mendrzyk, R.; Hilf, N.; Schoor, O.; Fritsche, J.; Mahr, A.; Maurer, D.; Vass, V.; Trautwein, C.; Lewandrowski, P.; Flohr, C.; Pohla, H.; Stanczak, J. J.; Bronte, V.; Mandruzzato, S.; Biedermann, T.; Pawelec, G.; Derhovanessian, E.; Yamagishi, H.; Miki, T.; Hongo, F.; Takaha, N.; Hirakawa, K.; Tanaka, H.; Stevanovic, S.; Frisch, J.; Mayer-Mokler, A.; Kirner, A.; Rammensee, H.-G.; Reinhardt, C.; Singh-Jasuja, H., Multipeptide immune response to cancer vaccine

IMA901 after single-dose cyclophosphamide associates with longer patient survival. *Nat Med* **2012,** *18* (8), 1254-1261.

11. De Flora, S.; Bonanni, P., The prevention of infection-associated cancers. *Carcinogenesis* **2011,** *32* (6), 787-795.

12. Doorbar, J., Molecular biology of human papillomavirus infection and cervical cancer. *Clinical Science* **2006,** *110* (5), 525-541.

13. Lowy, D. R., Prophylactic human papillomavirus vaccines. *Journal of Clinical Investigation* **2006,** *116* (5), 1167-1173.

14. Frazer, I. H.; Lowy, D. R.; Schiller, J. T., Prevention of cancer through immunization: Prospects and challenges for the 21st century. *Eur J Immunol* **2007,** *37 Suppl 1*, S148-55.

15. Butterfield, L. H., Cancer vaccines. *BMJ* **2015,** *350* (apr22 14), h988-h988.

16. Zerbini, A.; Pilli, M.; Penna, A.; Pelosi, G.; Schianchi, C.; Molinari, A.; Schivazappa, S.; Zibera, C.; Fagnoni, F. F.; Ferrari, C.; Missale, G., Radiofrequency thermal ablation of hepatocellular carcinoma liver nodules can activate and enhance tumor-specific T-cell responses. *Cancer Res* **2006,** *66* (2), 1139-46.

17. Feltkamp, M. C.; Smits, H. L.; Vierboom, M. P.; Minnaar, R. P.; de Jongh, B. M.; Drijfhout, J. W.; ter Schegget, J.; Melief, C. J.; Kast, W. M., Vaccination with cytotoxic T lymphocyte epitope-containing peptide protects against a tumor induced by human papillomavirus type 16-transformed cells. *Eur J Immunol* **1993,** *23* (9), 2242-9.

18. Rosenberg, S. A.; Sherry, R. M.; Morton, K. E.; Scharfman, W. J.; Yang, J. C.; Topalian, S. L.; Royal, R. E.; Kammula, U.; Restifo, N. P.; Hughes, M. S.; Schwartzentruber, D.; Berman, D. M.; Schwarz, S. L.; Ngo, L. T.; Mavroukakis, S. A.; White, D. E.; Steinberg, S. M., Tumor progression can occur despite the induction of very high levels of self/tumor antigen-specific CD8+ T cells in patients with melanoma. *J Immunol* **2005,** *175* (9), 6169-76.

19. Aichele, P.; Brduscha-Riem, K.; Zinkernagel, R. M.; Hengartner, H.; Pircher, H., T cell priming versus T cell tolerance induced by synthetic peptides. *J Exp Med* **1995,** *182* (1), 261-6.

20. Bijker, M. S.; van den Eeden, S. J.; Franken, K. L.; Melief, C. J.; van der Burg, S. H.; Offringa, R., Superior induction of anti-tumor CTL immunity by extended peptide vaccines involves prolonged, DC-focused antigen presentation. *Eur J Immunol* **2008,** *38* (4), 1033-42.

21. Toes, R. E.; Offringa, R.; Blom, R. J.; Melief, C. J.; Kast, W. M., Peptide vaccination can lead to enhanced tumor growth through specific T-cell tolerance induction. *Proceedings of the National Academy of Sciences of the United States of America* **1996,** *93* (15), 7855-7860.

22. Toes, R. E.; Blom, R. J.; Offringa, R.; Kast, W. M.; Melief, C. J., Enhanced tumor outgrowth after peptide vaccination. Functional deletion of tumor-specific CTL induced by peptide vaccination can lead to the inability to reject tumors. *J Immunol* **1996,** *156* (10), 3911-8.

23. Toes, R. E.; van der Voort, E. I.; Schoenberger, S. P.; Drijfhout, J. W.; van Bloois, L.; Storm, G.; Kast, W. M.; Offringa, R.; Melief, C. J., Enhancement of tumor outgrowth through CTL tolerization after peptide vaccination is avoided by peptide presentation on dendritic cells. *J Immunol* **1998,** *160* (9), 4449-56.

24. Zwaveling, S.; Ferreira Mota, S. C.; Nouta, J.; Johnson, M.; Lipford, G. B.; Offringa, R.; van der Burg, S. H.; Melief, C. J., Established human papillomavirus type 16-expressing tumors are effectively eradicated following vaccination with long peptides. *J Immunol* **2002,** *169* (1), 350-8.

25. Khong, H. T.; Restifo, N. P., Natural selection of tumor variants in the generation of "tumor escape" phenotypes. *Nat Immunol* **2002,** *3* (11), 999-1005.

26. Galluzzi, L.; Vacchelli, E.; Fridman, W. H.; Galon, J.; Sautès-Fridman, C.; Tartour, E.; Zucman-Rossi, J.; Zitvogel, L.; Kroemer, G., Trial Watch: Monoclonal antibodies in cancer therapy. *OncoImmunology* **2012,** *1* (1), 28-37.

27. Banchereau, J.; Steinman, R. M., Dendritic cells and the control of immunity. *Nature* **1998,** *392* (6673), 245-52.

28. Steinman, R. M.; Banchereau, J., Taking dendritic cells into medicine. *Nature* **2007,** *449* (7161), 419-426.

29. Merad, M.; Sathe, P.; Helft, J.; Miller, J.; Mortha, A., The dendritic cell lineage: ontogeny and function of dendritic cells and their subsets in the steady state and the inflamed setting. *Annu Rev Immunol* **2013,** *31*, 563-604.

30. Palucka, K.; Banchereau, J., Cancer immunotherapy via dendritic cells. *Nat Rev Cancer* **2012,** *12* (4), 265-277.

31. Yang, S. C.; Hillinger, S.; Riedl, K.; Zhang, L.; Zhu, L.; Huang, M.; Atianzar, K.; Kuo, B. Y.; Gardner, B.; Batra, R. K.; Strieter, R. M.; Dubinett, S. M.; Sharma, S., Intratumoral administration of dendritic cells overexpressing CCL21 generates systemic antitumor responses and confers tumor immunity. *Clin Cancer Res* **2004,** *10* (8), 2891-901.

32. Hu, J.; Yuan, X.; Belladonna, M. L.; Ong, J. M.; Wachsmann-Hogiu, S.; Farkas, D. L.; Black, K. L.; Yu, J. S., Induction of potent antitumor immunity by intratumoral injection of interleukin 23-transduced dendritic cells. *Cancer Res* **2006,** *66* (17), 8887-96.

33. Fields, R. C.; Shimizu, K.; Mule, J. J., Murine dendritic cells pulsed with whole tumor lysates mediate potent antitumor immune responses in vitro and in vivo. *Proc Natl Acad Sci U S A* **1998,** *95* (16), 9482-7.

34. Mayordomo, J. I.; Zorina, T.; Storkus, W. J.; Zitvogel, L.; Celluzzi, C.; Falo, L. D.; Melief, C. J.; Ildstad, S. T.; Kast, W. M.; Deleo, A. B.; et al., Bone marrow-derived dendritic cells pulsed with synthetic tumour peptides elicit protective and therapeutic antitumour immunity. *Nat Med* **1995,** *1* (12), 1297-302.

35. Bonifaz, L. C.; Bonnyay, D. P.; Charalambous, A.; Darguste, D. I.; Fujii, S.; Soares, H.; Brimnes, M. K.; Moltedo, B.; Moran, T. M.; Steinman, R. M., In vivo targeting of antigens to maturing dendritic cells via the DEC-205 receptor improves T cell vaccination. *J Exp Med* **2004,** *199* (6), 815-24.

36. Klechevsky, E.; Flamar, A. L.; Cao, Y.; Blanck, J. P.; Liu, M.; O'Bar, A.; Agouna-Deciat, O.; Klucar, P.; Thompson-Snipes, L.; Zurawski, S.; Reiter, Y.; Palucka, A. K.; Zurawski, G.; Banchereau, J., Cross-priming CD8+ T cells by targeting antigens to human dendritic cells through DCIR. *Blood* **2010,** *116* (10), 1685-97.

37. Viaud, S.; Thery, C.; Ploix, S.; Tursz, T.; Lapierre, V.; Lantz, O.; Zitvogel, L.; Chaput, N., Dendritic cell-derived exosomes for cancer immunotherapy: what's next? *Cancer Res* **2010,** *70* (4), 1281-5.

38. Zitvogel, L.; Regnault, A.; Lozier, A.; Wolfers, J.; Flament, C.; Tenza, D.; Ricciardi-Castagnoli, P.; Raposo, G.; Amigorena, S., Eradication of established murine tumors using a novel cell-free vaccine: dendritic cell derived exosomes. *Nat Med* **1998,** *4* (5), 594-600.

39. Munich, S.; Sobo-Vujanovic, A.; Buchser, W. J.; Beer-Stolz, D.; Vujanovic, N. L., Dendritic cell exosomes directly kill tumor cells and activate natural killer cells via TNF superfamily ligands. *Oncoimmunology* **2012,** *1* (7), 1074-1083.

40. Bonifaz, L.; Bonnyay, D.; Mahnke, K.; Rivera, M.; Nussenzweig, M. C.; Steinman, R. M., Efficient targeting of protein antigen to the dendritic cell receptor DEC-205 in the steady state leads to antigen presentation on major histocompatibility complex class I products and peripheral CD8+ T cell tolerance. *J Exp Med* **2002,** *196* (12), 1627-38.

41. Hawiger, D.; Inaba, K.; Dorsett, Y.; Guo, M.; Mahnke, K.; Rivera, M.; Ravetch, J. V.; Steinman, R. M.; Nussenzweig, M. C., Dendritic cells induce peripheral T cell unresponsiveness under steady state conditions in vivo. *J Exp Med* **2001,** *194* (6), 769-79.

42. Chiang, C. L.-L.; Benencia, F.; Coukos, G., Whole Tumor Antigen Vaccines. *Seminars in immunology* **2010,** *22* (3), 132-143.

43. Simons, J. W.; Carducci, M. A.; Mikhak, B.; Lim, M.; Biedrzycki, B.; Borellini, F.; Clift, S. M.; Hege, K. M.; Ando, D. G.; Piantadosi, S.; Mulligan, R.; Nelson, W. G., Phase I/II trial of an allogeneic cellular immunotherapy in hormone-naive prostate cancer. *Clin Cancer Res* **2006,** *12* (11 Pt 1), 3394-401.

44. Michael, A.; Ball, G.; Quatan, N.; Wushishi, F.; Russell, N.; Whelan, J.; Chakraborty, P.; Leader, D.; Whelan, M.; Pandha, H., Delayed disease progression after

allogeneic cell vaccination in hormone-resistant prostate cancer and correlation with immunologic variables. *Clin Cancer Res* **2005,** *11* (12), 4469-78.

45. Jaffee, E. M.; Hruban, R. H.; Biedrzycki, B.; Laheru, D.; Schepers, K.; Sauter, P. R.; Goemann, M.; Coleman, J.; Grochow, L.; Donehower, R. C.; Lillemoe, K. D.; O'Reilly, S.; Abrams, R. A.; Pardoll, D. M.; Cameron, J. L.; Yeo, C. J., Novel allogeneic granulocyte-macrophage colony-stimulating factor-secreting tumor vaccine for pancreatic cancer: a phase I trial of safety and immune activation. *J Clin Oncol* **2001,** *19* (1), 145-56.

46. Zitvogel, L.; Kepp, O.; Senovilla, L.; Menger, L.; Chaput, N.; Kroemer, G., Immunogenic Tumor Cell Death for Optimal Anticancer Therapy: The Calreticulin Exposure Pathway. *Clinical Cancer Research* **2010,** *16* (12), 3100-3104.

47. Ma, Y.; Conforti, R.; Aymeric, L.; Locher, C.; Kepp, O.; Kroemer, G.; Zitvogel, L., How to improve the immunogenicity of chemotherapy and radiotherapy. *Cancer and Metastasis Reviews* **2011,** *30* (1), 71-82.

48. Rosenberg, S. A.; Yang, J. C.; Sherry, R. M.; Kammula, U. S.; Hughes, M. S.; Phan, G. Q.; Citrin, D. E.; Restifo, N. P.; Robbins, P. F.; Wunderlich, J. R.; Morton, K. E.; Laurencot, C. M.; Steinberg, S. M.; White, D. E.; Dudley, M. E., Durable complete responses in heavily pretreated patients with metastatic melanoma using T-cell transfer immunotherapy. *Clin Cancer Res* **2011,** *17* (13), 4550-7.

49. June, C. H.; Blazar, B. R.; Riley, J. L., Engineering lymphocyte subsets: tools, trials and tribulations. *Nat Rev Immunol* **2009,** *9* (10), 704-716.

50. Baeuerle, P. A.; Reinhardt, C., Bispecific T-Cell Engaging Antibodies for Cancer Therapy. *Cancer Research* **2009,** *69* (12), 4941-4944.

51. Leach, D. R.; Krummel, M. F.; Allison, J. P., Enhancement of antitumor immunity by CTLA-4 blockade. *Science* **1996,** *271* (5256), 1734-6.

52. Agarwala, S. S., Current systemic therapy for metastatic melanoma. *Expert Review of Anticancer Therapy* **2009,** *9* (5), 587-595.

53. Rosenberg, S. A.; Packard, B. S.; Aebersold, P. M.; Solomon, D.; Topalian, S. L.; Toy, S. T.; Simon, P.; Lotze, M. T.; Yang, J. C.; Seipp, C. A.; et al., Use of tumor-infiltrating lymphocytes and interleukin-2 in the immunotherapy of patients with metastatic melanoma. A preliminary report. *N Engl J Med* **1988,** *319* (25), 1676-80.

54. Dudley, M. E.; Wunderlich, J. R.; Robbins, P. F.; Yang, J. C.; Hwu, P.; Schwartzentruber, D. J.; Topalian, S. L.; Sherry, R.; Restifo, N. P.; Hubicki, A. M.; Robinson, M. R.; Raffeld, M.; Duray, P.; Seipp, C. A.; Rogers-Freezer, L.; Morton, K. E.; Mavroukakis, S. A.; White, D. E.; Rosenberg, S. A., Cancer Regression and Autoimmunity in Patients After Clonal Repopulation with Antitumor Lymphocytes. *Science (New York, N.Y.)* **2002,** *298* (5594), 850-854.

55. Houot, R.; Schultz, L. M.; Marabelle, A.; Kohrt, H., T-cell-based Immunotherapy: Adoptive Cell Transfer and Checkpoint Inhibition. *Cancer Immunology Research* **2015,** *3* (10), 1115-1122.

56. Lawrence, M. S.; Stojanov, P.; Polak, P.; Kryukov, G. V.; Cibulskis, K.; Sivachenko, A.; Carter, S. L.; Stewart, C.; Mermel, C. H.; Roberts, S. A.; Kiezun, A.; Hammerman, P. S.; McKenna, A.; Drier, Y.; Zou, L.; Ramos, A. H.; Pugh, T. J.; Stransky, N.; Helman, E.; Kim, J.; Sougnez, C.; Ambrogio, L.; Nickerson, E.; Shefler, E.; Cortes, M. L.; Auclair, D.; Saksena, G.; Voet, D.; Noble, M.; DiCara, D.; Lin, P.; Lichtenstein, L.; Heiman, D. I.; Fennell, T.; Imielinski, M.; Hernandez, B.; Hodis, E.; Baca, S.; Dulak, A. M.; Lohr, J.; Landau, D. A.; Wu, C. J.; Melendez-Zajgla, J.; Hidalgo-Miranda, A.; Koren, A.; McCarroll, S. A.; Mora, J.; Lee, R. S.; Crompton, B.; Onofrio, R.; Parkin, M.; Winckler, W.; Ardlie, K.; Gabriel, S. B.; Roberts, C. W.; Biegel, J. A.; Stegmaier, K.; Bass, A. J.; Garraway, L. A.; Meyerson, M.; Golub, T. R.; Gordenin, D. A.; Sunyaev, S.; Lander, E. S.; Getz, G., Mutational heterogeneity in cancer and the search for new cancer-associated genes. *Nature* **2013,** *499* (7457), 214-8.

57. Yannelli, J. R.; Hyatt, C.; McConnell, S.; Hines, K.; Jacknin, L.; Parker, L.; Sanders, M.; Rosenberg, S. A., Growth of tumor-infiltrating lymphocytes from human solid cancers: summary of a 5-year experience. *Int J Cancer* **1996,** *65* (4), 413-21.

58. Bollard, C. M.; Rooney, C. M.; Heslop, H. E., T-cell therapy in the treatment of post-transplant lymphoproliferative disease. *Nat Rev Clin Oncol* **2012,** *9* (9), 510-519.

59. Louis, C. U.; Straathof, K.; Bollard, C. M.; Ennamuri, S.; Gerken, C.; Lopez, T. T.; Huls, M. H.; Sheehan, A.; Wu, M. F.; Liu, H.; Gee, A.; Brenner, M. K.; Rooney, C. M.; Heslop, H. E.; Gottschalk, S., Adoptive transfer of EBV-specific T cells results in sustained clinical responses in patients with locoregional nasopharyngeal carcinoma. *J Immunother* **2010,** *33* (9), 983-90.

60. Bollard, C. M.; Gottschalk, S.; Torrano, V.; Diouf, O.; Ku, S.; Hazrat, Y.; Carrum, G.; Ramos, C.; Fayad, L.; Shpall, E. J.; Pro, B.; Liu, H.; Wu, M. F.; Lee, D.; Sheehan, A. M.; Zu, Y.; Gee, A. P.; Brenner, M. K.; Heslop, H. E.; Rooney, C. M., Sustained complete responses in patients with lymphoma receiving autologous cytotoxic T lymphocytes targeting Epstein-Barr virus latent membrane proteins. *J Clin Oncol* **2014,** *32* (8), 798-808.

61. Morgan, R. A.; Dudley, M. E.; Wunderlich, J. R.; Hughes, M. S.; Yang, J. C.; Sherry, R. M.; Royal, R. E.; Topalian, S. L.; Kammula, U. S.; Restifo, N. P.; Zheng, Z.; Nahvi, A.; de Vries, C. R.; Rogers-Freezer, L. J.; Mavroukakis, S. A.; Rosenberg, S. A., Cancer regression in patients after transfer of genetically engineered lymphocytes. *Science* **2006,** *314* (5796), 126-9.

62. Robbins, P. F.; Morgan, R. A.; Feldman, S. A.; Yang, J. C.; Sherry, R. M.; Dudley, M. E.; Wunderlich, J. R.; Nahvi, A. V.; Helman, L. J.; Mackall, C. L.; Kammula, U. S.; Hughes, M. S.; Restifo, N. P.; Raffeld, M.; Lee, C. C.; Levy, C. L.; Li, Y. F.; El-Gamil, M.; Schwarz, S. L.; Laurencot, C.; Rosenberg, S. A., Tumor regression in patients

with metastatic synovial cell sarcoma and melanoma using genetically engineered lymphocytes reactive with NY-ESO-1. *J Clin Oncol* **2011,** *29* (7), 917-24.

63. Morgan, R. A.; Chinnasamy, N.; Abate-Daga, D.; Gros, A.; Robbins, P. F.; Zheng, Z.; Dudley, M. E.; Feldman, S. A.; Yang, J. C.; Sherry, R. M.; Phan, G. Q.; Hughes, M. S.; Kammula, U. S.; Miller, A. D.; Hessman, C. J.; Stewart, A. A.; Restifo, N. P.; Quezado, M. M.; Alimchandani, M.; Rosenberg, A. Z.; Nath, A.; Wang, T.; Bielekova, B.; Wuest, S. C.; Akula, N.; McMahon, F. J.; Wilde, S.; Mosetter, B.; Schendel, D. J.; Laurencot, C. M.; Rosenberg, S. A., Cancer regression and neurological toxicity following anti-MAGE-A3 TCR gene therapy. *J Immunother* **2013,** *36* (2), 133-51.

64. Johnson, L. A.; Morgan, R. A.; Dudley, M. E.; Cassard, L.; Yang, J. C.; Hughes, M. S.; Kammula, U. S.; Royal, R. E.; Sherry, R. M.; Wunderlich, J. R.; Lee, C. C.; Restifo, N. P.; Schwarz, S. L.; Cogdill, A. P.; Bishop, R. J.; Kim, H.; Brewer, C. C.; Rudy, S. F.; VanWaes, C.; Davis, J. L.; Mathur, A.; Ripley, R. T.; Nathan, D. A.; Laurencot, C. M.; Rosenberg, S. A., Gene therapy with human and mouse T-cell receptors mediates cancer regression and targets normal tissues expressing cognate antigen. *Blood* **2009,** *114* (3), 535-46.

65. Parkhurst, M. R.; Yang, J. C.; Langan, R. C.; Dudley, M. E.; Nathan, D. A.; Feldman, S. A.; Davis, J. L.; Morgan, R. A.; Merino, M. J.; Sherry, R. M.; Hughes, M. S.; Kammula, U. S.; Phan, G. Q.; Lim, R. M.; Wank, S. A.; Restifo, N. P.; Robbins, P. F.; Laurencot, C. M.; Rosenberg, S. A., T cells targeting carcinoembryonic antigen can mediate regression of metastatic colorectal cancer but induce severe transient colitis. *Mol Ther* **2011,** *19* (3), 620-6.

66. Linette, G. P.; Stadtmauer, E. A.; Maus, M. V.; Rapoport, A. P.; Levine, B. L.; Emery, L.; Litzky, L.; Bagg, A.; Carreno, B. M.; Cimino, P. J.; Binder-Scholl, G. K.; Smethurst, D. P.; Gerry, A. B.; Pumphrey, N. J.; Bennett, A. D.; Brewer, J. E.; Dukes, J.; Harper, J.; Tayton-Martin, H. K.; Jakobsen, B. K.; Hassan, N. J.; Kalos, M.; June, C. H., Cardiovascular toxicity and titin cross-reactivity of affinity-enhanced T cells in myeloma and melanoma. *Blood* **2013,** *122* (6), 863-71.

67. Barrett, D. M.; Singh, N.; Porter, D. L.; Grupp, S. A.; June, C. H., Chimeric Antigen Receptor Therapy for Cancer. *Annual Review of Medicine* **2014,** *65* (1), 333-347.

68. Sadelain, M.; Brentjens, R.; Riviere, I., The basic principles of chimeric antigen receptor design. *Cancer Discov* **2013,** *3* (4), 388-98.

69. Essand, M.; Loskog, A. S. I., Genetically engineered T cells for the treatment of cancer. *Journal of Internal Medicine* **2013,** *273* (2), 166-181.

70. Mezzanzanica, D.; Canevari, S.; Mazzoni, A.; Figini, M.; Colnaghi, M. I.; Waks, T.; Schindler, D. G.; Eshhar, Z., Transfer of chimeric receptor gene made of variable regions of tumor-specific antibody confers anticarbohydrate specificity on T cells. *Cancer Gene Ther* **1998,** *5* (6), 401-7.

71. Kershaw, M. H.; Teng, M. W.; Smyth, M. J.; Darcy, P. K., Supernatural T cells: genetic modification of T cells for cancer therapy. *Nat Rev Immunol* **2005,** *5* (12), 928-40.

72. Beard, B. C.; Keyser, K. A.; Trobridge, G. D.; Peterson, L. J.; Miller, D. G.; Jacobs, M.; Kaul, R.; Kiem, H. P., Unique integration profiles in a canine model of long-term repopulating cells transduced with gammaretrovirus, lentivirus, or foamy virus. *Hum Gene Ther* **2007,** *18* (5), 423-34.

73. Rethwilm, A., Foamy virus vectors: an awaited alternative to gammaretro- and lentiviral vectors. *Curr Gene Ther* **2007,** *7* (4), 261-71.

74. Zhao, Y.; Moon, E.; Carpenito, C.; Paulos, C. M.; Liu, X.; Brennan, A. L.; Chew, A.; Carroll, R. G.; Scholler, J.; Levine, B. L., Multiple injections of electroporated autologous T cells expressing a chimeric antigen receptor mediate regression of human disseminated tumor. *Cancer research* **2010,** *70* (22), 9053-9061.

75. Huang, X.; Wilber, A. C.; Bao, L.; Tuong, D.; Tolar, J.; Orchard, P. J.; Levine, B. L.; June, C. H.; McIvor, R. S.; Blazar, B. R.; Zhou, X., Stable gene transfer and expression in human primary T cells by the Sleeping Beauty transposon system. *Blood* **2006,** *107* (2), 483-91.

76. Hoogenboom, H. R., Selecting and screening recombinant antibody libraries. *Nat Biotech* **2005,** *23* (9), 1105-1116.

77. Dao, T.; Pankov, D.; Scott, A.; Korontsvit, T.; Zakhaleva, V.; Xu, Y.; Xiang, J.; Yan, S.; de Morais Guerreiro, M. D.; Veomett, N.; Dubrovsky, L.; Curcio, M.; Doubrovina, E.; Ponomarev, V.; Liu, C.; O'Reilly, R. J.; Scheinberg, D. A., Therapeutic bispecific T-cell engager antibody targeting the intracellular oncoprotein WT1. *Nat Biotech* **2015,** *33* (10), 1079-1086.

78. James, S. E.; Greenberg, P. D.; Jensen, M. C.; Lin, Y.; Wang, J.; Till, B. G.; Raubitschek, A. A.; Forman, S. J.; Press, O. W., Antigen sensitivity of CD22-specific chimeric TCR is modulated by target epitope distance from the cell membrane. *The Journal of Immunology* **2008,** *180* (10), 7028-7038.

79. Dustin, M. L.; Depoil, D., New insights into the T cell synapse from single molecule techniques. *Nat Rev Immunol* **2011,** *11* (10), 672-84.

80. Irving, B. A.; Weiss, A., The cytoplasmic domain of the T cell receptor zeta chain is sufficient to couple to receptor-associated signal transduction pathways. *Cell* **1991,** *64* (5), 891-901.

81. Arnett, K. L.; Harrison, S. C.; Wiley, D. C., Crystal structure of a human CD3-ε/δ dimer in complex with a UCHT1 single-chain antibody fragment. *Proceedings of the National Academy of Sciences of the United States of America* **2004,** *101* (46), 16268-16273.

82. Romeo, C.; Amiot, M.; Seed, B., Sequence requirements for induction of cytolysis by the T cell antigen/Fc receptor zeta chain. *Cell* **1992,** *68* (5), 889-97.

83. Romeo, C.; Seed, B., Cellular immunity to HIV activated by CD4 fused to T cell or Fc receptor polypeptides. *Cell* **1991,** *64* (5), 1037-46.

84. Bruhns, P., Properties of mouse and human IgG receptors and their contribution to disease models. *Blood* **2012,** *119* (24), 5640-9.

85. Letourneur, F.; Klausner, R. D., T-cell and basophil activation through the cytoplasmic tail of T-cell-receptor zeta family proteins. *Proc Natl Acad Sci U S A* **1991,** *88* (20), 8905-9.

86. Chen, L.; Flies, D. B., Molecular mechanisms of T cell co-stimulation and co-inhibition. *Nature reviews. Immunology* **2013,** *13* (4), 227-242.

87. Harding, F. A.; McArthur, J. G.; Gross, J. A.; Raulet, D. H.; Allison, J. P., CD28-mediated signalling co-stimulates murine T cells and prevents induction of anergy in T-cell clones. *Nature* **1992,** *356* (6370), 607-609.

88. Maher, J.; Brentjens, R. J.; Gunset, G.; Riviere, I.; Sadelain, M., Human T-lymphocyte cytotoxicity and proliferation directed by a single chimeric TCR[zeta] /CD28 receptor. *Nat Biotech* **2002,** *20* (1), 70-75.

89. Gong, M. C.; Latouche, J.-B.; Krause, A.; Heston, W. D. W.; Bander, N. H.; Sadelain, M., Cancer Patient T Cells Genetically Targeted to Prostate-Specific Membrane Antigen Specifically Lyse Prostate Cancer Cells and Release Cytokines in Response to Prostate-Specific Membrane Antigen. *Neoplasia (New York, N.Y.)* **1999,** *1* (2), 123-127.

90. Savoldo, B.; Ramos, C. A.; Liu, E.; Mims, M. P.; Keating, M. J.; Carrum, G.; Kamble, R. T.; Bollard, C. M.; Gee, A. P.; Mei, Z.; Liu, H.; Grilley, B.; Rooney, C. M.; Heslop, H. E.; Brenner, M. K.; Dotti, G., CD28 costimulation improves expansion and persistence of chimeric antigen receptor-modified T cells in lymphoma patients. *J Clin Invest* **2011,** *121* (5), 1822-6.

91. Batlevi, C. L.; Matsuki, E.; Brentjens, R. J.; Younes, A., Novel immunotherapies in lymphoid malignancies. *Nat Rev Clin Oncol* **2016,** *13* (1), 25-40.

92. Stephan, M. T.; Ponomarev, V.; Brentjens, R. J.; Chang, A. H.; Dobrenkov, K. V.; Heller, G.; Sadelain, M., T cell-encoded CD80 and 4-1BBL induce auto- and transcostimulation, resulting in potent tumor rejection. *Nat Med* **2007,** *13* (12), 1440-9.

93. Markley, J. C.; Sadelain, M., IL-7 and IL-21 are superior to IL-2 and IL-15 in promoting human T cell-mediated rejection of systemic lymphoma in immunodeficient mice. *Blood* **2010,** *115* (17), 3508-19.

94. Pegram, H. J.; Lee, J. C.; Hayman, E. G.; Imperato, G. H.; Tedder, T. F.; Sadelain, M.; Brentjens, R. J., Tumor-targeted T cells modified to secrete IL-12 eradicate systemic tumors without need for prior conditioning. *Blood* **2012,** *119* (18), 4133-4141.

95. Kakarla, S.; Gottschalk, S., CAR T cells for solid tumors: armed and ready to go? *Cancer journal (Sudbury, Mass.)* **2014,** *20* (2), 151-155.

96. Lamers, C. H.; Willemsen, R.; van Elzakker, P.; van Steenbergen-Langeveld, S.; Broertjes, M.; Oosterwijk-Wakka, J.; Oosterwijk, E.; Sleijfer, S.; Debets, R.; Gratama, J. W., Immune responses to transgene and retroviral vector in patients treated with ex vivo-engineered T cells. *Blood* **2011,** *117* (1), 72-82.

97. Maus, M. V.; Haas, A. R.; Beatty, G. L.; Albelda, S. M.; Levine, B. L.; Liu, X.; Zhao, Y.; Kalos, M.; June, C. H., T cells expressing chimeric antigen receptors can cause anaphylaxis in humans. *Cancer immunology research* **2013,** *1*, 26-31.

98. Riddell, S. R.; Elliott, M.; Lewinsohn, D. A.; Gilbert, M. J.; Wilson, L.; Manley, S. A.; Lupton, S. D.; Overell, R. W.; Reynolds, T. C.; Corey, L.; Greenberg, P. D., T-cell mediated rejection of gene-modified HIV-specific cytotoxic T lymphocytes in HIV-infected patients. *Nat Med* **1996,** *2* (2), 216-23.

99. Maude, S. L.; Barrett, D.; Teachey, D. T.; Grupp, S. A., Managing Cytokine Release Syndrome Associated With Novel T Cell-Engaging Therapies. *Cancer journal (Sudbury, Mass.)* **2014,** *20* (2), 119-122.

100. Schneider, H.; Downey, J.; Smith, A.; Zinselmeyer, B. H.; Rush, C.; Brewer, J. M.; Wei, B.; Hogg, N.; Garside, P.; Rudd, C. E., Reversal of the TCR stop signal by CTLA-4. *Science* **2006,** *313* (5795), 1972-5.

101. Egen, J. G.; Allison, J. P., Cytotoxic T lymphocyte antigen-4 accumulation in the immunological synapse is regulated by TCR signal strength. *Immunity* **2002,** *16* (1), 23-35.

102. Walunas, T. L.; Lenschow, D. J.; Bakker, C. Y.; Linsley, P. S.; Freeman, G. J.; Green, J. M.; Thompson, C. B.; Bluestone, J. A., CTLA-4 can function as a negative regulator of T cell activation. *Immunity* **1994,** *1* (5), 405-413.

103. Krummel, M. F.; Allison, J. P., CD28 and CTLA-4 have opposing effects on the response of T cells to stimulation. *Journal of Experimental Medicine* **1995,** *182* (2), 459-465.

104. Brunner, M. C.; Chambers, C. A.; Chan, F. K. M.; Hanke, J.; Winoto, A.; Allison, J. P., CTLA-4-mediated inhibition of early events of T cell proliferation. *Journal of Immunology* **1999,** *162* (10), 5813-5820.

105. Ribas, A., Clinical Development of the Anti–CTLA-4 Antibody Tremelimumab. *Seminars in Oncology* **2010,** *37* (5), 450-454.

106. Phan, G. Q.; Yang, J. C.; Sherry, R. M.; Hwu, P.; Topalian, S. L.; Schwartzentruber, D. J.; Restifo, N. P.; Haworth, L. R.; Seipp, C. A.; Freezer, L. J.; Morton, K. E.; Mavroukakis, S. A.; Duray, P. H.; Steinberg, S. M.; Allison, J. P.; Davis, T. A.; Rosenberg, S. A., Cancer regression and autoimmunity induced by cytotoxic T

lymphocyte-associated antigen 4 blockade in patients with metastatic melanoma. *Proceedings of the National Academy of Sciences* **2003,** *100* (14), 8372-8377.

107. Hodi, F. S.; O'Day, S. J.; McDermott, D. F.; Weber, R. W.; Sosman, J. A.; Haanen, J. B.; Gonzalez, R.; Robert, C.; Schadendorf, D.; Hassel, J. C.; Akerley, W.; van den Eertwegh, A. J. M.; Lutzky, J.; Lorigan, P.; Vaubel, J. M.; Linette, G. P.; Hogg, D.; Ottensmeier, C. H.; Lebbé, C.; Peschel, C.; Quirt, I.; Clark, J. I.; Wolchok, J. D.; Weber, J. S.; Tian, J.; Yellin, M. J.; Nichol, G. M.; Hoos, A.; Urba, W. J., Improved Survival with Ipilimumab in Patients with Metastatic Melanoma. *New England Journal of Medicine* **2010,** *363* (8), 711-723.

108. Pardoll, D. M., The blockade of immune checkpoints in cancer immunotherapy. *Nat Rev Cancer* **2012,** *12* (4), 252-264.

109. Taube, J. M.; Anders, R. A.; Young, G. D.; Xu, H.; Sharma, R.; McMiller, T. L.; Chen, S.; Klein, A. P.; Pardoll, D. M.; Topalian, S. L.; Chen, L., Colocalization of Inflammatory Response with B7-H1 Expression in Human Melanocytic Lesions Supports an Adaptive Resistance Mechanism of Immune Escape. *Science translational medicine* **2012,** *4* (127), 127ra37-127ra37.

110. Ahmadzadeh, M.; Johnson, L. A.; Heemskerk, B.; Wunderlich, J. R.; Dudley, M. E.; White, D. E.; Rosenberg, S. A., Tumor antigen–specific CD8 T cells infiltrating the tumor express high levels of PD-1 and are functionally impaired. *Blood* **2009,** *114* (8), 1537-1544.

111. Kyi, C.; Postow, M. A., Checkpoint blocking antibodies in cancer immunotherapy. *FEBS Letters* **2014,** *588* (2), 368-376.

112. Velu, V.; Titanji, K.; Zhu, B.; Husain, S.; Pladevega, A.; Lai, L.; Vanderford, T. H.; Chennareddi, L.; Silvestri, G.; Freeman, G. J.; Ahmed, R.; Amara, R. R., Enhancing SIV-specific immunity in vivo by PD-1 blockade. *Nature* **2009,** *458* (7235), 206-210.

113. Zou, W.; Chen, L., Inhibitory B7-family molecules in the tumour microenvironment. *Nat Rev Immunol* **2008,** *8* (6), 467-77.

114. Dong, H.; Strome, S. E.; Salomao, D. R.; Tamura, H.; Hirano, F.; Flies, D. B.; Roche, P. C.; Lu, J.; Zhu, G.; Tamada, K.; Lennon, V. A.; Celis, E.; Chen, L., Tumor-associated B7-H1 promotes T-cell apoptosis: A potential mechanism of immune evasion. *Nat Med* **2002,** *8* (8), 793-800.

115. Rosenwald, A.; Wright, G.; Leroy, K.; Yu, X.; Gaulard, P.; Gascoyne, R. D.; Chan, W. C.; Zhao, T.; Haioun, C.; Greiner, T. C.; Weisenburger, D. D.; Lynch, J. C.; Vose, J.; Armitage, J. O.; Smeland, E. B.; Kvaloy, S.; Holte, H.; Delabie, J.; Campo, E.; Montserrat, E.; Lopez-Guillermo, A.; Ott, G.; Muller-Hermelink, H. K.; Connors, J. M.; Braziel, R.; Grogan, T. M.; Fisher, R. I.; Miller, T. P.; LeBlanc, M.; Chiorazzi, M.; Zhao, H.; Yang, L.; Powell, J.; Wilson, W. H.; Jaffe, E. S.; Simon, R.; Klausner, R. D.; Staudt, L. M., Molecular diagnosis of primary mediastinal B cell lymphoma identifies a

clinically favorable subgroup of diffuse large B cell lymphoma related to Hodgkin lymphoma. *J Exp Med* **2003,** *198* (6), 851-62.

116. Poole, R. M., Pembrolizumab: First Global Approval. *Drugs* **2014,** *74* (16), 1973-1981.

117. Hamid, O.; Robert, C.; Daud, A.; Hodi, F. S.; Hwu, W.-J.; Kefford, R.; Wolchok, J. D.; Hersey, P.; Joseph, R. W.; Weber, J. S.; Dronca, R.; Gangadhar, T. C.; Patnaik, A.; Zarour, H.; Joshua, A. M.; Gergich, K.; Elassaiss-Schaap, J.; Algazi, A.; Mateus, C.; Boasberg, P.; Tumeh, P. C.; Chmielowski, B.; Ebbinghaus, S. W.; Li, X. N.; Kang, S. P.; Ribas, A., Safety and Tumor Responses with Lambrolizumab (Anti–PD-1) in Melanoma. *The New England journal of medicine* **2013,** *369* (2), 134-144.

118. Robert, C.; Schachter, J.; Long, G. V.; Arance, A.; Grob, J. J.; Mortier, L.; Daud, A.; Carlino, M. S.; McNeil, C.; Lotem, M.; Larkin, J.; Lorigan, P.; Neyns, B.; Blank, C. U.; Hamid, O.; Mateus, C.; Shapira-Frommer, R.; Kosh, M.; Zhou, H.; Ibrahim, N.; Ebbinghaus, S.; Ribas, A., Pembrolizumab versus Ipilimumab in Advanced Melanoma. *New England Journal of Medicine* **2015,** *372* (26), 2521-2532.

119. Garber, K., Bispecific antibodies rise again. *Nature Reviews Drug Discovery* **2014,** *13* (11), 799-801.

120. Mullard, A., FDA approves first bispecific. *Nat Rev Drug Discov* **2015,** *14* (1), 7-7.

121. Nagorsen, D.; Kufer, P.; Baeuerle, P. A.; Bargou, R., Blinatumomab: a historical perspective. *Pharmacology & therapeutics* **2012,** *136* (3), 334-342.

122. Haas, C.; Krinner, E.; Brischwein, K.; Hoffmann, P.; Lutterbüse, R.; Schlereth, B.; Kufer, P.; Baeuerle, P. A., Mode of cytotoxic action of T cell-engaging BiTE antibody MT110. *Immunobiology* **2009,** *214* (6), 441-453.

123. Russell, J. H.; Ley, T. J., Lymphocyte-mediated cytotoxicity. *Annu Rev Immunol* **2002,** *20*, 323-70.

124. Klinger, M.; Brandl, C.; Zugmaier, G.; Hijazi, Y.; Bargou, R. C.; Topp, M. S.; Gokbuget, N.; Neumann, S.; Goebeler, M.; Viardot, A.; Stelljes, M.; Bruggemann, M.; Hoelzer, D.; Degenhard, E.; Nagorsen, D.; Baeuerle, P. A.; Wolf, A.; Kufer, P., Immunopharmacologic response of patients with B-lineage acute lymphoblastic leukemia to continuous infusion of T cell-engaging CD19/CD3-bispecific BiTE antibody blinatumomab. *Blood* **2012,** *119* (26), 6226-6233.

125. Wuellner, U.; Klupsch, K.; Buller, F.; Attinger-Toller, I.; Santimaria, R.; Zbinden, I.; Henne, P.; Grabulovski, D.; Bertschinger, J.; Brack, S., Bispecific CD3/HER2 Targeting FynomAb Induces Redirected T Cell-Mediated Cytolysis with High Potency and Enhanced Tumor Selectivity. *Antibodies* **2015,** *4* (4).

126. Lutterbuese, R.; Raum, T.; Kischel, R.; Hoffmann, P.; Mangold, S.; Rattel, B.; Friedrich, M.; Thomas, O.; Lorenczewski, G.; Rau, D.; Schaller, E.; Herrmann, I.; Wolf, A.; Urbig, T.; Baeuerle, P. A.; Kufer, P., T cell-engaging BiTE antibodies specific for EGFR potently eliminate KRAS- and BRAF-mutated colorectal cancer cells. *Proceedings of the National Academy of Sciences of the United States of America* **2010,** *107* (28), 12605-12610.

127. Osada, T.; Patel, S. P.; Hammond, S. A.; Osada, K.; Morse, M. A.; Lyerly, H. K., CEA/CD3-bispecific T cell-engaging (BiTE) antibody-mediated T lymphocyte cytotoxicity maximized by inhibition of both PD1 and PD-L1. *Cancer Immunology, Immunotherapy* **2015,** *64* (6), 677-688.

128. Laszlo, G. S.; Gudgeon, C. J.; Harrington, K. H.; Walter, R. B., T-cell ligands modulate the cytolytic activity of the CD33/CD3 BiTE antibody construct, AMG 330. *Blood Cancer Journal* **2015,** *5*, e340.

129. Hammond, S. A.; Lutterbuese, R.; Roff, S.; Lutterbuese, P.; Schlereth, B.; Bruckheimer, E.; Kinch, M. S.; Coats, S.; Baeuerle, P. A.; Kufer, P.; Kiener, P. A., Selective targeting and potent control of tumor growth using an EphA2/CD3-Bispecific single-chain antibody construct. *Cancer Res* **2007,** *67* (8), 3927-35.

130. Torisu-Itakura, H.; Schoellhammer, H. F.; Sim, M. S.; Irie, R. F.; Hausmann, S.; Raum, T.; Baeuerle, P. A.; Morton, D. L., Redirected lysis of human melanoma cells by a MCSP/CD3-bispecific BiTE antibody that engages patient-derived T cells. *J Immunother* **2011,** *34* (8), 597-605.

131. Dreier, T.; Baeuerle, P. A.; Fichtner, I.; Grun, M.; Schlereth, B.; Lorenczewski, G.; Kufer, P.; Lutterbuse, R.; Riethmuller, G.; Gjorstrup, P.; Bargou, R. C., T cell costimulus-independent and very efficacious inhibition of tumor growth in mice bearing subcutaneous or leukemic human B cell lymphoma xenografts by a CD19-/CD3-bispecific single-chain antibody construct. *J Immunol* **2003,** *170* (8), 4397-402.

132. Bargou, R.; Leo, E.; Zugmaier, G.; Klinger, M.; Goebeler, M.; Knop, S.; Noppeney, R.; Viardot, A.; Hess, G.; Schuler, M.; Einsele, H.; Brandl, C.; Wolf, A.; Kirchinger, P.; Klappers, P.; Schmidt, M.; Riethmuller, G.; Reinhardt, C.; Baeuerle, P. A.; Kufer, P., Tumor regression in cancer patients by very low doses of a T cell-engaging antibody. *Science* **2008,** *321* (5891), 974-7.

133. Nagorsen, D.; Bargou, R.; Ruttinger, D.; Kufer, P.; Baeuerle, P. A.; Zugmaier, G., Immunotherapy of lymphoma and leukemia with T-cell engaging BiTE antibody blinatumomab. *Leuk Lymphoma* **2009,** *50* (6), 886-91.

134. Dawson, J. P.; Berger, M. B.; Lin, C.-C.; Schlessinger, J.; Lemmon, M. A.; Ferguson, K. M., Epidermal Growth Factor Receptor Dimerization and Activation Require Ligand-Induced Conformational Changes in the Dimer Interface. *Molecular and Cellular Biology* **2005,** *25* (17), 7734-7742.

135. Schlessinger, J., Cell Signaling by Receptor Tyrosine Kinases. *Cell* **2000,** *103* (2), 211-225.

136. Brooks, A. J.; Dai, W.; O'Mara, M. L.; Abankwa, D.; Chhabra, Y.; Pelekanos, R. A.; Gardon, O.; Tunny, K. A.; Blucher, K. M.; Morton, C. J.; Parker, M. W.; Sierecki, E.; Gambin, Y.; Gomez, G. A.; Alexandrov, K.; Wilson, I. A.; Doxastakis, M.; Mark, A. E.; Waters, M. J., Mechanism of Activation of Protein Kinase JAK2 by the Growth Hormone Receptor. *Science* **2014,** *344* (6185).

137. Brownlie, R. J.; Zamoyska, R., T cell receptor signalling networks: branched, diversified and bounded. *Nat Rev Immunol* **2013,** *13* (4), 257-269.

138. Idriss, H. T.; Naismith, J. H., TNF alpha and the TNF receptor superfamily: structure-function relationship(s). *Microsc Res Tech* **2000,** *50* (3), 184-95.

139. Massagué, J.; Gomis, R. R., The logic of TGFβ signaling. *FEBS Letters* **2006,** *580* (12), 2811-2820.

140. Klemm, J. D.; Schreiber, S. L.; Crabtree, G. R., Dimerization as a regulatory mechanism in signal transduction. *Annu Rev Immunol* **1998,** *16*, 569-92.

141. Heldin, C.-H., Dimerization of cell surface receptors in signal transduction. *Cell* **1995,** *80* (2), 213-223.

142. Oltval, Z. N.; Milliman, C. L.; Korsmeyer, S. J., Bcl-2 heterodimerizes in vivo with a conserved homolog, Bax, that accelerates programed cell death. *Cell* **1993,** *74* (4), 609-619.

143. Hai, T.; Curran, T., Cross-family dimerization of transcription factors Fos/Jun and ATF/CREB alters DNA binding specificity. *Proc Natl Acad Sci U S A* **1991,** *88* (9), 3720-4.

144. Fegan, A.; White, B.; Carlson, J. C. T.; Wagner, C. R., Chemically Controlled Protein Assembly: Techniques and Applications. *Chemical Reviews* **2010,** *110* (6), 3315-3336.

145. Diver, S. T.; Schreiber, S. L., Single-Step Synthesis of Cell-Permeable Protein Dimerizers That Activate Signal Transduction and Gene Expression. *Journal of the American Chemical Society* **1997,** *119* (22), 5106-5109.

146. Spencer, D.; Wandless, T.; Schreiber, S.; Crabtree, G., Controlling signal transduction with synthetic ligands. *Science* **1993,** *262* (5136), 1019-1024.

147. Carlson, J. C. T.; Sidhartha, S. J.; Flenniken, M.; Chou, T.-F.; Siegel, R. A.; Wagner, C. R., Chemically controlled self-assembly of protein nanorings. *J. Amer. Chem. Soc.* **2006,** *128*, 7630-7638.

148. Ho, S. N.; Biggar, S. R.; Spencer, D. M.; Schreiber, S. L.; Crabtree, G. R., Dimeric ligands define a role for transcriptional activation domains in reinitiation. *Nature* **1996,** *382* (6594), 822-826.

149. Belshaw, P. J.; Ho, S. N.; Crabtree, G. R.; Schreiber, S. L., Controlling protein association and subcellular localization with a synthetic ligand that induces heterodimerization of proteins. *Proceedings of the National Academy of Sciences* **1996,** *93* (10), 4604-4607.

150. Rivera, V. M.; Clackson, T.; Natesan, S.; Pollock, R.; Amara, J. F.; Keenan, T.; Magari, S. R.; Phillips, T.; Courage, N. L.; Cerasoli, F.; Holt, D. A.; Gilman, M., A humanized system for pharmacologic control of gene expression. *Nat Med* **1996,** *2* (9), 1028-1032.

151. Farrar, M. A.; Alberola-lla, J.; Perlmutter, R. M., Activation of the Raf-1 kinase cascade by coumermycin-induced dimerization. *Nature* **1996,** *383* (6596), 178-181.

152. Kopytek, S. J.; Standaert, R. F.; Dyer, J. C. D.; Hu, J. C., Chemically induced dimerization of dihydrofolate reductase by a homobifunctional dimer of methotrexate. *Chemistry & biology* **2000,** *7* (5), 313-321.

153. Voss, S.; Wu, Y.-W., Tandem Orthogonal Chemically Induced Dimerization. *ChemBioChem* **2013,** *14* (13), 1525-1527.

154. Schweitzer, B. I.; Dicker, A. P.; Bertino, J. R., Dihydrofolate reductase as a therapeutic target. *The FASEB Journal* **1990,** *4* (8), 2441-2452.

155. Matthews, D.; Alden, R.; Bolin, J.; Freer, S.; Hamlin, R.; Xuong, N.; Kraut, J.; Poe, M.; Williams, M.; Hoogsteen, K., Dihydrofolate reductase: x-ray structure of the binary complex with methotrexate. *Science* **1977,** *197* (4302), 452-455.

156. Appleman, J. R.; Howell, E. E.; Kraut, J.; Kühl, M.; Blakley, R. L., Role of aspartate 27 in the binding of methotrexate to dihydrofolate reductase from Escherichia coli. *Journal of Biological Chemistry* **1988,** *263* (19), 9187-9198.

157. Bolin, J. T.; Filman, D. J.; Matthews, D. A.; Hamlin, R. C.; Kraut, J., Crystal structures of Escherichia coli and Lactobacillus casei dihydrofolate reductase refined at 1.7 A resolution. I. General features and binding of methotrexate. *J Biol Chem* **1982,** *257* (22), 13650-62.

158. Carlson, J. C. T.; Kanter, A.; Thuduppathy, G. R.; Cody, V.; Pineda, P. E.; McIvor, R. S.; Wagner, C. R., Designing Protein Dimerizers: The Importance of Ligand Conformational Equilibria. *Journal of the American Chemical Society* **2003,** *125* (6), 1501-1507.

159. Kopytek, S. J.; Standaert, R. F.; Dyer, J. C.; Hu, J. C., Chemically induced dimerization of dihydrofolate reductase by a homobifunctional dimer of methotrexate. *Chem Biol* **2000,** *7* (5), 313-21.

160. Li, Q.; So, C. R.; Fegan, A.; Cody, V.; Sarikaya, M.; Vallera, D. A.; Wagner, C. R., Chemically Self-Assembled Antibody Nanorings (CSANs): Design and Characterization of an Anti-CD3 IgM Biomimetic. *Journal of the American Chemical Society* **2010,** *132* (48), 17247-17257.

161. Ercolani, G., Physical Basis of Self-Assembly Macrocyclizations. *The Journal of Physical Chemistry B* **1998,** *102* (29), 5699-5703.

162. Fegan, A.; Kumarapperuma, S. C.; Wagner, C. R., Chemically self-assembled antibody nanostructures as potential drug carriers. *Mol. Pharmeceutics* **2012,** *9*, 3218-3227.

163. Bayle, J. H.; Grimley, J. S.; Stankunas, K.; Gestwicki, J. E.; Wandless, T. J.; Crabtree, G. R., Rapamycin Analogs with Differential Binding Specificity Permit Orthogonal Control of Protein Activity. *Chemistry & Biology* **2006,** *13* (1), 99-107.

164. Czlapinski, J. L.; Schelle, M. W.; Miller, L. W.; Laughlin, S. T.; Kohler, J. J.; Cornish, V. W.; Bertozzi, C. R., Conditional Glycosylation in Eukaryotic Cells Using a Biocompatible Chemical Inducer of Dimerization. *Journal of the American Chemical Society* **2008,** *130* (40), 13186-13187.

165. Li, Q.; Hapka, D.; Chen, H.; Vallera, D. A.; Wagner, C. R., Self-Assembly of Antibodies by Chemical Induction. *Angewandte Chemie* **2008,** *120* (52), 10333-10336.

166. Shen, J.; Vallera, D. A.; Wagner, C. R., Prosthetic Antigen Receptors. *J Am Chem Soc* **2015,** *137* (32), 10108-11.

167. Taira, K.; Benkovic, S. J., Evaluation of the importance of hydrophobic interactions in drug binding to dihydrofolate reductase. *Journal of Medicinal Chemistry* **1988,** *31* (1), 129-137.

168. Sousou, T.; Friedberg, J., Rituximab in Indolent Lymphomas. *Seminars in Hematology* **2010,** *47* (2), 133-142.

169. Loffler, A.; Gruen, M.; Wuchter, C.; Schriever, F.; Kufer, P.; Dreier, T.; Hanakam, F.; Baeuerle, P. A.; Bommert, K.; Karawajew, L.; Dorken, B.; Bargou, R. C., Efficient elimination of chronic lymphocytic leukaemia B cells by autologous T cells with a bispecific anti-CD19/anti-CD3 single-chain antibody construct. *Leukemia* **2003,** *17* (5), 900-9.

170. Blattman, J. N.; Greenberg, P. D., Cancer immunotherapy: a treatment for the masses. *Science* **2004,** *305* (5681), 200-205.

171. Ferrone, S.; Whiteside, T. L., Tumor Microenvironment and Immune Escape. *Surgical Oncology Clinics of North America* **2007,** *16* (4), 755-774.

172. Vonderheide, R. H.; June, C. H., Engineering T cells for cancer: our synthetic future. *Immunological reviews* **2014,** *257* (1), 7-13.

173. June, C. H.; Maus, M. V.; Plesa, G.; Johnson, L. A.; Zhao, Y. B.; Levine, B. L.; Grupp, S. A.; Porter, D. L., Engineered T cells for cancer therapy. *Cancer Immunology Immunotherapy* **2014,** *63* (9), 969-975.

174. Maus, M. V.; Grupp, S. A.; Porter, D. L.; June, C. H., Antibody-modified T cells: CARs take the front seat for hematologic malignancies. *Blood* **2014,** *123* (17), 2625-2635.

175. Qasim, W.; Thrasher, A. J., Progress and prospects for engineered T cell therapies. *British Journal of Haematology* **2014,** *166* (6), 818-829.

176. Porter, D. L., Levine, B. L., Kalos, M., Bagg, A. & June, C. H., Chimeric Antigen Receptor-Modified T cells in chronic Lymphoid Leukemia. *The New England Journal of Medicine* **2011,** *365*, 9.

177. Brentjens, R. J.; Davila, M. L.; Riviere, I.; Park, J.; Wang, X.; Cowell, L. G.; Bartido, S.; Stefanski, J.; Taylor, C.; Olszewska, M.; others, CD19-targeted T cells rapidly induce molecular remissions in adults with chemotherapy-refractory acute lymphoblastic leukemia. *Science translational medicine* **2013,** *5* (177), 177ra38-177ra38.

178. Levine, B., Performance-enhancing drugs: design and production of redirected chimeric antigen receptor (CAR) T cells. *Cancer gene therapy* **2015**.

179. Baum, C.; Kustikova, O.; Modlich, U.; Li, Z.; Fehse, B., Mutagenesis and oncogenesis by chromosomal insertion of gene transfer vectors. *Human gene therapy* **2006,** *17* (3), 253-263.

180. Li, Q.; Hapka, D.; Chen, H.; Vallera, D. A.; Wagner, C. R., Self-Assembly of Antibodies by Chemical Induction. *Angew. Chemie, Inter. Ed.* **2008,** *47* (52), 10179-10182.

181. Fegan, A.; Kumarapperuma, S. C.; Wagner, C. R., Chemically Self-Assembled Antibody Nanostructures as Potential Drug Carriers. *Molecular pharmaceutics* **2012,** *9* (11), 3218-3227.

182. Carlson, J. C. T.; Jena, S. S.; Flenniken, M.; Chou, T.-f.; Siegel, R. A.; Wagner, C. R., Chemically Controlled Self-Assembly of Protein Nanorings. *Journal of the American Chemical Society* **2006,** *128* (23), 7630-7638.

183. Piccaluga, P. P.; Arpinati, M.; Candoni, A.; Laterza, C.; Paolini, S.; Gazzola, A.; Sabattini, E.; Visani, G.; Pileri, S. A., Surface antigens analysis reveals significant expression of candidate targets for immunotherapy in adult acute lymphoid leukemia. *Leukemia & Lymphoma* **2011,** *52* (2), 325-327.

184. Haas, K. M.; Sen, S.; Sanford, I. G.; Miller, A. S.; Poe, J. C.; Tedder, T. F., CD22 ligand binding regulates normal and malignant B lymphocyte survival in vivo. *The Journal of Immunology* **2006,** *177* (5), 3063-3073.

185. Haso, W.; Lee, D. W.; Shah, N. N.; Stetler-Stevenson, M.; Yuan, C. M.; Pastan, I. H.; Dimitrov, D. S.; Morgan, R. A.; FitzGerald, D. J.; Barrett, D. M.; Wayne, A. S.;

Mackall, C. L.; Orentas, R. J., Anti-CD22-chimeric antigen receptors targeting B-cell precursor acute lymphoblastic leukemia. *Blood* **2013,** *121* (7), 1165-1174.

186. Leonard, J. P.; Link, B. K., Immunotherapy of non-Hodgkin's lymphoma with hLL2 (epratuzumab, an anti-CD22 monoclonal antibody) and Hu1D10 (apolizumab). *Seminars in Oncology* **2002,** *29* (1), 81-86.

187. Du, X.; Beers, R.; FitzGerald, D. J.; Pastan, I., Differential Cellular Internalization of Anti-CD19 and -CD22 Immunotoxins Results in Different Cytotoxic Activity. *Cancer Research* **2008,** *68* (15), 6300-6305.

188. Amini, H.; Ahmadiani, A., Rapid and simultaneous determination of sulfamethoxazole and trimethoprim in human plasma by high-performance liquid chromatography. *Journal of Pharmaceutical and Biomedical Analysis* **2007,** *43* (3), 1146-1150.

189. Feldmann, A.; Arndt, C.; Töpfer, K.; Stamova, S.; Krone, F.; Cartellieri, M.; Koristka, S.; Michalk, I.; Lindemann, D.; Schmitz, M.; others, Novel humanized and highly efficient bispecific antibodies mediate killing of prostate stem cell antigen-expressing tumor cells by CD8+ and CD4+ T cells. *The Journal of Immunology* **2012,** *189* (6), 3249-3259.

190. Marchand, M.; Weynants, P.; Rankin, E.; Arienti, F.; Belli, F.; Parmiani, G.; Cascinelli, N.; Bourlond, A.; Vanwijck, R.; Humblet, Y.; et al., Tumor regression responses in melanoma patients treated with a peptide encoded by gene MAGE-3. *Int J Cancer* **1995,** *63* (6), 883-5.

191. Yaddanapudi, K.; Mitchell, R. A.; Eaton, J. W., Cancer vaccines. *OncoImmunology* **2013,** *2* (3), e23403.

192. Akira, S., Mammalian Toll-like receptors. *Current Opinion in Immunology* **2003,** *15* (1), 5-11.

193. Krieg, A. M.; Yi, A. K.; Schorr, J.; Davis, H. L., The role of CpG dinucleotides in DNA vaccines. *Trends Microbiol* **1998,** *6* (1), 23-7.

194. Hartmann, G.; Weeratna, R. D.; Ballas, Z. K.; Payette, P.; Blackwell, S.; Suparto, I.; Rasmussen, W. L.; Waldschmidt, M.; Sajuthi, D.; Purcell, R. H.; Davis, H. L.; Krieg, A. M., Delineation of a CpG phosphorothioate oligodeoxynucleotide for activating primate immune responses in vitro and in vivo. *J Immunol* **2000,** *164* (3), 1617-24.

195. Krieg, A. M.; Yi, A. K.; Matson, S.; Waldschmidt, T. J.; Bishop, G. A.; Teasdale, R.; Koretzky, G. A.; Klinman, D. M., CpG motifs in bacterial DNA trigger direct B-cell activation. *Nature* **1995,** *374* (6522), 546-9.

196. Klinman, D. M.; Yi, A.-K.; Beaucage, S. L.; Conover, J.; Krieg, A. M., CpG motifs present in bacteria DNA rapidly induce lymphocytes to secrete interleukin 6,

interleukin 12, and interferon gamma. *Proceedings of the national academy of sciences* **1996,** *93* (7), 2879-2883.

197. Martin-Orozco, E.; Kobayashi, H.; Van Uden, J.; Nguyen, M. D.; Kornbluth, R. S.; Raz, E., Enhancement of antigen-presenting cell surface molecules involved in cognate interactions by immunostimulatory DNA sequences. *Int Immunol* **1999,** *11* (7), 1111-8.

198. Krieg, A. M., The role of CpG motifs in innate immunity. *Curr Opin Immunol* **2000,** *12* (1), 35-43.

199. Wagner, H., Bacterial CpG DNA activates immune cells to signal infectious danger. *Adv Immunol* **1999,** *73*, 329-68.

200. Klinman, D. M.; Verthelyi, D.; Takeshita, F.; Ishii, K. J., Immune Recognition of Foreign DNA: A Cure for Bioterrorism? *Immunity* **1999,** *11* (2), 123-129.

201. Mutwiri, G. K.; Nichani, A. K.; Babiuk, S.; Babiuk, L. A., Strategies for enhancing the immunostimulatory effects of CpG oligodeoxynucleotides. *J Control Release* **2004,** *97* (1), 1-17.

202. Cho, H. J.; Takabayashi, K.; Cheng, P. M.; Nguyen, M. D.; Corr, M.; Tuck, S.; Raz, E., Immunostimulatory DNA-based vaccines induce cytotoxic lymphocyte activity by a T-helper cell-independent mechanism. *Nat Biotechnol* **2000,** *18* (5), 509-14.

203. Zhang, X. Q.; Dahle, C. E.; Weiner, G. J.; Salem, A. K., A comparative study of the antigen-specific immune response induced by co-delivery of CpG ODN and antigen using fusion molecules or biodegradable microparticles. *J Pharm Sci* **2007,** *96* (12), 3283-92.

204. Ilyinskii, P. O.; Roy, C. J.; O'Neil, C. P.; Browning, E. A.; Pittet, L. A.; Altreuter, D. H.; Alexis, F.; Tonti, E.; Shi, J.; Basto, P. A.; Iannacone, M.; Radovic-Moreno, A. F.; Langer, R. S.; Farokhzad, O. C.; von Andrian, U. H.; Johnston, L. P. M.; Kishimoto, T. K., Adjuvant-carrying synthetic vaccine particles augment the immune response to encapsulated antigen and exhibit strong local immune activation without inducing systemic cytokine release. *Vaccine* **2014,** *32* (24), 2882-2895.

205. Diwan, M.; Tafaghodi, M.; Samuel, J., Enhancement of immune responses by co-delivery of a CpG oligodeoxynucleotide and tetanus toxoid in biodegradable nanospheres. *J Control Release* **2002,** *85* (1-3), 247-62.

206. Mammadov, R.; Cinar, G.; Gunduz, N.; Goktas, M.; Kayhan, H.; Tohumeken, S.; Topal, A. E.; Orujalipoor, I.; Delibasi, T.; Dana, A.; Ide, S.; Tekinay, A. B.; Guler, M. O., Virus-like nanostructures for tuning immune response. *Scientific Reports* **2015,** *5*, 16728.

207. Herbath, M.; Szekeres, Z.; Kovesdi, D.; Papp, K.; Erdei, A.; Prechl, J., Coadministration of antigen-conjugated and free CpG: effects of in vitro and in vivo interactions in a murine model. *Immunol Lett* **2014,** *160* (2), 178-85.

208. de Titta, A.; Ballester, M.; Julier, Z.; Nembrini, C.; Jeanbart, L.; van der Vlies, A. J.; Swartz, M. A.; Hubbell, J. A., Nanoparticle conjugation of CpG enhances adjuvancy for cellular immunity and memory recall at low dose. *Proceedings of the National Academy of Sciences* **2013,** *110* (49), 19902-19907.

209. Gangar, A.; Fegan, A.; Kumarapperuma, S. C.; Wagner, C. R., Programmable self-assembly of antibody-oligonucleotide conjugates as small molecule and protein carriers. *J Am Chem Soc* **2012,** *134* (6), 2895-7.

210. Gangar, A.; Fegan, A.; Kumarapperuma, S. C.; Huynh, P.; Benyumov, A.; Wagner, C. R., Targeted delivery of antisense oligonucleotides by chemically self-assembled nanostructures. *Mol Pharm* **2013,** *10* (9), 3514-8.

211. Utaisincharoen, P.; Anuntagool, N.; Chaisuriya, P.; Pichyangkul, S.; Sirisinha, S., CpG ODN activates NO and iNOS production in mouse macrophage cell line (RAW 264 ·7). *Clin Exp Immunol* **2002,** *128* (3), 467-73.

212. Radovic-Moreno, A. F.; Chernyak, N.; Mader, C. C.; Nallagatla, S.; Kang, R. S.; Hao, L.; Walker, D. A.; Halo, T. L.; Merkel, T. J.; Rische, C. H.; Anantatmula, S.; Burkhart, M.; Mirkin, C. A.; Gryaznov, S. M., Immunomodulatory spherical nucleic acids. *Proceedings of the National Academy of Sciences* **2015,** *112* (13), 3892-3897.

213. Zhu, F. G.; Reich, C. F.; Pisetsky, D. S., The role of the macrophage scavenger receptor in immune stimulation by bacterial DNA and synthetic oligonucleotides. *Immunology* **2001,** *103* (2), 226-34.

214. Chu, R. S.; Targoni, O. S.; Krieg, A. M.; Lehmann, P. V.; Harding, C. V., CpG Oligodeoxynucleotides Act as Adjuvants that Switch on T Helper 1 (Th1) Immunity. *The Journal of Experimental Medicine* **1997,** *186* (10), 1623-1631.

215. Shah, R.; Petersburg, J.; Gangar, A. C.; Fegan, A.; Wagner, C. R.; Kumarapperuma, S. C., In Vivo Evaluation of Site-Specifically PEGylated Chemically Self-Assembled Protein Nanostructures. *Molecular Pharmaceutics* **2016**.

216. Jegerlehner, A.; Maurer, P.; Bessa, J.; Hinton, H. J.; Kopf, M.; Bachmann, M. F., TLR9 Signaling in B Cells Determines Class Switch Recombination to IgG2a. *The Journal of Immunology* **2007,** *178* (4), 2415-2420.